Available online at www.sciencedirect.com
ScienceDirect
Atmospheric Environment 41 (2007) S80–S117
ATMOSPHERIC ENVIRONMENT
www.elsevier.com/locate/atmosenv

Atmospheric Environment Vol. 24A, No. 3, pp. 481–518, 1990.
Printed in Great Britain.

0004–6981/90 $3.00 + 0.00

A DETAILED MECHANISM FOR THE GAS-PHASE ATMOSPHERIC REACTIONS OF ORGANIC COMPOUNDS

WILLIAM P. L. CARTER*
Statewide Air Pollution Research Center, University of California, Riverside, CA 92521, U.S.A.

(*First received* 13 *February* 1989 *and in final form* 26 *May* 1989)

Abstract—A gas-phase reaction mechanism for the atmospheric photooxidations of over 100 alkanes, alkenes, aromatic hydrocarbons, alcohols, ethers and other compounds representative of the range of reactive organics emitted into polluted atmospheres is described. Most of these organic species are represented using generalized reactions with variable rate constants and product yield coefficients for which individual assignments were made or estimated. This mechanism employs 19 species to represent the reactive oxygenated and organic nitrate products, and includes the gas-phase reactions of SO_2, but does not include heterogeneous or liquid-phase reactions. The evaluation of this mechanism, by comparison of its predictions against the results of over 500 environmental chamber experiments, is described in a separate paper. This detailed mechanism can be used in assessments of relative atmospheric reactivities of organic compounds, and can provide the basis for the derivation of more condensed mechanisms for use in air quality simulation models.

Key word index: Atmospheric chemistry, photochemical smog, air pollution, computer modeling, air quality simulation models, kinetic mechanisms, gas-phase reactions, organic compounds, alkanes, alkenes, aromatic hydrocarbons, oxygenated organic compounds, organic nitrates, ozone, atmospheric reactivity.

INTRODUCTION

Photochemical ozone formation continues to be an important air pollution problem in many urban and downwind areas. Ozone is not emitted directly, but is formed from a complex series of reactions between emitted oxides of nitrogen (NO_x) and reactive organic gases (ROG). Reliable and scientifically valid methods of relating emissions of these species to ambient levels of O_3 are required to formulate appropriate and cost-effective control strategies to reduce O_3 levels in areas where this is a problem. Air quality simulation models (AQSMs) can be useful in this regard, provided that their components represent the latest scientific data concerning the major chemical and physical processes which are important in influencing O_3 formation. An important component of such models is the gas-phase chemical mechanism used to describe the atmospheric transformations of the emitted reactive chemical species.

A number of chemical mechanisms have been and are being used in air quality simulation models (e.g. Dodge, 1977; Falls and Seinfeld, 1978; Killus and Whitten, 1982; McRae *et al.*, 1982; Atkinson *et al.*, 1982; Penner and Walton, 1982; McRae and Seinfeld, 1983; Stockwell and Calvert, 1983; Stockwell, 1986; Lurmann *et al.*, 1986, 1987; Gery *et al.*, 1988; Hough, 1988 and references therein). While the more recent of these mechanisms are to a large extent based on the same body of laboratory kinetic data, different techniques and assumptions have been used to represent and condense the organic chemistry in the differing mechanisms. Differences in these mechanisms yield different O_3 control strategy requirements for identical meteorological, emissions and background air quality conditions (Jeffries *et al.*, 1981; Carter *et al.*, 1982b; Leone and Seinfeld, 1984a; Schafer and Seinfeld, 1985). Since it is unlikely that the many uncertainties in the atmospheric chemistry of organics will be reduced in the near term, or that AQSMs models will soon be able to incorporate mechanisms which represent the details of the atmospheric reactions of the many hundreds of emitted ROG species without significant approximation or condensation (even if these details were known), numerous researchers have recommended using more than one chemical mechanism in control strategy calculations (Schafer and Seinfeld, 1985; EPA, 1987). This may permit the uncertainties in the representation of the chemistry to be, at least partially, taken into account.

In this paper, an up-to-date detailed photochemical reaction mechanism developed for use in O_3 modeling and control strategy applications and in assessing the relative reactivities of different VOC species with respect to O_3 formation is described. The starting point in the development of this mechanism was the "ALW" mechanism of Atkinson *et al.* (1982), as updated in the "ADOM" mechanism developed by Lurmann *et al.* (1986) for use in acid deposition and long-range transport (LRT) modeling studies. The primary difference between this new mechanism and most others is that, instead of representing the many emitted organic compounds using a limited number of lumped species with fixed mechanistic parameters, the present mechanism includes assignments of kinetic and mechanistic parameters for over 100 individual

doi:10.1016/j.atmosenv.2007.10.061

alkanes, aromatics, alkenes and other species, with these compounds then being represented using generalized species and reactions with parameters derived based on those of the compound(s) being represented. Thus, at least in terms of the numbers of different organic compounds whose reactions can be separately represented, this is probably the most detailed mechanism which has been developed to date. This most recent and detailed SAPRC mechanism is the one whose major features are summarized in this paper.

The mechanism described in this paper has been tested against the results of over 550 environmental chamber experiments carried out in four different environmental chambers in two different laboratories (Carter, 1988a; Lurmann and Carter, 1989). Although the ability of a mechanism to simulate results of environmental chamber experiments does not prove its correctness, it is clearly important that it at least be shown not to be inconsistent with the available data. The performance of this mechanism in simulating the chamber data is comparable to previous versions of this mechanism which were evaluated against this data base (Carter *et al.*, 1986b; Lurmann *et al.*, 1987). For example, Fig. 1 shows plots of experimental vs calculated O_3 maximum yields in simulations of all experiments on this data base containing three or more different types of organics (Lurmann and Carter, 1989). In general, this and the previous version of the mechanism are able to predict maximum O_3 yields and rates of NO oxidation in most types of chamber experiments to within $\pm 30\%$, with variability in performance in simulations of individual runs being attributable, at least in part, to uncertainties in characterization of chamber effects (Carter *et al.*, 1986b). A publication described the testing of this and other recent mechanisms against these chamber data is in preparation.

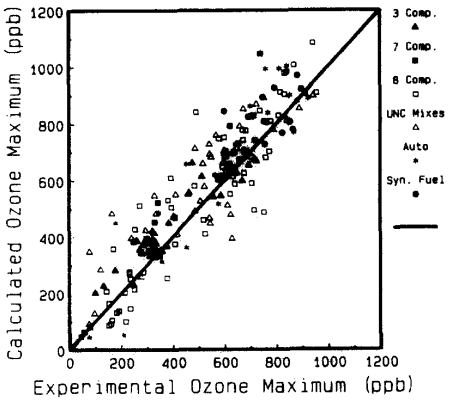

Fig. 1. Plot of experimental vs calculated ozone yields in simulations of organic mixture–NO_x–air environmental chamber experiments (from Lurmann and Carter, 1989).

LISTING OF THE MECHANISM

The detailed gas-phase atmospheric photochemical transformation mechanism is given in Tables 1–9. The species used explicitly in the mechanism are listed in Table 1, and their reactions and rate constant parameters are listed in Table 2. The absorption coefficients and quantum yields used in the photolysis reactions included in Table 2 are listed in Table 3. A set of generalized reactions with variable kinetic and mechanistic parameters are used to represent the reactions of individual alkane, aromatic, alkene (other than ethene) and other species. The types of parameters used for the alkane and aromatic species are summarized in Table 4, while those for the alkenes are summarized in Table 5. The kinetic and mechanistic parameters assigned for the individual alkanes and aromatics are given in Tables 6 and 7, respectively; the parameters assigned for alcohols, ethers and other miscellaneous species estimated to react with mechanisms similar to the alkanes are given in Table 8 and the parameters assigned for the alkenes are given in Table 9. Some of these detailed model species represent individual compounds, while others represent groups of compounds which are estimated to have similar reactivities. The tables documenting the mechanism include notes giving the sources of the rate constants and mechanistic assignments used. A discussion of the major features of this mechanism is given below.

DISCUSSION

The major features of the present mechanism are summarized in this section. The reports of Carter and co-workers (1986b, 1987, 1988a) should be consulted for details. A more complete discussion of the various portions of this mechanism and the treatments of the uncertain aspects of the chemistry cannot be given here because of space limitations.

Inorganic reactions

The inorganic reactions given in Table 2 are similar to those used in the other current atmospheric photochemical mechanisms (Lurmann *et al.*, 1986; Gery *et al.*, 1988), except that they were updated, primarily using the NASA (1987) evaluation. This update resulted in minor changes for a majority of the rate constants and for some of the absorption coefficients and quantum yields used in the photolysis reactions. In addition, several inorganic reactions which were neglected in the mechanisms of Atkinson *et al.* (1982) and Lurmann *et al.* (1986) were included in this mechanism to increase the range of conditions for which it is valid. These include (a) the explicit representation of the formation of ground state $O(^3P)$ oxygen atoms and the inclusion of its reactions (A3A and A3B) with NO_2; (b) the termolecular oxidation reaction (A7) of NO to NO_2; (c) the inclusion of reactions (A30A–A30D) between HO_2 and NO_3 and

Table 1. List of species in the detailed mechanism

No.	Name	Description
Active inorganic species*		
1	O3	Ozone
2	NO	Nitric oxide
3	NO2	Nitrogen dioxide
4	NO3	NO_3 radicals
5	N2O5	N_2O_5
6	HNO3	Nitric acid
7	HONO	Nitrous acid
8	HNO4	Peroxynitric acid
9	HO2.	HO_2 radicals
12	CO	Carbon monoxide
10	HO2H	Hydrogen peroxide
11	SO2	Sulphur dioxide
Active organic product species		
13	HCHO	Formaldehyde
14	CCHO	Acetaldehyde
15	PAN	Peroxy acetyl nitrate
16	RCHO	Propionaldehyde and lumped higher aldehydes
17	PPN	Peroxy propionyl nitrate and higher PAN analogues
18	ACET	Acetone
19	MEK	Methylethyl ketone and lumped higher ketones
20	RNO3	Lumped organic nitrates
21	GLY	Glyoxal
22	GPAN	PAN analogue formed from glyoxal
23	MGLY	Methyl glyoxal
24	PHEN	Phenol
25	CRES	Cresols and other alkyl phenols
26	BALD	Benzaldehyde and other aromatic aldehydes
27	PBZN	Peroxy benzoyl nitrate
28	NPHE	Nitrophenols and other aromatic nitro-compounds
29	AFG1	Unknown aromatic fragmentation product #1. (Formed from benzene, tetralin, and naphthalenes.)
30	AFG2	Unknown aromatic fragmentation product #2. (Formed from aromatics containing alkyl groups.)
31	–OOH	Chemical operator used to represent reactions at hydroperoxy groups
Active primary emitted species		
32	ETHE	Ethene
33+	AARn	*n*'th lumped group used to represent lumped alkanes and/or aromatics. (In general, there will be more than one such species.)
34+	OLEn	*n*'th lumped group used to represent lumped higher alkenes. (In general, there will be more than one such species.)
Active total peroxy radical species		
35	RO2.	Total alkyl peroxy radicals
36	RCO3.	Total peroxyacyl radicals
Product only species		
36	CO2	Carbon dioxide
37	H2SO4	Sulphuric acid
38	H2	Hydrogen
39	–C	"Lost carbon." Used to account for carbon balance.
40	–N	"Lost nitrogen ." Used to account for nitrogen balance. (Primarily represents C_1–C_3 organic nitrates and dinitrophenols, whose reactions are neglected.)
Steady state† inorganic species		
41	HO.	Hydroxyl radicals
42	O	Ground state oxygen atoms
43	O*1D2	Excited oxygen atoms
Steady state organic radical species		
44	HOCOO.	Intermediate formed in the $HCHO + HO_2$ reaction
45	CCO–O2.	Peroxy acetyl radicals
46	C2CO–O2.	Higher peroxyacyl radicals
47	BZ–CO–O2.	Peroxy benzoyl radicals
48	HCOCO–O2.	Peroxyacyl radical formed from glyoxal

Table 1. (*Contd.*)

No.	Name	Description
49	BZ–O.	Phenoxy radicals
50	BZ(NO2)–O.	Phenoxy-type radicals containing nitro-groups
Steady state chemical "operators"		
51	O3OL–SB	Chemical operator used to account for the oxidation of SO_2 by ozone–alkene reaction intermediates (This is a product-only species if reactions of SO_2 are removed from the mechanism.)
52	RO2–R.	Chemical operator used to represent NO to NO_2 Conversion with generation of HO_2 radicals
53	RO2–X.	Chemical operator used to represent NO consumption and alkyl nitrate formation
54	RO2–NP.	Chemical operator used to represent NO consumption and nitrophenol formation
55	RO2–XN.	Chemical operator used to represent NO sink reactions
56	R2O2.	Chemical operator used to represent extra NO to NO_2 conversions
Constant species		
57	O2	Oxygen
58	M	Air
59	HV	Light factor (1.0 = normal intensity)
60	H2O	Water

*"Active" species are those which undergo chemical reaction and for which the steady state approximation is not applied.

†"Steady state" species are those where the steady state approximation can be employed.

Table 2. List of reactions and rate constant parameters for the detailed reaction mechanism

Label*	Rate parameters† (*A*	E_a	*B*)	Reaction‡	Notes
Inorganic reactions					
A1	Phot Set = NO2			NO2 + HV = NO + O	1,2
A2	6.00E–34	0.0	−2.3	O + O2 + M = O3 + M	3
A3A	6.50E–12	−0.238	0.0	O + NO2 = NO + O2	3
A3B	See note 4			O + NO2 = NO3 + M	3,4
A4	2.00E–12	2.782	0.0	O3 + NO = NO2 + O2	3
A5	1.40E–13	4.968	0.0	O3 + NO2 = O2 + NO3	3
A6	1.70E–11	−0.298		NO + NO3 = #2 NO2	3
A7	3.30E–39	−1.050	0.0	NO + NO + O2 = #2 NO2	5
A8	See note 6			NO2 + NO3 = N2O5	3,6
A9	See note 7			N2O5 = NO2 + NO3	3,7
A10	1.00E–21	0.0	0.0	N2O5 + H2O = #2 HNO3	8
A11	2.50E–14	2.44	0.0	NO2 + NO3 = NO + NO2 + O2	9
A12A	Phot Set = NO3NO			NO3 + HV = NO + O2	10
A12B	Phot Set = NO3NO2			NO3 + HV = NO2 + O	10
A13A	Phot Set = O3O3P			O3 + HV = O + O2	11
A13B	Phot Set = O3O1D			O3 + HV = O*1D2 + O2	12
A14	2.20E–10	0.0	0.0	O*1D2 + H2O = #2 HO.	3
A15	1.92E–11	−0.251	0.0	O*1D2 + M = O + M	13
A16	See note 14			HO. + NO = HONO	3,14
A17	Phot Set = HONO			HONO + HV = HO. + NO	15
A18	See note 16			HO. + NO2 = HNO3	3, 16
A19	6.45E–15	−1.652	0.0	HO. + HNO3 = H2O + NO3	17
A20	(Ignored)			HNO3 + HV = HO. + NO2	18
A21	2.40E–13	0.0	0.0	HO. + CO = HO2. + CO2	19
A22	1.60E–12	1.87	0.0	HO. + O3 = HO2. + O2	3
A23	3.70E–12	−0.48	0.0	HO2. + NO = HO. + NO2	3
A24	See note 20			HO2. + NO2 = HNO4	3,20
A25	See note 21			HNO4 = HO2. + NO2	3,21
A26	(Ignored)			HNO4 + HV = products	18
A27	1.30E–12	−0.755	0.0	HNO4 + HO. = H2O + NO2 + O2	3
A28	1.10E–14	0.994	0.0	HO2. + O3 = HO. + #2 O2	3
A29A	2.20E–13	−1.23	0.0	HO2. + HO2. = HO2H + O2	22
A29A	1.90E–33	−1.95	0.0	HO2. + HO2. + M = HO2H + O2 + M	22
A29C	3.10E–34	−5.60	0.0	HO2. + HO2. + H2O = HO2H + O2 + H2O	22
A29D	6.60E–35	−6.32	0.0	HO2. + HO2. + H2O = HO2H + O2 + H2O	22

Table 2 (*Contd.*)

Label*	Rate parameters† (*A*	E_a	*B*)	Reaction‡	Notes
A30A	Same *k* as A29A			NO3 + HO2. = HNO3 + O2	23
A30B	Same *k* as A29B			NO3 + HO2. + M = HNO3 + O2 + M	23
A30C	Same *k* as A29C			NO3 + HO2. + H2O = HNO3 + O2 + H2O	23
A30A	Same *k* as A29D			NO3 + HO2. + H2O = HNO3 + O2 + H2O	23
A31	Phot Set = H2O2			HO2H + HV = #2 HO.	24
A32	3.30E–12	0.397	0.0	HO2H + HO. = HO2. + H2O	3
A33	4.60E–11	−0.457	0.0	HO. + HO2. = H2O + O2	3
Reactions of SO2					
SR1	See note 25			SO2 + HO. = HO2. + H2SO4	3,25
SR2	2.30E–17	0.0	0.0	O3OL–SB + H2O =	26
SR3	1.00E–13	0.0	0.0	O3OL–SB + SO2 = H2SO4	26
Lumped alkyl and acyl peroxy radical reactions					27
B1	4.20E–12	−0.360	0.0	RO2. + NO = NO	28
B2	5.10E–12	−0.397	0.0	RCO3. + NO = NO	28
B3	(Ignored)			RO2. + NO2 = NO2	29
B4	See note 30			RCO3. + NO2 = NO2	30
B5	3.40E–13	−1.590	0.0	RO2. + HO2. = HO2.	31
B6	3.40E–13	−1.590	0.0	RCO3. + HO2. = HO2.	31
B8	1.00E–15	0.0	0.0	RO2. + RO2. =	32
B9	1.86E–12	−1.053	0.0	RO2. + RCO3. =	33
B10	2.80E–12	−1.053	0.0	RCO3. + RCO3. =	34
Reactions of other peroxy radical operators					35
B11	Same *k* as B1			RO2–R. + NO = NO2 + HO2	36
B12	Same *k* as B5			RO2–R. + HO2. = –OOH	36,37
B13	Same *k* as B8			RO2–R. + RO2. = RO2. + #0.5 HO2.	36
B14	Same *k* as B9			RO2–R. + RCO3. = RCO3. + #0.5 HO2.	36
B19	Same *k* as B1			RO2–N. + NO = RNO3	38
B20	Same *k* as B5			RO2–N. + HO2. = –OOH + MEK + #1.5–C	37,38
B21	Same *k* as B8			RO2–N. + RO2. = RO2. + #0.5 HO2. + MEK + #1.5–C	38
B22	Same *k* as B9			RO2–N. + RCO3. = RCO3. + #0.5 HO2. + MEK + #1.5–C	38
G2	Same *k* as B1			RO2–NP. + NO = NPHE	39
G3	Same *k* as B5			RO2–NP. + HO2. = –OOH + #6–C	37,39
G4	Same *k* as B8			RO2–NP. + RO2. = RO2. + #0.5 HO2. + #6–C	39
G5	Same *k* as B9			RO2–NP. + RCO3. = RCO3. + HO2. + #6–C	39
B23	Same *k* as B1			RO2–XN. + NO = –N	40
B24	Same *k* as B5			RO2–XN. + HO2. = –OOH	37,40
B25	Same *k* as B8			RO2–XN. + RO2. = RO2. + #0.5 HO2.	40
B26	Same *k* as B9			RO2–XN. + RCO3. = RCO3. + HO2.	40
B15	Same *k* as B1			R2O2. + NO = NO2	41
B16	Same *k* as B5			R2O2. + HO2. =	37,41
B17	Same *k* as B8			R2O2. + RO2. = RO2.	41
B18	Same *k* as B9			R2O2. + RCO3. = RCO3.	41
Reactions of formaldehyde					
C1	Phot Set = HCHOAVGR			HCHO + HV = #2 HO2. + CO	42
C2	Phot Set = HCHOAVGM			HCHO + HV = H2 + CO	42
C3	1.13E–12	−1.288	2.0	HCHO + HO. = HO2. + CO + H2O	28
C4	9.70E–15	−1.242	0.0	HCHO + HO2. = HOCOO.	43
C4A	2.40E + 12	13.91	0.0	HOCOO. = HO2. + HCHO	43
C4B	Same *k* as B1			HOCOO. + NO = –C + NO2 + HO2.	43
C9	2.80E–12	5.00	0.0	HCHO + NO3 = HNO3 + HO2. + CO	44
Reactions of acetaldehyde and PAN					
C10	5.55E–12	−0.618	0.0	CCHO + HO. = CCO–O2. + H2O + RCO3.	28
C11A	Phot Set = CCHOR			CCHO + HV = CO + HO2. + HCHO + RO2–R. + RO2.	45
C11B	(Ignored)			CCHO + HV = CH4 + CO	45
C12	1.40E–12	3.696	0.0	CCHO + NO3 = HNO3 + CCO–O2. + RCO3.	28
C13	Same *k* as B2			CCO–O2. + NO = CO2 + NO2 + HCHO + RO2–R. + RO2.	46
C14	Same *k* as B4			CCO–O2. + NO2 = PAN	46
C15	Same *k* as B6			CCO–O2. + HO2. = –OOH + CO2 + HCHO	37,46
C16	Same *k* as B9			CCO–O2. + RO2. = RO2. + #0.5 HO2. + CO + HCHO	46
C17	Same *k* as B10			CCO–O2. + RCO3. = RCO3. + HO2. + CO2 + HCHO	46
C18	See note 47			PAN = CCO–O2. + NO2 + RCO3.	47

Table 2 (*Contd.*)

Label*	Rate parameters† (*A*	E_a	*B*)	Reaction‡	Notes
Reactions of propionaldehyde and PPN (also used for lumped higher aldehydes and lumped higher acyl peroxy nitrates)					
C25	8.50E-12	−0.50	0.0	RCHO + HO. = C2CO–O2. + RCO3.	48
C26	Phot Set = RCHO			RCHO + HV = CCHO + RO2–R. + RO2. + CO + HO2.	49
C27	1.40E-12	3.696	0.0	NO3 + RCHO = HNO3 + C2CO–O2. + RCO3.	50
C28	Same *k* as B2			C2CO–O2. + NO = CCHO + RO2–R. + CO2 + NO2 + RO2.	46
C29	8.40E-12	0.0	0.0	C2CO–O2. + NO2 = PPN	51
C30	Same *k* as B6			C2CO–O2. + HO2. = –OOH + CCHO + CO2	37, 46
C31	Same *k* as B9			C2CO–O2. + RO2. = RO2. + #0.5 HO2. + CCHO + CO2	46
C32	Same *k* as B10			C2CO–O2. + RCO3. = RCO3. + HO2. + CCHO + CO2	46
C33	1.60E + 17	27.966	0.0	PPN = C2CO–O2. + NO2 + RCO3.	28
Reactions of acetone					
C38	1.92E-13	−0.11	2.0	ACET + HO. = #0.8 "MGLY + RO2–R." + #0.2 "R2O2. + HCHO + CCO–O2. + RCO3." + RO2.	28, 52
C39	Phot Set = ACETONE			ACET + HV = CCO–O2. + HCHO + RO2–R. + RCO3. + RO2.	53
Reactions of methyl ethyl ketone and lumped higher ketones					
C44	2.92E-13	−0.823	2.0	MEK + HO. = H2O + #0.5 "CCHO + HCHO + CCO–O2. + C2CO–O2." + RCO3. + #1.5 "R2O2. + RO2."	54
C57	Phot Set = KETONE			MEK + HV = CCO–O2. + CCHO + RO2–R. + RCO3. + RO2.	55
Reactions of the lumped alkyl nitrate					
C95	2.19E-11	1.408	0.0	RNO3 + HO. = NO2 + #0.155 MEK + #1.05 RCHO + #0.48 CCHO + #0.16 HCHO + #0.11 –C + #1.39 "R2O2. + RO2."	56
Reactions of glyoxal and its PAN *analogue*					
C58A	Phot Set = GLYOXAL1			GLY + HV = #0.8 HO2. + #0.45 HCHO + #1.55 CO	57
C58B	Phot Set = GLYOXAL2			GLY + HV = #0.13 HCHO + #1.87 CO	58
C59	1.14E-11	0.0	0.0	GLY + HO. = #0.6 HO2. + #1.2 CO + #0.4 "HCOCO–O2. + RCO3."	59
C60	Same *k* as C12			GLY + NO3 = HNO3 + #0.6 HO2. + #1.2 CO + #0.4 "HCOCO–O2. + RCO3."	60
C62	Same *k* as B2			HCOCO–O2. + NO = NO2 + CO2 + CO + HO2.	46
C63	Same *k* as B4			HCOCO–O2. + NO2 = GPAN	46
C65	Same *k* as B6			HCOCO–O2. + HO2. = –OOH + CO2 + CO	37, 46
C66	Same *k* as B9			HCOCO–O2. + RO2. = RO2. + #0.5 HO2. + CO2 + CO	46
C67	Same *k* as B10			HCOCO–O2. + RCO3. = RCO3. + HO2. + CO2 + CO	46
C64	Same *k* as C18			GPAN = HCOCO–O2. + NO2 + RCO3.	61
Reactions of methyl glyoxal					
C68A	Phot Set = MEGLYOX1			MGLY + HV = HO2. + CO + CCO–O2. + RCO3.	62
C68B	Phot Set = MEGLYOX2			MGLY + HV = HO2. + CO + CCO–O2. + RCO3.	63
C69	1.72E-11	0.0	0.0	MGLY + HO. = CO + CCO–O2. + RCO3.	64
C70	Same *k* as C12			MGLY + NO3 = HNO3 + CO + CCO–O2. + RCO3.	60
Reactions of phenol					
G46	2.63E-11	0.0	0.0	HO. + PHEN = #0.15 RO2–NP. + #0.85 RO2–R. + #0.2 GLY + #4.7–C + RO2.	65
G51	3.60E-12	0.0	0.0	NO3 + PHEN = HNO3 + BZ–O.	28
Reaction of cresols and other alkylphenols					
G52	4.20E-11	0.0	0.0	HO. + CRES = #0.15 RO2–NP. + #0.85 RO2–R. + #0.2 MGLY + #5.5 –C + RO2.	66
G57	2.10E-11	0.0	0.0	NO3 + CRES = HNO3 + BZ–O. + –C	67
Reactions of benzaldehyde, PBzN *and analogous aromatic compounds*					
G30	1.29E-11	0.0	0.0	BALD + HO. = BZ–CO–O2. + RCO3.	28
G31	Phot Set = BZCHO			BALD + HV = #7 –C	68
G32	1.40E-12	3.747	0.0	BALD + NO3 = HNO3 + BZ–CO–O2. + RCO3.	69
G33	Same *k* as B2			BZ–CO–O2. + NO = BZ–O. + CO2 + NO2 + R2O2. + RO2.	46
G36	Same *k* as B6			BZ–CO–O2. + HO2. = –OOH + CO2 + PHEN	37, 46
G34	8.40E-12	0.0	0.0	BZ–CO–O2. + NO2 = PBZN	51
G37	Same *k* as B9			BZ–CO–O2. + RO2. = RO2 + #0.5 HO2. + CO2 + PHEN	46
G38	Same *k* as B10			BZ–CO–O2. + RCO3. = RCO3. + HO2. + CO2 + PHEN	46
G35	1.60E + 15	25.90	0.0	PBZN = BZ–CO–O2. + NO2 + RCO3.	70

Table 2 (*Contd.*)

Label*	Rate parameters† (*A*	E_a	*B*)	Reaction‡	Notes
Reactions of phenoxy radicals and nitrophenols					
G43	1.30E−11	−0.596	0.0	BZ–O. + NO2 = NPHE	71
G44	Same *k* as B5			BZ–O. + HO2. = PHEN	72
G45	1.00E−3	0.0	0.0	BZ–O. = PHEN	73
G58	3.60E−12	0.0	0.0	NPHE + NO3 = HNO3 + BZ(NO2)–O.	74
G59	Same *k* as G43			BZ(NO2)–O. + NO2. = #2 –N + #6 –C	75
G60	Same *k* as B5			BZ(NO2)–O. + HO2. = NPHE	75
G61	Same *k* as G45			BZ(NO2)–O. = NPHE	75
Reactions of the uncharacterized aromatic ring-opening product #1					
G7	1.14E−11	0.0	0.0	AFG1 = HCOCO–O2. + RCO3.	76, 77
G8	Phot Set = AROMUNK1			AFG1 + HV = HO2. + HCOCO–O2. + RCO3.	76, 78
Reactions of the uncharacterized aromatic ring-opening product #2					
G9	1.72E−11	0.0	0.0	HO. + AFG2 = C2CO–O2. + RCO3.	79, 80
G10	Phot Set = AROMUNK2			AFG2 + HV = HO2. + CO + CCO–O2. + RCO3.	79, 81
Reactions of the lumped hydroperoxide group					
B7	Phot Set = CO2H			–OOH + HV = HO2. + HO.	37, 82
B7A	1.18E−12	−0.254	0.0	HO. + –OOH = HO.	37, 83
B7B	1.79E−12	−0.435	0.0	HO. + –OOH = RO2–R. + RO2.	37, 83
Reactions of ethene					
D1	1.96E−12	−0.870	0.0	ETHE + HO. = #0.22 CCHO + #1.56 HCHO + RO2–R. + RO2.	28, 84
D6	1.20E−14	5.226	0.0	ETHE + O3 = HCHO + #0.37 O3OL–SB + #0.44 CO + #0.56 –C + #0.12 HO2.	26, 28, 85
D8	1.04E−11	1.574	0.0	ETHE + O = HCHO + CO + HO2. + RO2–R. + RO2.	86
D9	1.96E−12	5.413	0.0	ETHE + NO3 = NO2 + #2 HCHO + R2O2. + RO2.	85, 87
General alkane and aromatic reactions					
AnOH	See note 88			HO. + AARn = #AnRR RO2–R. + #AnNR RO2–N. + #AnXN RO2–XN. + #AnNP RO2–NP. + #AnRH HO2. + #AnR2 R2O2. + #AnRO2 RO2. + #AnAl HCHO + #AnA2 CCHO + #AnA3 RCHO + #AnK3 ACET + #AnK4 MEK + #AnCO CO + #AnC2 CO2 + #AnPH PHEN + #AnCR CRES + #AnBZ BALD + #AnGL GLY + #AnMG MGLY + #AnU1 AFG1 + AnU2 AFG2 + #AnXC –C	89
General alkene reactions					
OnOH	See note 89			OLEn + HO. = #OnP1R HCHO + #OnP2R CCHO + #OnP3R RCHO + #OnP4R ACET + #OnP5R MEK + #OnPR RO2–R. + #OnPN RO2–N. + RO2. + #OnOHXC –C	89
OnO3	See note 89			OLEn + O3 = #OnO3A1 HCHO + #OnO3A2 CCHO + #OnO3A3 RCHO + #OnO3K3 ACET + #OnO3K4 MEK + #OnO3MG MGLY + #OnO3CO CO + #OnO3SB O3OL–SB + #OnO3P1 CCO–O2. + #OnO3P2 C2CO–O2. + #OnO3RH HO2. + #OnO3OH HO. + #OnO3RR RO2–R. + #OnO3R2 R2O2. + #OnO3RO2 RO2. + #OnO3PS RCO3. + #OnO3XC –C	26, 89
OnOA	See note 89			OLEn + O = #0.4 HO2. + #0.5 "MEK + RCHO" + #OnOAXC –C	89
OnN3	See note 89			OLEn + NO3 = NO2 + #OnP1 HCHO + #OnP2 CCHO + #OnP3 RCHO + #OnP4 ACET + #OnP5 MEK + R2O2. + RO2. + #OnN3XC –C	89

*Reaction label notation of Carter *et al.* (1986b) and Carter (1988a) is employed.

†Except as indicated otherwise, rate constants for reactions in this table are given by the expression

$$k = A(T/300)^B \exp(-E_a/RT)$$

where k and A are in cm, molecule, s units, T is the temperature in K and R is 0.0019872 kcal deg^{-1} mole^{-1}. If a note is

Table 2 Footnote (*Contd.*)

referenced which indicates that the "falloff expression" is used, then the rate constant is both temperature and pressure dependent and is given by

$$k = [(k_0 \times M)/(1 + [k_0 \times M/k_\infty])] \times f^g$$

where

$$g = 1/[1 + (\log 10[k_0 \times M/k_\infty]/n)^2].$$

M is the pressure in molecules cm^{-3}. The notes for the reactions give the expressions for k_0 and k_∞. Unless indicated otherwise in the notes, $f = 0.6$ and $n = 1$.

‡If a number or symbol preceded by a "#" appears in the list of reaction products, then that number or symbol is a product yield coefficient. If no coefficient is given, then the yield is 1.0. If a product coefficient is given followed by a list of products enclosed by double quotes, then that coefficient gives the yields of all the products given in the list.

Documentation notes:

(1) Absorption cross-section and quantum yields for all photolysis reactions are listed in Table 3. See listing for the indicated "Photolysis Set."
(2) Absorption coefficients and quantum yields for NASA (1987).
(3) Recommendation of NASA (1987).
(4) Falloff expression used, where $k_0 = 9.0 \times 10^{-32}(T/300)^{-2.0}$ and $k_\infty = 2.2 \times 10^{-11}$.
(5) This reaction not listed by NASA (1987). Recommendation of Atkinson and Lloyd (1984) used.
(6) Falloff expression used where $k_0 = 2.2 \times 10^{-30}(T/300)^{-4.3}$ and $k_\infty = 1.5 \times 10^{-12}(T/300)^{-0.5}$.
(7) Rate constant given by $k(A9) = k(A8) \times 9.09 \times 10^{26} \exp(-22.26/RT)$.
(8) The $N_2O_5 + H_2O$ reaction is assumed to have both a homogeneous and heterogeneous component based on the results of Tuazon *et al.* (1983). Reaction (A10) represents the "homogeneous" component. The rate constant is derived from the rate of formation of gas-phase HNO_3 by Tuazon *et al.* (1983), and is strictly valid for 298 K only.
(9) This reaction not found in NASA (1987). Rate constant by Graham and Johnston (1978) used, as recommended by Atkinson and Lloyd (1984).
(10) The NO_3 absorption coefficients and quantum yields are based on the evaluation of Carter *et al.* (1986b). The absorption cross-sections used are based on the discussion of Atkinson and Lloyd (1984). The quantum yields used are those of Magnotta and Johnston (1980), divided by a factor of 1.5 to yield unit quantum yields at 580–590 nm. [The NASA (1987) recommendations could not be used because they give no absorption coefficients below 600 nm, and make no recommendation for the quantum yields.]
(11) The absorption coefficients for 280–320 nm are from Bass and Paur (1985), and those for >320 are those used by Carter *et al.* (1986b). The quantum yields were calculated from those used for the O(1D) path, assuming that the total quantum yield is 1.
(12) The absorption coefficients are from Bass and Paur (1985), and the quantum yields are those recommended by NASA (1987) for $T = 300$ K. The temperature dependence of the ozone photolysis reaction is ignored in this mechanism.
(13) The rate constants for air are based on $k = 1.8 \times 10^{-11} e^{110/T}$ for the N_2 reaction and $k = 3.2 \times 10^{-11} e^{70/T}$ for the O_2 reaction (NASA 1987), assuming M = 21% O_2 + 79% N_2.
(14) Falloff expression used where $k_0 = 7.0 \times 10^{-31}(T/300)^{-2.6}$, and $k_\infty = 1.5 \times 10^{-11}(T/300)^{-0.5}$.
(15) The absorption coefficients of Stockwell and Calvert (1978), which are consistent with the recommendation of NASA (1987), are used. Unit quantum yields are assumed.
(16) Falloff expression used where $k_0 = 2.6 \times 10^{-30}(T/300)^{-3.2}$ and $k_\infty = 2.4 \times 10^{-11}(T/300)^{-1.3}$.
(17) The rate constants were calculated for 1 atm and $T = 270$, 300 and 330 K, using the expression given by NASA (1987). A and E_a were calculated for using least squares. This rate constant expression is thus valid for 1 atm pressure only.
(18) The photolysis of nitric and peroxynitric acids are ignored in this mechanism.
(19) The rate constant for 1 atm pressure was calculated using the expression given by NASA (1987). The temperature dependence is assumed to be small.
(20) Falloff expression used where $k_0 = 1.8 \times 10^{-31}(T/300)^{-3.2}$ and $k_\infty = 4.7 \times 10^{-12}(T/300)^{-1.4}$.
(21) Rate constant given by $k(A25) = k(A24) \times 4.76 \times 10^{26} e^{-21.66/RT}$.
(22) The temperature, pressure and H_2O dependence used for this reaction is based on the data of Kircher and Sander (1984), as discussed by Carter *et al.* (1986b). [NASA (1987) does not give H_2O dependences.] Reaction (A29D) is based on $k = 2.7 \times 10^{-54} e^{6.32/RT}$ for $HO_2 + HO_2 + M + H_2O$, assuming 1 atm pressure.
(23) Assumed to have same rate constant and pressure and H_2O depencences as the $HO_2 + HO_2$ reaction.
(24) Absorption cross-section based on NASA (1987) recommendation. Unit quantum yields assumed.
(25) Falloff expression used where $k_0 = 3.0 \times 10^{-31}(T/300)^{-3.3}$ and $k_\infty = 1.5 \times 10^{-12}$.
(26) As discussed in the text, the chemical operator O3OL–SB is used to account for the oxidation of SO_2 by stabilized Criegee biradicals formed in the ozone + alkene reactions. This zero-carbon pseudo-species is formed in the mechanism whenever Criegee biradicals are stabilized. The rate constants for its reactions (with H_2O and SO_2) are based on those recommended by Atkinson (1990) for Criegee biradicals. The rate constant for the SO_2 reaction is unknown, and the arbitrary value assumed by Carter *et al.* (1986b) is used. The rate constant for the H_2O reaction is based on $k(.CH_2O_2. + H_2O)/k(.CH_2O_2. + SO_2) = 2.3 \times 10^{-4}$, from Suto *et al.* (1985), as given by Atkinson (1990). Atkinson (1990) recommends that the reactions of Criegee biradicals with NO and NO_2 can be neglected.
(27) As discussed in the text, RO2. and RCO3. are chemical "operators" which are used to represent the total peroxy radical concentrations for the purpose of determining branching ratios for $RO_2/RCO_3 + NO$, NO_2, HO_2 or peroxy reactions. Each reaction which forms an alkylperoxy radical is represented as forming an equal amount of "RO2.", and likewise for acyl peroxy radicals and "RCO_3.". Note that these operators have no mass and are not radicals; they are just used for the calculation of branching ratios. Thus, these "reactions" have no effect on any species other than RO2. or RCO3. themselves. The steady state approximation must not be used for these species, or the model will not operate properly under NO_x-free or light-free conditions.
(28) The rate constant expression for this reaction is based on the recommendation of Atkinson (1990).
(29) The reactions of alkyl peroxy radicals with NO_2 are ignored because of the rapid decomposition of the alkyl peroxynitrate back to reactants.
(30) Falloff expression used where $k_0 = 1.95 \times 10^{-28}(T/300)^{-4.0}$ and $k_\infty = 8.4 \times 10^{-12}$ and $f = 0.27$. This is derived using the

Table 2 Footnote (*Contd.*)

rate expression for $T=298$ K recommended by Atkinson *et al.* (1989b) for the reaction of NO_2 with acetyl peroxy radicals. The temperature dependence for k_0 is assumed to be the same as Atkinson *et al.* (1989b) recommended for $CH_3O_2+NO_2$.

(31) The rate constant expression is recommended by Atkinson (1990), based on data for the reactions of HO_2 with methyl and ethyl peroxy radicals. The HO_2 + acetyl peroxy radical reaction is assumed to have the same rate constant.

(32) See Carter *et al.* (1986b) for discussion of the choice of this rate constant, which is based on the approximate range of rate constants appropriate for secondary peroxy radicals. As discussed by Atkinson (1990), peroxy + peroxy radical rate constants can vary over orders of magnitude, but separate representation of each of the possible cross reactions would substantially increase the size and complexity of the mechanism without significantly affecting its major predictions. Test calculations discussed by Carter *et al.* (1986b) show that use of this approximation does not result in significant differences in results of simulations of propene + *n*-butane–NO_x–air mixtures compared with models including separate reactions of all these peroxy + peroxy reactions, with the appropriate rate constants for each. See text.

(33) Derived using the $T=289$ K rate constant for $CH_3O_2+CH_3C(O)O_2$, and the activation energies for $CH_3C(O)O_2+CH_3C(O)O_2$ recommended by Atkinson *et al.* (1989b).

(34) Based on the expression recommended by Atkinson *et al.* (1989b) for the self-reaction $CH_3C(O)O_2$.

(35) The chemical operators RO2–R., RO2–N., RO2–NP., RO2–XN. and R2O2. are used to represent net effects of reactions of individual peroxy radicals in the presence or absence of NO_x. These are discussed in detail by Lurmann *et al.* (1987) and Carter *et al.* (1987). The kinetics of their reactions are assumed to be the same as used for RO2., shown above. The steady state approximation can be used for all of these species.

(36) The operator RO2–R. is used to represent peroxy radical reactions where the net effect in the presence of NO_x is the conversion of NO to NO_2 and the generation of HO_2. In the absence of NO_x, the net effect is either reaction with HO_2 to form a hydroperoxide group or reaction with another peroxy radical. By analogy with the self-reaction of methyl peroxy radicals (see Atkinson, 1988), peroxy + peroxy radical reactions are assumed to react via a radical forming route half the time, with the radical formed being represented by HO_2. This operator is a zero carbon radical species.

(37) This mechanism does not represent the reactions of the organic hydroperoxides formed in peroxy + HO_2 reactions separately, but instead represents them, in effect, by the same set of organic species which would be formed if their precursor peroxy radicals reacted with NO, plus the zero-carbon lumped structure group "–OOH". This species is used to represent the effects of radical generation and NO to NO_2 conversions caused by photolysis or OH radical reactions at this group. This mechanism has –OOH being formed whenever a peroxy radical reacts with HO_2 to form an organic hydroperoxide. See text.

(38) The operator RO2–N. is a radical species which is used to represent peroxy radical reactions where the net effect in the presence of NO_x is reaction with NO to form alkyl nitrates, which are represented by RNO3. In the absence of NO_x, the net effect is either reaction with HO_2 to form a hydroperoxide group or reaction with another peroxy radical in a manner analgous to the reactions of RO2–R., above, except that this is a five-carbon operator (since RNO3 has five carbons). MEK + "lost carbon" is used to represent these carbons when these radicals react in the absence of NO_x.

(39) The operator RO2–NP. is exactly analogous to RO2–N. except it is used in aromatic mechanisms where nitrophenols are used to represent the product of the peroxy + NO reaction, rather than the lumped alkyl nitrate RNO3. It is a radical species with six carbons. The reactions of the product(s) formed when the radicals this represents react in the absence of NO_x are ignored, except for reactions of hydroperoxide groups.

(40) The operator RO2–XN. is analogous to RO2–N. and RO2–NP. except the reactions of the nitrogen-containing product formed when the radicals it represents react with NO are ignored. It is used primarily to represent the effects of formation of C_3 or smaller organic nitrates, which react slowly in the atmosphere. It is a zero-carbon radical species.

(41) The operator R2O2. is a zero-carbon, non radical species which is used to represent the net effect of the additional NO to NO_2 conversions resulting from multi-step photooxidation mechanisms involving second- and subsequent-generation peroxy radicals. Its destruction by 'reactions' with HO_2 or other peroxy radicals represents the fact that when peroxy radicals react via these routes, the additional NO to NO_2 conversions in multi-step mechanisms do not take place.

(42) The formaldehyde cross-section values were derived by averaging 1 nm values derived by Jeffries (University of North Carolina, private communication, 1988) from the data of Bass *et al.* (1980) and Moortgat *et al.* (1983). Averaging these data is recommended by NASA (1987), but their data lack adequate resolution. The quantum yields are derived from those tabulated by NASA (1987) in 10 nm intervals. Data between 10 nm intervals were obtained by interpolating the tabulated 10 nm average values.

(43) The mechanism and rate constants used for the $HCHO+HO_2$ reactions are those recommended by Atkinson *et al.* (1989b). The reactions of the formic acid expected to be formed are ignored. –C is given as the product to indicate that the carbon in formic acid is 'lost'. Note that the rate constant for reaction (C4B) is assumed to be the same as used for other peroxy radical + NO reactions in the mechanism.

(44) The Arrhenius parameters for this reaction were derived based on the NASA (1987) and Atkinson *et al.* (1989b) recommendation of $k=6.0\times10^{-16}$ for $T=298$ K and an estimated A of 2.8×10^{-12}, which is 2× the A for NO_3 + acetaldehyde recommended by Atkinson (1990).

(45) Absorption coefficients and quantum yields for acetaldehyde are those recommended by Baulch *et al.* (1984). Values used are also tabulated by Atkinson (1988). The photolysis route forming molecular products has no significant effect on model predictions and is ignored.

(46) Except as noted, all acyl peroxy radical reactions are assumed to have the same rate constants as used for the lumped peroxy radical species RCO3.

(47) Falloff expression used where $k_0=6.30\times10^{-2}e^{-25.406/RT}$, $k_\infty=2.20\times10^{16}e^{-26.698/RT}$ and $f=0.27$. This rate constant expression is recommended by Atkinson *et al.* (1989b).

(48) Rate constant for $T=298$ K recommended by Atkinson (1990). Temperature dependence estimated by Carter *et al.* (1986b) assumed.

(49) The absorption coefficients used are from Calvert and Pitts (1966). The quantum yields based on the data of Heicklen *et al.* (1986).

(50) Assumed to react with the same kinetics as used for NO_3 + acetaldehyde.

(51) The high pressure limit recommended by Atkinson (1990) for the acetyl peroxy + NO_2 rate constant is used for the corresponding reaction of propionyl and benzoyl peroxy radicals. Note that using different rate constants for the NO_2

Table 2 Footnote (*Contd.*)

reactions of the RCO_3's results in a slight inaccuracy in the calculation of the total RCO_3 levels. However, this should be minor, especially if most of the RCO_3 is $CCO\text{–}O_2$.

(52) Mechanism is based on $CH_3\text{–}CO\text{–}CH_2\text{–}O\cdot$ branching ratio estimates given by Atkinson (1990).

(53) The absorption coefficients for acetone were taken from the data base developed for the RADM model (NCAR, 1987), provided by Stockwell (1988). They are consistent with the values tabulated in Calvert and Pitts (1966). The quantum yields are based on those of Meyrahn *et al.* (1986), as recommended by Atkinson *et al.* (1989b).

(54) Kinetic parameters recommended by Atkinson (1990). The mechanism used is that assumed by Carter *et al.* (1986a).

(55) The absorption coefficients used for MEK are from Calvert and Pitts (1966). The overall MEK quantum yield of 0.1 was derived based on fits to UNC chamber data as determined by Carter *et al.* (1986b).

(56) The OH + lumped alkyl nitrate mechanism consists of the average of the reactions of the lumped C4 nitrate and the lumped C7 nitrate used in the mechanism of Carter *et al.* (1986b). These reactions, given in terms of the species in the present mechanism, are as follows:

C4ONO2 + HO· = NO2 + #.2 MEK + #.96 CCHO + #.32 "HCHO + RCHO" + #1.12 "R2O2· + RO2·"

C7ONO2 + HO· = NO2 + #.11 MEK + #.1.78 RCHO + #1.22 –C + #1.66 "R2O2· + RO2·"

with $k = 2.0 \times 10^{-11} e^{-2.018/RT}$ and $3.00 \times 10^{-11} e^{-1.289/RT}$, respectively. The Arrhenius parameters for the lumped reaction were determined from their calculated rate constants at 270, 300 and 330 K. Note that the lumped alkyl nitrate species in this mechanism is represented as having five carbons, not 5.5 as would be the case for the average of C4ONO2 and C7ONO2.

(57) Reaction (C58A) refers to photolysis at the shorter wavelength band. The quantum yields are based on data of Langford and Moore (1984), and references therein. The absorption coefficients are from Plum *et al.* (1983). See text.

(58) Reaction (C58B) refers to photolysis at the longer wavelength band. The quantum yields and absorption coefficients are from Plum *et al.* (1983).

(59) Rate constant and product yields recommended by Atkinson (1988).

(60) Assumed to have the same kinetics as NO_3 + acetaldehyde. Assumed to have the same analogous mechanism as the OH radical reaction.

(61) This is assumed to have the same kinetics as the decomposition of PAN.

(62) Reaction (C68a) represents photolysis of methyl glyxoal in the shorter wavelength region. Quantum yields are assumed to be unity by analogy with photolysis of glyoxal at the low wavelength region. Absorption coefficients are from Plum *et al.* (1983).

(63) Reaction (C68B) represents photolysis at the longer wavelength region. Quantum yields and absorption coefficients are based on the data of Plum *et al.* (1983).

(64) Rate constant recommended by Atkinson (1990). The initially formed $CH_3\text{–}CO\text{–}CO\cdot$ radical is estimated to decompose rapidly to $CO + CH_3CO$.

(65) Rate constant recommended by Atkinson (1990). The mechanism is assumed to be analogous to the empirical mechanism derived for *o*-cresol (see note 66).

(66) The rate constant used is that recommended by Atkinson (1990) for *o*-cresol. The mechanism for the reaction of OH radicals with phenolic compounds is unknown, and is not represented explicitly. The empirical mechanism used is that derived by Carter *et al.* (1986b) based on model simulations of the *o*-cresol–NO_x–air chamber run EC–281 (Atkinson *et al.*, 1980). To fit the data in that run, it is assumed to proceed via a radical propagating and radical terminating path, with the amount of termination being adjusted to be 0.15, in order to fit the reactivity observed in that run. In addition, assuming a methyglyoxal yield of 0.8 allows the PAN yields observed in run EC–281 to be fit. Reactions of other products formed are neglected. See text.

(67) Rate constant recommended by Atkinson (1990) for *o*-cresol.

(68) Absorption coefficients from the data of Majer *et al.* (1969) for benzaldehyde in *n*-hexane. They must be considered to be only qualitative in nature, though they are not as uncertain as the quantum yields. The overall quantum yield of 0.05 was adjusted to fit the benzaldehyde consumption rate observed in toluene + benzaldehyde runs EC–337 and EC–339 (Pitts *et al.*, 1979). The quantum yield is assumed to be independent of wavelength, because no data concerning its wavelength dependence are available. The products formed from benzaldehyde photolysis are unknown, except that both radical formation and benzene formation appear to be minor. It is assumed that the benzaldehyde photooxidation products are unreactive.

(69) Kinetics estimated based on 298 K rate constant given by Atkinson (1990), and assuming the *A* factor is the same as for the reaction of NO_3 + acetaldehyde.

(70) Rate expression based on data of Kenley and Hendry (1982).

(71) This is based on the general recommendation for Atkinson (1990) for alkoxy + NO_2 reactions at the high pressure limit.

(72) This is assumed to react with the same rate constant as used for peroxy + HO_2 reactions (see below), and to form phenol + O_2.

(73) This reaction is included to avoid problems if BZ–O· is ever formed under conditions where HO_2 and NO_2 are very low (which is considered to be unlikely under most reasonable conditions), and can be considered to represent its reaction with organics present. The rate constant is arbitrary, and is such that this process becomes significant only if $[NO_2] \lesssim 3 \times 10^{-6}$ ppm and $[HO_2] < 1 \times 10^5$ ppm.

(74) This reaction is assumed to have the same rate constant as the analogous reaction of phenol. Reaction of nitrophenols with NO_3 is assumed to dominate over reaction with OH radicals, so the latter is ignored.

(75) These reactions are assumed to be analogous to the corresponding reactions of phenoxy radicals (BZ–O). The di-nitro compound formed in reaction G59 is assumed to condense into the aerosol phase, and thus its gas-phase reactions are ignored.

(76) This pseudo-species AFG1 is used to represent the contribution of uncharacterized aromatic ring-opening products to the overall reactivity of benzene, naphthalene and other aromatics which do not have alkyl groups. Its reactions are assumed to be like glyoxal, that is, it photolyzes more rapidly to form radicals, and photolyzes primarily at lower wavelengths. Its yield in the reactions of the parent compound are adjusted to fit overall reactivity observed in the aromatic–NO_x–air runs.

(77) Assumed to have the same rate constant as used for glyoxal. The mechanism is essentially arbitrary, but formation of a

Table 2 Footnote (*Contd.*)

PAN analogue tends to result in somewhat better predictions of maximum ozone yields in aromatic systems, and is analogous to what is assumed for uncharacterized ring fragmentation products in other mechanisms. The glyoxal PAN analogoue is used to avoid the predicted formation of PAN in systems where no alkyl groups are present.

(78) The rate of this photolysis is essentially arbitrary, though it is assumed to be rapid to simulate results of benzene–NO_x–air irradiations. It is arbitrarily assumed to be 10 times slower than the analogous photolysis of AFG2, the alkyl-containing uncharacterized aromatic ring fragmentation product. The spectral response for the photolysis of both AFG1 and AFG2 is adjusted so the same mechanism can fit the results of aromatic–NO_x–air runs carried out in the SAPRC indoor Teflon chamber (ITC) with blacklight irradiation as in the SAPRC evacuable chamber with solar simulator irradiation. See Carter *et al.* (1987).

(79) The pseudo-species AFG2 is used to represent the contribution of uncharacterized aromatic ring-opening products to the overall reactivity of toluene, xylenes, alkyl naphthalenes and other aromatic compounds with alkyl side groups. Its reactions are assumed to be like methyl glyoxal, except that it photolyzes more rapidly and primarily at lower wavelengths. Its yield in the reactions of the parent compound are adjusted to fit overall reactivity observed in the aromatic–NO_x–air runs.

(80) The rate constant for the corresponding reaction of methyl glyoxal is used. PPN is used to represent the PAN analogus which are assumed to be formed from these uncharacterized products. This is consistent with the use of PPN to represent all the higher PAN analogues, other than those which are explicitly represented.

(81) The photolysis rate of this reaction is essentially arbitrary, except that it must be assumed to be rapid to fit the results of aromatic–NO_x–air irradiations carried out in the SAPRC ITC, and that the spectral response of the photolysis reaction is derived from simulations of runs carried out in the SAPRC EC and ITC, as discussed above for AFG1. It is assumed to have the same mechanism as the photolysis of methyl glyoxal.

(82) The absorption coefficients used for the lumped hydroperoxide group are those measured by Molina and Arguello (1979) for methyl hydroperoxide, as recommended by NASA (1987). Quantum yields of unity are assumed.

(83) The rate constant for the reactions of OH radicals at the hydroperoxide group are based on data of Niki *et al.* (1983) and Vaghjani and Ravishankara (1989) for methyl hydroperoxide, as discussed by Atkinson (1990). Reaction (B7A) represents the processes where OH abstracts from the carbon alpha to the –OOH group, which is followed by formation of OH and the corresponding carbonyl, e.g.

$$OH + CH_3OOH \rightarrow H_2O + .CH_2OOH$$

$$.CH_2OOH \rightarrow HCHO + OH.$$

Reaction (B7B) represents the process where OH abstracts from the –OOH group, resulting in the formation of the corresponding peroxide. Reaction at other sites is ignored, since the –OOH group is probably preserved in those cases, and their reactions are represented by the reactions of the species used to represent the carbon-containing portion of the hydroperoxide.

(84) Product yields are based on data of Niki *et al.* (1981). Acetaldehyde is used to represent the glycolaldehyde formed in this reaction.

(85) The mechanism used is consistent with the generalized alkene mechanism discussed in the text.

(86) The rate expression and mechanism are based on recommendations of Atkinson and Lloyd (1984). This is the same as used by Carter *et al.* (1986). The ketene + H_2 pathway is ignored.

(87) The $T = 298$ K rate constant is based on the recommendation of Atkinson (1989). The Arrhenius A factor is assumed to be the same as the OH + ethene reaction.

(88) This generalized reaction is included for each generalized species AARn, where $n = 1, 2$, etc. These are used to represent one or more alkane, aromatic or other species in the mechanism which reacts significantly only with hydroxyl radicals. The values of the OH radical rate constant and the mechanistic parameters are determined by the individual compound, or group of compounds, which AARn represents. The mechanistic parameters used in this generalized alkane/aromatic reaction are listed and described in Table 4, and the values of the parameters used for individual species are given in Tables 6–8. Some of the product yield parameters in this reaction are determined from the assigned values for the other parameters as indicated in Table 4. The derivation of the parameters for the alkane, aromatic and other species represented by AARn is described in the text.

(89) These generalized reactions are included for each generalized species OLEn (where $n = 1$, 2, etc.), which are used to represent one or more nonethane alkene species. The values of the rate constants and the mechanistic parameters for these generalized reactions are determined by those for the compound or compounds being represented. The mechanistic and product yield parameters used in these generalized reactions are described in Table 5. Most of the product yield parameters depend on the alkane structural parameters $p_1, \ldots, p_5$, and (for the OH radical reactions) the nitrate yield parameter, p_N, as indicated in Table 5. The chemical principles and estimates behind the derivation of the relationships between the product yield parameters and the structural parameters for the various alkene reactions are described in the text. The values of the rate constants, structural parameters and nitrate yield parameters for the individual nonethene alkene species are listed in Table 9.

(d) the reaction (A33) of OH radicals with HO_2. The reactions of $O(^3P)$ atoms with NO_2 and the thermal oxidation of NO can be important under relatively high NO_x conditions in many environmental chamber experiments, in fossil-fueled power plant plumes and, perhaps, urban NO_x source areas under high pollution conditions. The reaction of HO_2 with NO_3 may be important under conditions of low (but not totally depleted) NO_x and at night-time. The inclusion of the OH + HO_2 reaction affects the predictions of H_2O_2 levels, an important aspect of acid deposition models (NCAR, 1987). In addition, the explicit inclusion of $O(^3P)$ atom formation permits its reactions with alkenes to be included; these are non-negligible radical sources in some of the environmental chamber experiments used to evaluate the mechanism (Carter *et al.*, 1986b). Although there are many conditions where the inclusion of these reactions have negligible effects on

Table 3. Tabulation of absorption coefficients and quantum yields for all photolysis reactions in the detailed mechanism*

WL (nm)	Abs (cm^2)	QY	WL (nm)	Abs (cm^2)	QY	WL (nm)	Abs (cm^2)	QY
Photolysis file = NO2								
250.0	2.83E-20	1.000	255.0	1.45E-20	1.000	260.0	1.90E-20	1.000
265.0	2.05E-20	1.000	270.0	3.13E-20	1.000	275.0	4.02E-20	1.000
280.0	5.54E-20	1.000	285.0	6.99E-20	1.000	290.0	8.18E-20	0.999
295.0	9.67E-20	0.998	300.0	1.17E-19	0.997	305.0	1.66E-19	0.996
310.0	1.76E-19	0.995	315.0	2.25E-19	0.994	320.0	2.54E-19	0.993
325.0	2.79E-19	0.992	330.0	2.99E-19	0.991	335.0	3.45E-19	0.990
340.0	3.88E-19	0.989	345.0	4.07E-19	0.988	350.0	4.10E-19	0.987
355.0	5.13E-19	0.986	360.0	4.51E-19	0.984	365.0	5.78E-19	0.983
370.0	5.42E-19	0.981	375.0	5.35E-19	0.979	380.0	5.99E-19	0.975
381.0	5.98E-19	0.974	382.0	5.97E-19	0.973	383.0	5.96E-19	0.972
384.0	5.95E-19	0.971	385.0	5.94E-19	0.969	386.0	5.95E-19	0.967
387.0	5.96E-19	0.966	388.0	5.98E-19	0.964	389.0	5.99E-19	0.962
390.0	6.00E-19	0.960	391.0	5.98E-19	0.959	392.0	5.96E-19	0.957
393.0	5.93E-19	0.953	394.0	5.91E-19	0.950	395.0	5.89E-19	0.942
396.0	6.06E-19	0.922	397.0	6.24E-19	0.870	398.0	6.41E-19	0.820
399.0	6.59E-19	0.760	400.0	6.76E-19	0.695	401.0	6.67E-19	0.635
402.0	6.58E-19	0.560	403.0	6.50E-19	0.485	404.0	6.41E-19	0.425
405.0	6.32E-19	0.350	406.0	6.21E-19	0.290	407.0	6.10E-19	0.225
408.0	5.99E-19	0.185	409.0	5.88E-19	0.153	410.0	5.77E-19	0.130
411.0	5.88E-19	0.110	412.0	5.98E-19	0.094	413.0	6.09E-19	0.083
414.0	6.19E-19	0.070	415.0	6.30E-19	0.059	416.0	6.29E-19	0.048
417.0	6.27E-19	0.039	418.0	6.26E-19	0.030	419.0	6.24E-19	0.023
420.0	6.23E-19	0.018	421.0	6.18E-19	0.012	422.0	6.14E-19	0.008
423.0	6.09E-19	0.004	424.0	6.05E-19	0.000	425.0	6.00E-19	0.000
Photolysis file = NO3NO								
585.0	2.77E-18	0.000	590.0	5.14E-18	0.250	595.0	4.08E-18	0.400
600.0	2.83E-18	0.250	605.0	3.45E-18	0.200	610.0	1.48E-18	0.200
615.0	1.96E-18	0.100	620.0	3.58E-18	0.100	625.0	9.25E-18	0.050
630.0	5.66E-18	0.050	635.0	1.45E-18	0.030	640.0	1.11E-18	0.000
Photolysis file = NO3NO2								
400.0	0.00E-01	1.000	405.0	3.00E-20	1.000	410.0	4.00E-20	1.000
415.0	5.00E-20	1.000	420.0	8.00E-20	1.000	425.0	1.00E-19	1.000
430.0	1.30E-19	1.000	435.0	1.80E-19	1.000	440.0	1.90E-19	1.000
445.0	2.20E-19	1.000	450.0	2.80E-19	1.000	455.0	3.30E-19	1.000
460.0	3.70E-19	1.000	465.0	4.30E-19	1.000	470.0	5.10E-19	1.000
475.0	6.00E-19	1.000	480.0	6.40E-19	1.000	485.0	6.90E-19	1.000
490.0	8.80E-19	1.000	495.0	9.50E-19	1.000	500.0	1.01E-18	1.000
505.0	1.10E-18	1.000	510.0	1.32E-18	1.000	515.0	1.40E-18	1.000
520.0	1.45E-18	1.000	525.0	1.48E-18	1.000	530.0	1.94E-18	1.000
535.0	2.04E-18	1.000	540.0	1.81E-18	1.000	545.0	1.81E-18	1.000
550.0	2.36E-18	1.000	555.0	2.68E-18	1.000	560.0	3.07E-18	1.000
565.0	2.53E-18	1.000	570.0	2.54E-18	1.000	575.0	2.74E-18	1.000
580.0	3.05E-18	1.000	585.0	2.77E-18	1.000	590.0	5.14E-18	0.750
595.0	4.08E-18	0.600	600.0	2.83E-18	0.550	605.0	3.45E-18	0.400
610.0	1.45E-18	0.300	615.0	1.96E-18	0.250	620.0	3.58E-18	0.200
625.0	9.25E-18	0.150	630.0	5.66E-18	0.050	635.0	1.45E-18	0.000
Photolysis file = O3O3P								
280.0	3.97E-18	0.100	281.0	3.60E-18	0.100	282.0	3.24E-18	0.100
283.0	3.01E-18	0.100	284.0	2.73E-18	0.100	285.0	2.44E-18	0.100
286.0	2.21E-18	0.100	287.0	2.01E-18	0.100	288.0	1.76E-18	0.100
289.0	1.58E-18	0.100	290.0	1.41E-18	0.100	291.0	1.26E-18	0.100
292.0	1.10E-18	0.100	293.0	9.89E-19	0.100	294.0	8.59E-19	0.100
295.0	7.70E-19	0.100	296.0	6.67E-19	0.100	297.0	5.84E-19	0.100
298.0	5.07E-19	0.100	299.0	4.52E-19	0.100	300.0	3.92E-19	0.100
301.0	3.42E-19	0.100	302.0	3.06E-19	0.100	303.0	2.60E-19	0.100
304.0	2.37E-19	0.100	305.0	2.01E-19	0.112	306.0	1.79E-19	0.149
307.0	1.56E-19	0.197	308.0	1.38E-19	0.259	309.0	1.25E-19	0.339
310.0	1.02E-19	0.437	311.0	9.17E-20	0.546	312.0	7.88E-20	0.652
313.0	6.77E-20	0.743	314.0	6.35E-20	0.816	315.0	5.10E-20	0.872
316.0	4.61E-20	0.916	317.0	4.17E-20	0.949	318.0	3.72E-20	0.976
319.0	2.69E-20	0.997	320.0	3.23E-20	1.000	330.0	6.70E-21	1.000
340.0	1.70E-21	1.000	350.0	4.00E-22	1.000	355.0	0.00E-01	1.000
400.0	0.00E-01	1.000	450.0	1.60E-22	1.000	500.0	1.34E-21	1.000

Table 3. (*Contd.*)

WL (nm)	Abs (cm^2)	*QY*	WL (nm)	Abs (cm^2)	*QY*	WL (nm)	Abs (cm^2)	*QY*
550.0	3.32E-21	1.000	600.0	5.06E-21	1.000	650.0	2.45E-21	1.000
700.0	8.70E-22	1.000	750.0	3.20E-22	1.000	800.0	1.60E-22	1.000
900.0	0.00E-01	1.000						
Photolysis file = O3O1D								
280.0	3.97E-18	0.900	281.0	3.60E-18	0.900	282.0	3.24E-18	0.900
283.0	3.01E-18	0.900	284.0	2.73E-18	0.900	285.0	2.44E-18	0.900
286.0	2.21E-18	0.900	287.0	2.01E-18	0.900	288.0	1.76E-18	0.900
289.0	1.58E-18	0.900	290.0	1.41E-18	0.900	291.0	1.26E-18	0.900
292.0	1.10E-18	0.900	293.0	9.89E-19	0.900	294.0	8.59E-19	0.900
295.0	7.70E-19	0.900	296.0	6.67E-19	0.900	297.0	5.84E-19	0.900
298.0	5.07E-19	0.900	299.0	4.52E-19	0.900	300.0	3.92E-19	0.900
301.0	3.42E-19	0.900	302.0	3.06E-19	0.900	303.0	2.60E-19	0.900
304.0	2.37E-19	0.900	305.0	2.01E-19	0.888	306.0	1.79E-19	0.851
307.0	1.56E-19	0.803	308.0	1.38E-19	0.741	309.0	1.25E-19	0.661
310.0	1.02E-19	0.563	311.0	9.17E-20	0.454	312.0	7.88E-20	0.348
313.0	6.77E-20	0.257	314.0	6.35E-20	0.184	315.0	5.10E-20	0.128
316.0	4.61E-20	0.084	317.0	4.17E-20	0.051	318.0	3.72E-20	0.024
319.0	2.69E-20	0.003	320.0	3.23E-20	0.000			
Photolysis file = HONO								
311.0	0.00E-01	1.000	312.0	2.00E-21	1.000	313.0	4.20E-21	1.000
314.0	4.60E-21	1.000	315.0	4.20E-21	1.000	316.0	3.00E-21	1.000
317.0	4.60E-21	1.000	318.0	3.60E-20	1.000	319.0	6.10E-20	1.000
320.0	2.10E-20	1.000	321.0	4.27E-20	1.000	322.0	4.01E-20	1.000
323.0	3.93E-20	1.000	324.0	4.01E-20	1.000	325.0	4.04E-20	1.000
326.0	3.13E-20	1.000	327.0	4.12E-20	1.000	328.0	7.55E-20	1.000
329.0	6.64E-20	1.000	330.0	7.29E-20	1.000	331.0	8.70E-20	1.000
332.0	1.38E-19	1.000	333.0	5.91E-20	1.000	334.0	5.91E-20	1.000
335.0	6.45E-20	1.000	336.0	5.91E-20	1.000	337.0	4.58E-20	1.000
338.0	1.91E-19	1.000	339.0	1.63E-19	1.000	340.0	1.05E-19	1.000
341.0	8.70E-20	1.000	342.0	3.35E-19	1.000	343.0	2.01E-19	1.000
344.0	1.02E-19	1.000	345.0	8.54E-20	1.000	346.0	8.32E-20	1.000
347.0	8.20E-20	1.000	348.0	7.49E-20	1.000	349.0	7.13E-20	1.000
350.0	6.83E-20	1.000	351.0	1.74E-19	1.000	352.0	1.14E-19	1.000
353.0	3.71E-19	1.000	354.0	4.96E-19	1.000	355.0	2.46E-19	1.000
356.0	1.19E-19	1.000	357.0	9.35E-20	1.000	358.0	7.78E-20	1.000
359.0	7.29E-20	1.000	360.0	6.83E-20	1.000	361.0	6.90E-20	1.000
362.0	7.32E-20	1.000	363.0	9.00E-20	1.000	364.0	1.21E-19	1.000
365.0	1.33E-19	1.000	366.0	2.13E-19	1.000	367.0	3.52E-19	1.000
368.0	4.50E-19	1.000	369.0	2.93E-19	1.000	370.0	1.19E-19	1.000
371.0	9.46E-20	1.000	372.0	8.85E-20	1.000	373.0	7.44E-20	1.000
374.0	4.77E-20	1.000	375.0	2.70E-20	1.000	376.0	1.90E-20	1.000
377.0	1.50E-20	1.000	378.0	1.90E-20	1.000	379.0	5.80E-20	1.000
380.0	7.78E-20	1.000	381.0	1.14E-19	1.000	382.0	1.40E-19	1.000
383.0	1.72E-19	1.000	384.0	1.99E-19	1.000	385.0	1.90E-19	1.000
386.0	1.19E-19	1.000	387.0	5.65E-20	1.000	388.0	3.20E-20	1.000
389.0	1.90E-20	1.000	390.0	1.20E-20	1.000	391.0	5.00E-21	1.000
392.0	0.00E-01	1.000						
Photolysis file = H2O2								
250.0	8.30E-20	1.000	255.0	6.70E-20	1.000	260.0	5.20E-20	1.000
265.0	4.20E-20	1.000	270.0	3.20E-20	1.000	275.0	2.50E-20	1.000
280.0	2.00E-20	1.000	285.0	1.50E-20	1.000	290.0	1.13E-20	1.000
295.0	8.70E-21	1.000	300.0	6.60E-21	1.000	305.0	4.90E-21	1.000
310.0	3.70E-21	1.000	315.0	2.80E-21	1.000	320.0	2.00E-21	1.000
325.0	1.50E-21	1.000	330.0	1.20E-21	1.000	335.0	9.00E-22	1.000
340.0	7.00E-22	1.000	345.0	5.00E-22	1.000	350.0	3.00E-22	1.000
355.0	0.00E-01	1.000						
Photolysis file = HCHOAVGR								
281.0	1.62E-20	0.602	282.0	9.77E-21	0.614	283.0	5.96E-21	0.626
284.0	3.31E-20	0.638	285.0	4.09E-20	0.650	286.0	2.42E-20	0.662
287.0	1.22E-20	0.674	288.0	2.19E-20	0.686	289.0	3.14E-20	0.698
290.0	1.54E-20	0.710	291.0	1.49E-20	0.717	292.0	9.59E-21	0.724
293.0	3.22E-20	0.731	294.0	5.45E-20	0.738	295.0	4.07E-20	0.745
296.0	2.41E-20	0.752	297.0	1.79E-20	0.759	298.0	3.16E-20	0.766
299.0	2.81E-20	0.773	300.0	1.14E-20	0.780	301.0	1.27E-20	0.779

Table 3. (*Contd.*)

WL (nm)	Abs (cm^2)	QY	WL (nm)	Abs (cm^2)	QY	WL (nm)	Abs (cm^2)	QY
Photolysis file = HCHOAVGR (*Contd.*)								
302.0	1.21E-20	0.778	303.0	2.78E-20	0.777	304.0	5.40E-20	0.776
305.0	5.30E-20	0.775	306.0	4.13E-20	0.774	307.0	2.23E-20	0.773
308.0	1.77E-20	0.772	309.0	2.43E-20	0.771	310.0	2.00E-20	0.770
311.0	9.15E-21	0.755	312.0	1.05E-20	0.740	313.0	1.43E-20	0.725
314.0	3.07E-20	0.710	315.0	4.05E-20	0.695	316.0	3.29E-20	0.680
317.0	3.77E-20	0.665	318.0	3.10E-20	0.650	319.0	1.22E-20	0.635
320.0	1.26E-20	0.620	321.0	1.48E-20	0.589	322.0	7.70E-21	0.558
323.0	4.66E-21	0.527	324.0	7.11E-21	0.496	325.0	1.51E-20	0.465
326.0	3.90E-20	0.434	327.0	3.50E-20	0.403	328.0	1.49E-20	0.372
329.0	2.30E-20	0.341	330.0	3.05E-20	0.310	331.0	1.43E-20	0.279
332.0	4.22E-21	0.248	333.0	2.01E-21	0.217	334.0	1.66E-21	0.186
335.0	9.68E-22	0.155	336.0	1.57E-21	0.124	337.0	3.27E-21	0.093
338.0	1.38E-20	0.062	339.0	3.18E-20	0.031	340.0	2.39E-20	0.000
Photolysis file = HCHOAVGM								
281.0	1.62E-20	0.341	282.0	9.77E-21	0.332	283.0	5.96E-21	0.323
284.0	3.31E-20	0.314	285.0	4.09E-20	0.305	286.0	2.42E-20	0.296
287.0	1.22E-20	0.287	288.0	2.19E-20	0.278	289.0	3.14E-20	0.269
290.0	1.54E-20	0.260	291.0	1.49E-20	0.256	292.0	9.59E-21	0.252
293.0	3.22E-20	0.248	294.0	5.45E-20	0.244	295.0	4.07E-20	0.240
296.0	2.41E-20	0.236	297.0	1.79E-20	0.232	298.0	3.16E-20	0.228
299.0	2.81E-20	0.224	300.0	1.14E-20	0.220	301.0	1.27E-20	0.221
302.0	1.21E-20	0.222	303.0	2.78E-20	0.223	304.0	5.40E-20	0.224
305.0	5.30E-20	0.225	306.0	4.13E-20	0.226	307.0	2.23E-20	0.227
308.0	1.77E-20	0.228	309.0	2.43E-20	0.229	310.0	2.00E-20	0.230
311.0	9.15E-21	0.245	312.0	1.05E-20	0.260	313.0	1.43E-20	0.275
314.0	3.07E-20	0.290	315.0	4.50E-20	0.305	316.0	3.29E-20	0.320
317.0	3.77E-20	0.335	318.0	3.10E-20	0.350	319.0	1.22E-20	0.365
320.0	1.26E-20	0.380	321.0	1.48E-20	0.411	322.0	7.70E-21	0.442
323.0	4.66E-21	0.473	324.0	7.11E-21	0.504	325.0	1.51E-20	0.535
326.0	3.90E-20	0.566	327.0	3.50E-20	0.597	328.0	1.49E-20	0.628
329.0	2.30E-20	0.659	330.0	3.05E-20	0.690	331.0	1.43E-20	0.690
332.0	4.22E-21	0.690	333.0	2.01E-21	0.690	334.0	1.66E-21	0.690
335.0	9.68E-22	0.690	336.0	1.57E-21	0.690	337.0	3.27E-21	0.690
338.0	1.38E-20	0.690	339.0	3.18E-20	0.690	340.0	2.39E-20	0.690
341.0	8.91E-21	0.661	342.0	6.91E-21	0.632	343.0	1.40E-20	0.603
344.0	1.13E-20	0.574	345.0	3.94E-21	0.545	346.0	9.93E-22	0.516
347.0	7.18E-22	0.487	348.0	6.70E-22	0.458	349.0	7.21E-22	0.429
350.0	1.87E-22	0.400	351.0	8.57E-22	0.372	352.0	5.46E-21	0.344
353.0	1.39E-20	0.316	354.0	1.39E-20	0.288	355.0	6.64E-21	0.260
356.0	1.97E-21	0.232	357.0	4.27E-22	0.204	358.0	3.22E-22	0.176
359.0	2.57E-22	0.148	360.0	3.73E-22	0.120			
Photolysis file = CCHOR								
260.0	2.00E-20	0.310	270.0	3.40E-20	0.390	280.0	4.50E-20	0.580
290.0	4.90E-20	0.530	295.0	4.50E-20	0.480	300.0	4.30E-20	0.430
305.0	3.40E-20	0.370	315.0	2.10E-20	0.170	320.0	1.80E-20	0.100
325.0	1.10E-20	0.040	330.0	6.90E-21	0.000			
Photolysis file = RCHO								
280.0	5.26E-20	0.960	290.0	5.77E-20	0.910	300.0	5.05E-20	0.860
310.0	3.68E-20	0.600	320.0	1.66E-20	0.360	330.0	6.49E-21	0.200
340.0	1.44E-21	0.080	345.0	0.00E-01	0.20			
Photolysis file = ACETONE								
279.8	5.30E-20	0.560	283.7	5.30E-20	0.460	287.8	5.10E-20	0.360
292.0	4.40E-20	0.250	296.3	3.50E-20	0.210	300.5	3.00E-20	0.150
303.0	2.80E-20	0.120	304.0	2.50E-20	0.110	305.0	2.30E-20	0.100
306.0	2.10E-20	0.090	307.0	2.00E-20	0.080	308.0	1.80E-20	0.070
309.0	1.70E-20	0.060	310.0	1.50E-20	0.050	311.0	1.40E-20	0.048
312.0	1.30E-20	0.046	313.0	1.20E-20	0.043	314.0	1.10E-20	0.041
316.0	9.20E-21	0.037	320.0	5.30E-21	0.028	325.0	2.80E-21	0.031
330.0	1.90E-21	0.033	335.0	0.00E-01	0.036			
Photolysis file = KETONE								
210.0	1.10E-21	0.100	220.0	1.20E-21	0.100	230.0	4.60E-21	0.100
240.0	1.30E-20	0.100	250.0	2.68E-20	0.100	260.0	4.21E-20	0.100

Table 3. (*Contd.*)

WL (nm)	Abs (cm^2)	QY	WL (nm)	Abs (cm^2)	QY	WL (nm)	Abs (cm^2)	QY
270.0	5.54E–20	0.100	280.0	5.92E–20	0.100	290.0	5.16E–20	0.100
300.0	3.44E–20	0.100	310.0	1.53E–20	0.100	320.0	4.60E–21	0.100
330.0	1.10E–21	0.100	340.0	0.00E–01	0.100			
Photolysis file = GLYOXAL1								
230.0	2.87E–21	1.000	235.0	2.87E–21	1.000	240.0	4.30E–21	1.000
245.0	5.73E–21	1.000	250.0	8.60E–21	1.000	255.0	1.15E–20	1.000
260.0	1.43E–20	1.000	265.0	1.86E–20	1.000	270.0	2.29E–20	1.000
275.0	2.58E–20	1.000	280.0	2.87E–20	1.000	285.0	3.30E–20	1.000
290.0	3.15E–20	1.000	295.0	3.30E–20	1.000	300.0	3.58E–20	1.000
305.0	2.72E–20	1.000	310.0	2.72E–20	1.000	312.5	2.87E–20	1.000
315.0	2.29E–20	1.000	320.0	1.43E–20	1.000	325.0	1.15E–20	1.000
327.5	1.43E–20	1.000	330.0	1.15E–20	1.000	335.0	2.87E–21	1.000
340.0	0.00E–01	1.000						
Photolysis file = GLYOXAL2								
355.0	0.00E–01	0.029	360.0	2.29E–21	0.029	365.0	2.87E–21	0.029
370.0	8.03E–21	0.029	375.0	1.00E–20	0.029	380.0	1.72E–20	0.029
382.0	1.58E–20	0.029	384.0	1.49E–20	0.029	386.0	1.49E–20	0.029
388.0	2.87E–20	0.029	390.0	3.15E–20	0.029	391.0	3.24E–20	0.029
392.0	3.04E–20	0.029	393.0	2.23E–20	0.029	394.0	2.63E–20	0.029
395.0	3.04E–20	0.029	396.0	2.63E–20	0.029	397.0	2.43E–20	0.029
398.0	3.24E–20	0.029	399.0	3.04E–20	0.029	400.0	2.84E–20	0.029
401.0	3.24E–20	0.029	402.0	4.46E–20	0.029	403.0	5.27E–20	0.029
404.0	4.26E–20	0.029	405.0	3.04E–20	0.029	406.0	3.04E–20	0.029
407.0	2.84E–20	0.029	408.0	2.43E–20	0.029	409.0	2.84E–20	0.029
410.0	6.08E–20	0.029	411.0	5.07E–20	0.029	411.5	6.08E–20	0.029
412.0	4.86E–20	0.029	413.0	8.31E–20	0.029	413.5	6.48E–20	0.029
414.0	7.50E–20	0.029	414.5	8.11E–20	0.029	415.0	8.11E–20	0.029
415.5	6.89E–20	0.029	416.0	4.26E–20	0.029	417.0	4.86E–20	0.029
418.0	5.88E–20	0.029	419.0	6.69E–20	0.029	420.0	3.85E–20	0.029
421.0	5.67E–20	0.029	421.5	4.46E–20	0.029	422.0	5.27E–20	0.029
422.5	1.05E–19	0.029	423.0	8.51E–20	0.029	424.0	6.08E–20	0.029
425.0	7.29E–20	0.029	426.0	1.18E–19	0.029	426.5	1.30E–19	0.029
427.0	1.07E–19	0.029	428.0	1.66E–19	0.029	429.0	4.05E–20	0.029
430.0	5.07E–20	0.029	431.0	4.86E–20	0.029	432.0	4.05E–20	0.029
433.0	3.65E–20	0.029	434.0	4.05E–20	0.029	434.5	6.08E–20	0.029
435.0	5.07E–20	0.029	436.0	8.11E–20	0.029	436.5	1.13E–19	0.029
437.0	5.27E–20	0.029	438.0	1.01E–19	0.029	438.5	1.38E–19	0.029
439.0	7.70E–20	0.029	440.0	2.47E–19	0.029	441.0	8.11E–20	0.029
442.0	6.08E–20	0.029	443.0	7.50E–20	0.029	444.0	9.32E–20	0.029
445.0	1.13E–19	0.029	446.0	5.27E–20	0.029	447.0	2.43E–20	0.029
448.0	2.84E–20	0.029	449.0	3.85E–20	0.029	450.0	6.08E–20	0.029
451.0	1.09E–19	0.029	451.5	9.32E–20	0.029	452.0	1.22E–19	0.029
453.0	2.39E–19	0.029	454.0	1.70E–19	0.029	455.0	3.40E–19	0.029
455.5	4.05E–19	0.029	456.0	1.01E–19	0.029	457.0	1.62E–20	0.029
458.0	1.22E–20	0.029	458.0	1.42E–20	0.029	459.0	4.05E–21	0.029
460.0	4.05E–21	0.029	460.5	6.08E–21	0.029	461.0	2.03E–21	0.029
462.0	0.00E–01	0.029						
Photolysis file = MEGLYOX1								
220.0	2.10E–21	1.000	225.0	2.10E–21	1.000	230.0	4.21E–21	1.000
235.0	7.57E–21	1.000	240.0	9.25E–21	1.000	245.0	8.41E–21	1.000
250.0	9.25E–21	1.000	255.0	9.25E–21	1.000	260.0	9.67E–21	1.000
265.0	1.05E–20	1.000	270.0	1.26E–20	1.000	275.0	1.43E–20	1.000
280.0	1.51E–20	1.000	285.0	1.43E–20	1.000	290.0	1.47E–20	1.000
295.0	1.18E–20	1.000	300.0	1.14E–20	1.000	305.0	9.25E–21	1.000
310.0	6.31E–21	1.000	315.0	5.47E–21	1.000	320.0	3.36E–21	1.000
325.0	1.68E–21	1.000	330.0	8.41E–22	1.000	335.0	0.00E–01	1.000
Photolysis file = MEGLYOX2								
350.0	0.00E–01	0.107	354.0	4.21E–22	0.107	358.0	1.26E–21	0.107
360.0	2.10E–21	0.107	362.0	2.10E–21	0.107	364.0	2.94E–21	0.107
366.0	3.36E–21	0.107	368.0	4.21E–21	0.107	370.0	5.47E–21	0.107
372.0	5.89E–21	0.107	374.0	7.57E–21	0.107	376.0	7.99E–21	0.107
378.0	8.83E–21	0.107	380.0	1.01E–20	0.107	382.0	1.09E–20	0.107
384.0	1.35E–20	0.107	386.0	1.51E–20	0.107	388.0	1.72E–20	0.107
390.0	2.06E–20	0.107	392.0	2.10E–20	0.107	394.0	2.31E–20	0.107

Table 3. (*Contd.*)

WL (nm)	Abs (cm^2)	QY	WL (nm)	Abs (cm^2)	QY	WL (nm)	Abs (cm^2)	QY
Photolysis file = MEGLYOX2								
396.0	2.48E–20	0.107	398.0	2.61E–20	0.107	400.0	2.78E–20	0.107
402.0	2.99E–20	0.107	404.0	3.20E–20	0.107	406.0	3.79E–20	0.107
408.0	3.95E–20	0.107	410.0	4.33E–20	0.107	412.0	4.71E–20	0.107
414.0	4.79E–20	0.107	416.0	4.88E–20	0.107	418.0	5.05E–20	0.107
420.0	5.21E–20	0.107	422.0	5.30E–20	0.107	424.0	5.17E–20	0.107
426.0	5.30E–20	0.107	428.0	5.21E–20	0.107	430.0	5.55E–20	0.107
432.0	5.13E–20	0.107	434.0	5.68E–20	0.107	436.0	6.22E–20	0.107
438.0	6.06E–20	0.107	440.0	5.47E–20	0.107	441.0	6.14E–20	0.107
442.0	5.47E–20	0.107	443.0	5.55E–20	0.107	433.5	6.81E–20	0.107
444.0	5.97E–20	0.107	445.0	5.13E–20	0.107	446.0	4.88E–20	0.107
447.0	5.72E–20	0.107	448.0	5.47E–20	0.107	449.0	6.56E–20	0.107
450.0	5.05E–20	0.107	451.0	3.03E–20	0.107	452.0	4.29E–20	0.107
453.0	2.78E–20	0.107	454.0	2.27E–20	0.107	456.0	1.77E–20	0.107
458.0	8.41E–21	0.107	460.0	4.21E–21	0.107	464.0	1.68E–21	0.107
468.0	0.00E–01	0.107						
Photolysis file = BZCHO								
299.0	1.78E–19	0.050	304.0	7.40E–20	0.050	306.0	6.91E–20	0.050
309.0	6.41E–20	0.050	313.0	6.91E–20	0.050	314.0	6.91E–20	0.050
318.0	6.41E–20	0.050	325.0	8.39E–20	0.050	332.0	7.65E–20	0.050
338.0	8.88E–20	0.050	342.0	8.88E–20	0.050	346.0	7.89E–20	0.050
349.0	7.89E–20	0.050	354.0	9.13E–20	0.050	355.0	8.14E–20	0.050
364.0	5.67E–20	0.050	368.0	6.66E–20	0.050	369.0	8.39E–20	0.050
370.0	8.39E–20	0.050	372.0	3.45E–20	0.050	374.0	3.21E–20	0.050
376.0	2.47E–20	0.050	377.0	2.47E–20	0.050	380.0	3.58E–20	0.050
382.0	9.90E–21	0.050	386.0	0.00E–01	0.050			
Photolysis file = AROMUNK1								
200.0	7.90E–21	1.000	350.0	7.90E–21	1.000	360.0	0.00E–01	1.000
Photolysis file = AROMUNK2								
200.0	7.90E–20	1.000	350.0	7.90E–20	1.000	360.0	0.00E–01	1.000
Photolysis file = CO2H								
210.0	3.75E–19	1.000	220.0	2.20E–19	1.000	230.0	1.38E–19	1.000
240.0	8.80E–20	1.000	250.0	5.80E–20	1.000	260.0	3.80E–20	1.000
270.0	2.50E–20	1.000	280.0	1.50E–20	1.000	290.0	9.00E–21	1.000
300.0	5.80E–21	1.000	310.0	3.40E–21	1.000	320.0	1.90E–21	1.000
330.0	1.10E–21	1.000	340.0	6.00E–22	1.000	350.0	4.00E–22	1.000
360.0	0.00E–01	1.000						

*See notes for corresponding reaction on Table 2 for documentation of the sources of these values.

model predictions, we believe excluding them has relatively little advantage and unnecessarily limits the range of validity of the mechanism.

The most uncertain aspect of the inorganic mechanism is probably the assumed 'homogeneous' pathway for the $N_2O_5 + H_2O$ reaction (Reaction A10 in Table 2). The rate constant used for this reaction is based on assuming that the formation of gas-phase HNO_3 from N_2O_5 in humid air observed by Tuazon *et al.* (1983) reflects a homogeneous gas-phase process. (Note that Tuazon *et al.* (1983) cited their rate data as an upper limit to the homogeneous gas-phase rate constant.) However, more recent data (Atkinson *et al.*, 1986; Sverdrup *et al.*, 1987) show that the room temperature rate constant for the homogeneous gas-phase reaction is $< 1.5 \times 10^{-21}$ cm^3 $molecule^{-1}$ s^{-1}, and may well be orders of magnitude less (Sverdrup *et al.*, 1987). Nevertheless, this reaction is retained in the gas-phase mechanism, since analysis of air quality data (Atkinson *et al.*, 1986) suggests that a loss mechanism of N_2O_5 exists in the night-time lower troposphere, which can be represented, approximately, as an $N_2O_5 + H_2O$ reaction with approximately the rate constant assumed. The rate constant assumed for the N_2O_5 hydrolysis reaction is probably the most important single difference between the homogeneous inorganic reactions assumed in this mechanism compared to the latest version of the Carbon Bond mechanism documented by Gery *et al.* (1988), where a rate constant which is ~ 30% higher than used in this mechanism is employed.

Representation of the organic products

This mechanism employs 19 species to represent the reactions of the major organic photooxidation products. Like the ALW (Atkinson *et al.*, 1982) and the

Table 4. Description of kinetic and mechanistic parameters used in the generalized alkane and aromatic reaction mechanism (parameters shown are for reactions of the generalized alkane/aromatic species AARn, as listed in Table 2)

Parameter	Meaning
Kinetic parameters	
kAnOH	Rate constant for reaction with OH radicals
Mechanistic parameters affection radicals and/or NO_x	
AnRR	Amount of NO to NO_2 conversion with HO_2 formation. (Yield of RO_2–R.)
AnNR	Amount of reaction with NO to form reactive alkyl nitrates. (Yield of RO_2–N.)
AnXN	Amount of reaction with NO to form unreactive nitrates. (Yield of RO_2–XN.)
AnNP	Amount or reaction with NO to form aromatic nitro compounds. (Yield of RO_2–NP.)
AnRH	Direct HO_2 yield, with no NO to NO_2 conversion.
AnR2	Amount of extra NO to NO_2 conversion caused by secondarily formed peroxy radicals. (Yield of R_2O_2.)
Organic product yield parameters	
AnA1	Yield of formaldehyde (HCHO)
AnA2	Yield of acetaldehyde (CCHO)
AnA3	Yield of propionaldehyde and higher aldehydes (RCHO)
AnK3	Yield of acetone (ACET)
AnK4	Yield of higher ketones (MEK)
AnCO	Yield of CO
AnC2	Yield of CO_2
AnPH	Yield of phenol (PHEN)
AnCR	Yield of cresols or alkyl phenols (CRES)
AnBZ	Yield of aromatic aldehydes (BALD)
AnGL	Yield of glyoxal (GLY)
AnMG	Yield of methyl glyoxal (MGLY)
AnU1	Yield of unknown aromatic ring fragmentation product # 1 (AFG1)
AnU2	Yield of unknown aromatic ring fragmentation product # 2 (AFG2)
AnNC	Number of carbons in the alkane, aromatic or mixture being represented by AARn.
Parameters derived from the above parameters	
AnRO2	Total peroxy radical (RO2.) yield = AnRR + AnNR + AnNP + AnXN + AnR2
AnXC	"Lost" carbon in OH radical reaction. (Yield of –C.) = AnNC – 5 AnNR – 6 AnNP – AnA1 – 2 AnA2 – 3 AnA3 – 3 AnK3 – 4 AnK4 – AnCO – AnC2 – 6 AnPH – 7 AnCR – 7 AnBZ – 2 AnGL – 3 AnMG – 2 AnU1 – 3 AnU2

detailed ADOM (Lurmann *et al.*, 1986) mechanisms, the oxygenated products which are explicitly represented include formaldehyde (HCHO), acetaldehyde (CCHO), propionaldehyde and lumped higher aldehydes (RCHO), acetone (ACET), methyl ethyl ketone and lumped higher ketones (MEK), glyoxal (GLY), methylglyoxal (MGLY), cresols (CRES), peroxyacetyl nitrate (PAN), peroxypropionyl nitrate and higher PAN analogues (PPN) and the PAN analogue formed from glyoxal (GPAN). This mechanism also includes a lumped alkyl nitrate species (RNO_3), phenol (PHEN), nitrophenols (NPHE), benzaldehyde (BALD) and its PAN analogue (PBZN). By comparison, none of these latter five species are in the ALW mechanism, while the ADOM mechanism includes phenol and has several lumped alkyl nitrate species (making it more detailed in this regard), but does not include benzaldehyde, PBZN or nitrophenols. Finally, this mechanism uses two species used to represent uncharacterized aromatic fragmentation products (AFG1 and AFG2) and a lumped hydroperoxide species (–OOH), which are different from the representations used in the previous mechanisms.

The mechanisms and rate constants used for the reactions of the explicitly represented oxygenated and organic nitrate products are based primarily on the recent comprehensive reviews of Atkinson (1988, 1990), which in turn are based on the most recent kinetic and mechanistic data and our current estimates. However, the available laboratory data are insufficient to completely characterize the atmospheric reaction mechanisms of all these species. Therefore, a number of estimates had to be made, and parameters had to be derived based on fits of model simulations to the environmental chamber data. These cases are indicated in the notes given with the reactions in Table 2. The following points regarding these reactions are noted.

Formaldehyde. The major change in the updated formaldehyde mechanism is that the mechanism of the HO_2 + formaldehyde reactions was modified based on the new recommendations of Atkinson *et al.* (1989b).

Table 5. Description of kinetic and mechanistic parameters used in the generalized alkene reaction mechanism (parameters shown are for reactions of the generalized alkene species OLEn)

Parameter	Meaning
Kinetic parameters	
*k*OnOH	Rate constant for reaction with OH radicals
*k*OnO3	Rate constant for reaction with ozone
*k*OnN3	Rate constant for reaction with NO_3 radicals
*k*OnOA	Rate constant for reaction with $O(^3P)$ atoms
Structural parameters giving groups about the most reactive double bond	
OnP1	Number of $=CH_2$ groups
OnP2	Number of $=CHCH_3$ groups
OnP3	Number of =CHR groups, where R not H or CH_3
OnP4	Number of $=C(CH_3)_2$ groups
OnP5	Number of $=C(CH_3)$ (R) or $=CH_2$ groups
Other mechanistic parameters	
OnPN	Organic nitrate yield in the OH reaction. (Yield of RO_2–N.)
OnNC	Number of carbons in the alkene, or average number of carbons in the alkene mixture.

Product yield parameters derived from the above parameters

	Rxn.	Product	Derivation
OnPR	OH	RO2–R.	1 – OnPN
OnP1R		HCHO	OnPN × OnP1
OnP2R		CCHO	OnPN × OnP2
OnP3R		RCHO	OnPN × OnP3
OnP4R	OH	ACET	OnPN × OnP4
OnP5R		MEK	OnPN × OnP5
OnOHXC		Lost C	OnNC – OnP1R – 2 OnP2R – 3 OnP3R – 3 OnP4R – 4 OnP5R – 5 OnPN
OnO3A1	O_3	HCHO	0.5 (OnP1 + 0.3 OnP2 + 0.1 OnP5)
OnO3A2		CCHO	0.5 (OnP2 + 0.3 OnP3 + 0.1 OnP5)
OnO3A3		RCHO	0.5 OnP3
OnO3K3		ACET	0.5 OnP4
OnO3K4		MEK	0.5 (0.28 OnP2 + 0.42 OnP3 + 0.8 OnP4 + 0.8 OnP5)
OnO3MG		MGLY	0.5 (0.2 OnP4)
OnO3CO		CO	0.5 (0.44 OnP1 + 0.15 OnP2 + 0.15 OnP3)
OnO3SB		O3OL–SB	0.5 (0.37 OnP1 + 0.2 OnP2 + 0.2 OnP3)
OnO3P1		CCO–O2.	0.5 (0.1 OnP5)
OnO3P2		C2CO–O2.	0.5 (0.1 OnP5)
OnO3RH		HO2.	0.5 (0.12 OnP1 + 0.21 OnP2 + 0.21 OnP3)
OnO3OH		HO.	0.5 (0.12 OnP2 + 0.12 OnP3 + 0.2 OnP4 + 0.2 OnP5)
OnO3RR		ROR–R.	0.5 (0.27 OnP2 + 0.27 OnP3 + 0.2 OnP4)
OnO3R2		R2O2.	0.5 (0.3 OnP5)
OnO3RO2		RO2.	OnO3RR + OnO3R2
OnO3PS		RCO3.	OnO3P1 + OnOP2
OnO3XC		Lost C	OnNC – OnO3A1 – 2 OnO3A2 – 3 OnOA3 – 3 OnO3K3 – 4 OnO3K4 – 3 OnO3MG – OnO3CO – 2 OnOP1 – 3 OnO3P2
OnOAXC	O	Lost C	OnNC – 3.5
OnN3XC	NO_3	Lost C	OnNC – OnP1 – 2 OnP2 – 3 OnP3 – 3 OnP4 – 4 OnP5

Table 6. Listing of kinetic and mechanistic parameters assigned for the alkane detailed model species. Parameters are given for $T = 300$ [parameters for other temperatures are given by Carter *et al.* (1988a)]

		Product yield parameters†										
Name	*k*OH*	RR	NR	XN	R2	A1	A2	A3	K3	K4	CO	C2
METHANE‡	8.71E–15	1.000	0.000	0.000	0.000	1.000	0.000	0.000	0.000	0.000	0.000	0.000
ETHANE§	2.74E–13	1.000	0.000	0.000	0.000	0.000	1.000	0.000	0.000	0.000	0.000	0.000
PROPANE‖	1.22E–12	0.961	0.000	0.039	0.000	0.000	0.000	0.303	0.658	0.000	0.000	0.000
N-C4	2.56E–12	0.924	0.076	0.000	0.397	0.001	0.571	0.140	0.000	0.533	0.000	0.000
N-C5	3.96E–12	0.880	0.120	0.000	0.544	0.007	0.080	0.172	0.000	0.929	0.000	0.000
N-C6	5.36E–12	0.815	0.185	0.000	0.738	0.000	0.020	0.105	0.000	1.134	0.000	0.000
N-C7	6.76E–12	0.733	0.267	0.000	0.727	0.000	0.000	0.056	0.000	1.241	0.000	0.000
N-C8	8.16E–12	0.667	0.333	0.000	0.706	0.000	0.000	0.002	0.000	1.333	0.000	0.000
N-C9	9.56E–12	0.627	0.373	0.000	0.673	0.000	0.000	0.001	0.000	1.299	0.000	0.000
N-C10	1.10E–11	0.603	0.397	0.000	0.659	0.000	0.000	0.001	0.000	1.261	0.000	0.000
N-C11	1.24E–11	0.589	0.411	0.000	0.654	0.000	0.000	0.001	0.000	1.241	0.000	0.000
N-C12	1.38E–11	0.580	0.420	0.000	0.644	0.000	0.000	0.001	0.000	1.223	0.000	0.000

Table 6. (*Contd.*)

Name	kOH*	RR	NR	XN	Product yield parameters† R2	A1	A2	A3	K3	K4	CO	C2
N-C13	1.52E-11	0.573	0.427	0.000	0.638	0.000	0.000	0.001	0.000	1.211	0.000	0.000
N-C14	1.66E-11	0.569	0.431	0.000	0.634	0.000	0.000	0.001	0.000	1.202	0.000	0.000
N-C15	1.80E-11	0.566	0.434	0.000	0.631	0.000	0.000	0.001	0.000	1.196	0.000	0.000
ISO-C4	2.39E-12	0.973	0.027	0.000	0.744	0.744	0.000	0.229	0.744	0.000	0.000	0.000
ISO-C5	4.00E-12	0.933	0.064	0.002	0.734	0.000	0.614	0.133	0.611	0.303	0.000	0.000
BR-C5	4.00E-12	0.933	0.064	0.002	0.734	0.000	0.614	0.133	0.611	0.303	0.000	0.000
NEO-C5	7.55E-13	0.949	0.051	0.000	0.019	0.019	0.000	0.939	0.010	0.000	0.000	0.000
2-ME-C5	5.40E-12	0.873	0.122	0.005	0.749	0.006	0.023	0.545	0.223	0.724	0.000	0.000
3-ME-C5	5.76E-12	0.888	0.112	0.000	0.860	0.005	0.523	0.089	0.000	1.003	0.000	0.000
22-DMB	1.84E-12	0.847	0.153	0.000	0.960	0.295	0.303	0.372	0.295	0.542	0.000	0.000
23-DMB	5.44E-12	0.901	0.061	0.039	0.944	0.000	0.000	0.128	1.584	0.096	0.000	0.000
4-ME-C6	7.16E-12	0.815	0.182	0.002	0.842	0.000	0.127	0.329	0.000	1.119	0.000	0.000
24-DM-C5	6.84E-12	0.867	0.131	0.002	0.844	0.000	0.000	0.772	0.257	0.682	0.000	0.000
23-DM-C5	7.21E-12	0.860	0.128	0.011	1.101	0.036	0.253	0.185	0.390	0.960	0.000	0.000
ISO-C8	4.69E-12	0.811	0.188	0.001	0.942	0.111	0.000	0.747	0.251	0.643	0.000	0.000
CYCC5	5.62E-12	0.873	0.127	0.000	1.745	0.000	0.000	0.873	0.000	0.218	0.873	0.000
ME-CYCC5	7.10E-12	0.856	0.144	0.000	2.057	0.321	0.000	0.622	0.000	0.550	0.535	0.214
CYCC6	8.41E-12	0.807	0.193	0.000	0.352	0.003	0.000	0.333	0.000	0.816	0.000	0.003
ME-CYCC6	1.02E-11	0.784	0.216	0.000	0.977	0.100	0.001	0.474	0.000	0.979	0.003	0.046
ET-CYCC6	1.22E-11	0.737	0.263	0.000	1.464	0.185	0.310	0.393	0.000	0.930	0.010	0.185
3-ME-C6	7.16E-12	0.815	0.182	0.002	0.842	0.000	0.127	0.329	0.000	1.119	0.000	0.000
4-ME-C7	8.57E-12	0.753	0.244	0.002	0.803	0.000	0.000	0.352	0.000	1.204	0.000	0.000
4-ET-C7	1.05E-11	0.727	0.271	0.002	0.804	0.002	0.059	0.303	0.000	1.167	0.000	0.000
4-PR-C7	1.19E-11	0.696	0.301	0.002	0.775	0.000	0.004	0.328	0.000	1.139	0.000	0.000
BR-C6	5.40E-12	0.873	0.122	0.005	0.749	0.006	0.023	0.545	0.223	0.724	0.000	0.000
BR-C7	7.16E-12	0.815	0.182	0.002	0.842	0.000	0.127	0.329	0.000	1.119	0.000	0.000
BR-C8	8.57E-12	0.753	0.244	0.002	0.803	0.000	0.000	0.352	0.000	1.204	0.000	0.000
BR-C9	1.05E-11	0.727	0.271	0.002	0.804	0.002	0.059	0.303	0.000	1.167	0.000	0.000
Br-C10	1.19E-11	0.696	0.301	0.002	0.775	0.000	0.004	0.328	0.000	1.139	0.000	0.000
BR-C11	1.43E-11	0.754	0.246	0.000	1.273	0.021	0.054	0.090	0.000	1.862	0.000	0.000
BR-C12	1.57E-11	0.733	0.267	0.000	1.350	0.002	0.422	0.012	0.000	1.647	0.000	0.000
BR-C13	1.71E-11	0.715	0.285	0.000	1.226	0.002	0.008	0.111	0.000	1.819	0.000	0.000
BR-C14	1.85E-11	0.702	0.298	0.000	1.122	0.002	0.000	0.003	0.000	1.820	0.000	0.000
BR-C15	1.99E-11	0.690	0.310	0.000	1.103	0.001	0.000	0.003	0.000	1.790	0.000	0.000
CYC-C6	8.41E-12	0.807	0.193	0.000	0.352	0.003	0.000	0.333	0.000	0.816	0.000	0.003
CYC-C7	1.02E-11	0.784	0.216	0.000	0.977	0.100	0.001	0.474	0.000	0.979	0.003	0.046
CYC-C8	1.22E-11	0.737	0.263	0.000	1.464	0.185	0.310	0.393	0.000	0.930	0.010	0.185
CYC-C9	1.40E-11	0.756	0.244	0.000	1.970	0.283	0.264	0.502	0.000	1.056	0.000	0.264
CYC-C10	1.59E-11	0.739	0.261	0.000	1.874	0.208	0.390	0.228	0.000	1.359	0.011	0.208
CYC-C11	1.77E-11	0.767	0.233	0.000	1.855	0.236	0.376	0.144	0.000	1.464	0.001	0.184
CYC-C12	1.97E-11	0.757	0.243	0.000	2.040	0.202	0.437	0.110	0.000	1.708	0.001	0.169
CYC-C13	2.11E-11	0.738	0.261	0.000	1.638	0.104	0.243	0.198	0.000	1.649	0.002	0.074
CYC-C14	2.25E-11	0.725	0.274	0.001	1.498	0.069	0.070	0.439	0.000	1.516	0.002	0.048
CYC-C15	2.39E-11	0.714	0.283	0.002	1.611	0.040	0.027	0.465	0.000	1.719	0.002	0.036
C4C5¶	3.22E-12	0.927	0.072	0.001	0.604	0.188	0.316	0.168	0.339	0.441	0.000	0.000
C6PLUS¶	6.14E-12	0.808	0.184	0.008	0.844	0.022	0.042	0.252	0.350	0.876	0.000	0.000

*OH radical rate constant given in units of cm^3 $molecule^{-1}$ s^{-1}.

†Symbols for product yield parameters correspond to the notation used in Table 4.

‡Rate constants for reaction of OH radicals with methane were calculated using the expression $kOH = 6.255 \times 10^{-13} (T/300)^2 \exp(-2.548/RT)$, as recommended by Atkinson (1990). Formation of formaldehyde $+HO_2$ following one NO to NO_2 conversion is assumed to dominate.

§Rate constants for reactions of OH radicals with ethane were calculated using the expression $kOH = 1.278 \times 10^{-12} (T/300)^2 \exp(-0.918/RT)$, as recommended by Atkinson (1990). Formation of acetaldehyde $+HO_2$ following one NO to NO_2 conversion is assumed to dominate.

‖The rate constants, product yields and NO to NO_2 conversions for the C_{3+} alkanes were derived using a computer program as described in the text.

¶C4C5 and C6PLUS are the lumped alkane species used in the mechanism of Lurmann *et al.* (1987). They are included among the detailed model species for compatibility with that mechanism. The parameters for C4C5 were calculated by averaging those of N-C5, N-C5, ISO-C4 and ISO-C5. The parameters for C6PLUS were calculated by averaging those of N-C6, N-C7, N-C8, 23-DMB, 2-ME-C5, 23-DM-C5 and ISO-C8.

The net effect of these changes is that this overall process is much less important under atmospheric conditions than assumed previously.

The most important uncertainty in the formaldehyde mechanism concerns its absorption cross-sections, where there is a significant discrepancy in the literature. In particular, as discussed by Gery *et al.* (1988), the measurements of Bass *et al.* (1980) and

Table 7. Listing of kinetic and mechanistic parameters assigned for the aromatic species in the mechanism

Name	Rate parameters* A	E_a	Type	Value	Mechanistic parameters† Type	Value	Type	Value	Notes
BENZENE	2.50E−12	0.397	GL	0.207	PH	0.236	U1	0.490	1
			RH	0.236	RR	0.764			
TOLUENE	1.81E−12	−0.705	BZ	0.085	CR	0.260	GL	0.118	2
			MG	0.131	U2	0.410	RH	0.260	
			RR	0.740					
C2-BENZ	7.10E−12	0.000	BZ	0.085	CR	0.260	GL	0.118	3,4
			MG	0.131	U2	0.410	RH	0.260	
			RR	0.740					
I-C3-BEN	6.50E−12	0.000	BZ	0.085	CR	0.260	GL	0.118	3,4
			MG	0.131	U2	0.410	RH	0.260	
			RR	0.740					
N-C3-BEN	6.00E−12	0.000	BZ	0.085	CR	0.260	GL	0.118	3,4
			MG	0.131	U2	0.410	RH	0.260	
			RR	0.740					
S-C4-BEN	6.00E−12	0.000	BZ	0.085	CR	0.260	GL	0.118	3,5
			MG	0.131	U2	0.410	RH	0.260	
			RR	0.740					
***m*-XYLENE**	2.36E−11	0.000	BZ	0.040	CR	0.180	RH	0.180	4,6
			GL	0.108	MG	0.370	U2	0.666	
			RR	0.820					
***o*-XYLENE**	1.37E−11	0.000	BZ	0.040	CR	0.180	GL	0.108	4,7
			MG	0.370	U2	0.666	RH	0.180	
			RR	0.820					
***p*-XYLENE**	1.43E−11	0.000	BZ	0.040	CR	0.180	GL	0.108	4, 7
			MG	0.370	U2	0.666	RH	0.180	
			RR	0.820					
135-TMB	5.75E−11	0.000	BZ	0.030	CR	0.180	MG	0.620	4, 8
			U2	0.600	RH	0.180	RR	0.820	
123-TMB	3.27E−11	0.000	BZ	0.030	CR	0.180	MG	0.620	4, 8
			U2	0.600	RH	0.180	RR	0.820	
124-TMB	3.25E−11	0.000	BZ	0.030	CR	0.180	MG	0.620	4, 9
			U2	0.600	RH	0.180	RR	0.820	
NAPHTHAL	2.16E−11	0.000	PH	0.170	NP	0.140	U1	0.320	4, 10
			RH	0.170	RR	0.690			
23-DMN	7.70E−11	0.000	CR	0.040	NP	0.160	MG	0.490	4, 11
			U1	0.850	RH	0.040	RR	0.800	
ME-NAPH	5.20E−11	0.000	PH	0.085	CR	0.020	NP	0.150	12
			MG	0.245	U1	0.585	RH	0.105	
			RR	0.745					
TETRALIN	3.43E−11	0.000	PH	0.090	NP	0.120	RR	0.790	4, 13
			RH	0.090	U1	0.164			

*A is the Arrhenius activation energy in cm^3 $molecule^{-1}$ s^{-1}. E_a is the activation energy in kcal $mole^{-1}$.

†The symbols used to indicate the types of aromatic mechanistic parameters are based on the nomenclature used in Tables 2 and 4.

Documentation notes:

(1) Rate parameters based on data of Wallington *et al.* (1987), Witte *et al.* (1986) and data summarized by Atkinson (1986). Consisting with the $T=298$ K value tabulated by Atkinson (1990). Phenol yields based on the data of Atkinson *et al.* (1990a). Glyoxal yield based on data of Tuazon *et al.* (1986), and as given by Atkinson (1990). Aromatic fragmentation product yield adjusted to fit O3, NO and NO2 data in benzene–NO_x–air runs ITC-560, 561 and 562.

(2) Rate constant recommended by Atkinson (1990) for $T=213$–324 K at the high pressure limit. Benzaldehyde yield average of the data tabulated by Atkinson (1990). Alpha dicarbonyl yields averages of those of Bandow *et al.* (1985), Tuazon *et al.* (1986) and Gery *et al.* (1985) as summarized by Atkinson (1990). Yields of Shepson *et al.* (1984) seem to be somewhat low compared to more recent data, and were not used in computing the average. Cresol yields average of data of Gery *et al.* (1985) and Atkinson *et al.* (1989a). Previous data of Atkinson *et al.* (1983) and Leone *et al.* (1985) indicate lower yields of around 0.18, but use of the higher yields indicated by the newer data result in much better fits of model simulations to maximum ozone yields observed in SAPRC toluene–NO_x–air runs. Fragmentation product yields adjusted to fit the O_3, NO, NO_2 and PAN data of toluene–NO_x runs EC-266, EC-270, EC-271 and ITC-699 (Carter *et al.*, 1987; Carter, 1988a).

(3) Mechanistic parameters of toluene used for all mono-alkyl benzenes.

(4) $T=298$ rate constant recommended by Atkinson (1990). Temperature dependence expected to be small.

(5) Assumed to have the same rate constant as *n*-propyl benzene.

(6) Aromatic aldehyde yields based on estimates of Atkinson (1986) and data of Bandow and Washida (1985a). α-Dicarbonyl yields are averages of those of Bandow and Washida (1985a) and Tuazon *et al.* (1986) as summarized by Atkinson (1990). "Cresol" yields based on data of Gery *et al.* (1987). Aromatic fragmentation product yields adjusted to fit the O3, NO, NO_2, PAN and *m*-xylene data in *m*-xylene–NO_x–air runs EC-344, EC-345 and ITC-702 (Carter *et al.*, 1987; Carter, 1988a).

(7) The mechanistic parameters derived for *m*-xylene were used for all the xylenes and dialkyl benzenes, since there are insufficient chamber data to use to derive yields of uncharacterized fragmentation products for the others. Note in

Table 7 Foornote (*Contd.*)

particular that the α-dicarbonyl yields for the other xylenes are known (Bandow and Washida, 1985a; Tuazon *et al.*, 1986) to be different from those used in this mechanism, which are based on those for *m*-xylene.

(8) Aromatic aldehyde yield based on value derived by Atkinson (1986) from kinetics data. Phenolic product yields assumed to be the same as those assumed for xylenes. Methyl glyoxal yield average of values of Bandow and Washida (1985b) and Tuazon *et al.* (1986) and as summarized by Atkinson (1988). Aromatic fragmentation product yield adjusted to fit O3, NO, NO2, PAN and 135-TMB yields in 135-TMB–NO_x–air runs EC-901, EC-903, ITC-703, ITC-706 and ITC-709 (Carter *et al.*, 1987; Carter, 1988a).

(9) Product yield parameters for 1,3,5-trimethyl benzene used for all trialkyl benzenes.

(10) "Phenol" and "nitrophenol" (i.e. direct radical and NO_x sink) yields derived by Carter *et al.* (1987) based on fits to chamber data were used without further adjustment. Glyoxal yield arbitrarily set at zero; chamber simulations are not sensitive to this parameter. Aromatic fragmentation product yield adjusted based on fits to O_3, NO and NO_2 data in naphthalene–NO_x–air runs ITC-751, ITC-755, ITC-756, ITC-798 and ITC-802 (Carter *et al.*, 1987; Carter, 1988a).

(11) (2,3-DMN = 2,3-Dimethyl naphthalene.) "cresol" and "nitrophenol" (i.e. direct radical and NO_x sink) yields derived by Carter *et al.* (1987) based on fits to chamber data were used without further adjustement. Glyoxal yield arbitrarily set at zero; chamber simulations are not sensitive to this parameter. Aromatic fragmentation product yields adjusted based on fits to O3, NO, NO2, PAN and 23-DMN data in the 23-DMN–NO_x–air runs ITC-771, ITC-774, ITC-775 and ITC-806 (Carter *et al.*, 1987; Carter, 1988a).

(12) Rate constant given by Atkinson (1990) for 2-methyl naphthalene used. Mechanistic parameters used are averages of those derived for naphthalene and 2,3-dimethyl naphthalene.

(13) "Phenol" and "nitrophenol" (i.e. direct radical and NO_x sink) yields derived by Carter *et al.* (1987) based on fits to chamber data were used without further adjustment. Aromatic fragmentation product yields adjusted based on fits to O_3, NO, NO_2 and propene tracer data in tetralin–NO_x–air runs ITC-739, ITC-747, ITC-748, ITC-750 and ITC-802 (Carter *et al.*, 1987; Carter, 1988a).

Moortgat *et al.* (1983) yield predictions of the atmospheric photolysis rates of formaldehyde to yield radicals which differ by ~ 30%, with the Moortgat values giving the higher rate constants. Gery *et al.* (1987) use the Bass (1980) values for the latest version of the Carbon Bond mechanism because they give better results in model simulations of formaldehyde decay rates observed in the University of North Carolina outdoor chamber. On the other hand, the most recent IUPAC recommendation (Atkinson *et al.*, (1989b) is to use the data of Moortgat (1986), and recent unpublished data from our laboratories (H. W. Biermann, University of California, Riverside) also suggest that the higher Moortgat values are more likely to be correct. Because of this discrepancy, for the time being we still follow the NASA (1987) recommendation to use the average of the two sets of data. We hope that this discrepancy can be resolved in the near future, since the rate of photolysis of formaldehyde can significantly affect the predictions of airshed models as a whole.

Photolysis of other oxygenated products. Laboratory data are available concerning the absorption coefficients and quantum yields for the photolysis reactions of acetaldehyde, propionaldehyde and acetone, but the quantum yields for methyl ethyl ketone (MEK) had to be adjusted based on fits to results of a single UNC outdoor environmental chamber run (Carter *et al.*, 1986b). Laboratory data concerning the photolysis of MEK and other higher ketones under atmospheric conditions are needed. Note that the quantum yields for the ketone species appear to be significantly lower than unity, which is different from previous mechanism assumptions.

Lumped organic nitrates. The mechanisms used for the lumped organic nitrate species (RNO_3) is based on averaging the parameters estimated by Carter *et al.* (1986b) for the reactions of OH radicals with 2-butyl and 3-heptyl nitrates. The photolysis reactions of these higher nitrates are ignored, since it is estimated that the OH radical reaction will be a more important sink for these species under atmospheric conditions. However, the possibility that photolysis may have non-negligible effects on simulations of LRT conditions has not been adequately investigated. The species RNO_3 is used to represent only the C_{4+} alkyl nitrates. The C_2 and C_3 nitrates are ignored in this mechanism because (a) their formation is relatively important and (b) they are estimated to react relatively slowly under atmospheric conditions.

Glyoxal and methylglyoxal photolysis. The photolysis rates used in this mechanism for glyoxal and methylglyoxal are derived primarily, but not exclusively, from the data of Plum *et al.* (1983). They measured the absorption coefficients of these species over the wavelength region of interest for atmospheric modeling, and obtained an overall quantum yield for photolysis in the high wavelength (> 350 nm) band. However, the light source used by Plum *et al.* (1983) had a cut-off which precluded photolysis in the low wavelength (< 350 nm) band, and thus provided no information concerning photolysis in that region. Based on the data of Langford and Moore (1984), and references cited by them, we assume that glyoxal has a unit quantum yield for photodecomposition in the low wavelength region, and we also assume that photodissociation of methylglyoxal has a unit-efficiency in the short wavelength band. This differs from the previous versions of our mechanisms (Carter *et al.*, 1986b, 1987; Lurmann *et al.*, 1987), where the overall quantum yields of Plum *et al.* (1983) were assumed to be applicable over the entire wavelength region of relevance in the lower atmosphere. There are no details directly concerning the wavelength dependence

Table 8. Listing of kinetic and mechanistic parameters assigned for alcohols, ethers and acetylene

Name	Rate parameters†			Mechanistic parameters‡						
	k or A	E_a	B	Type	Value	Type	Value	Type	Value	Notes
MEOH	5.75E–13	−0.294	2	A1	1.000	RH	1.000			1,2
ETOH	5.56E–13	−1.057	2	A2	1.000	RH	1.000			1,2
ME–O–ME	1.04E–11	0.739	0	A3	1.000	RR	1.000			1,3
I-C3-OH	6.59E–13	−1.232	2	K3	1.000	RH	1.000			1,2
N-C3-OH	5.34E–12			A1	0.230	A2	0.230	A3	0.770	4,5
				RH	0.770	RR	0.230			
N-C4-OH	8.30E–12			A1	0.250	A2	0.120	A3	0.850	4,5
				K4	0.090	RH	0.600	RR	0.400	
				R2	0.060					
I-C4-OH	9.53E–12			K4	0.840	A2	0.240	RH	0.840	5,6
				RR	0.120					
T-C4-OH	3.86E–13	−0.640	2	RR	1.000	A1	1.000	K3	1.000	1,7
ET-GLYCL	7.70E–12			A2	1.000	RH	1.000			8, 9
PR-GLYCL	1.20E–11			A3	0.314	K4	0.686	RH	1.000	8,10
ACETYLEN	1.70E–12	0.463	0	GL	0.700	RH	0.300	RR	0.700	11

*Nomenclature employed: MEOH = methanol, ETOH = ethanol, ME–O–ME = dimethyl ether, I-C3-OH = isopropyl alcohol, N-C3-OH = *n*-propyl alcohol, N-C4-OH = *n*-butyl alcohol, I-C4-OH = isobutyl alcohol, T-C4-OH = *t*-butyl alcohol, ET-GLYCL = ethylene glycol or 1,2-ethanediol, PR-GLYCL = propylene glycol or 1,2-propanediol and ACETYLEN = acetylene.

†See footnote (b) of Table 2 for rate expression and units used. If no E_a or B are given then the temperature dependence is ignored in this mechanism.

‡The symbols used to represent the various types of mechanistic parameters are based on those employed in Tables 2 and 4.

Documentation notes:

(1) The rate parameters are recommended by Atkinson (1990).

(2) The reactions of these alcohols with OH radicals are assumed to result primarily in formation of α-hydroxy alkyl radicals, which is then assumed to react primarily with O_2 to form HO_2 + the corresponding carbonyl compound.

(3) Dimethyl ether is assumed to react to form CH_3–O–CHO (represented by RCHO in this mechanism) + HO_2 after one NO to NO_2 conversion.

(4) The rate constant for 298 K is recommended by Atkinson (1990). No recommendation is made concerning the temperature dependence of this rate constant, and it is ignored in this mechanism.

(5) The mechanisms for these compounds are based on estimates of initial OH radical reaction rates at various positions using the structure–activity estimates of Atkinson (1987), and the estimates for the subsequent reactions of the oxygenated radicals formed given by Carter and Atkinson (1985).

(6) Rate constant estimated using the structure–activity estimates of Atkinson (1987).

(7) The mechanism is based on assuming that most of the reaction occurs via initial reaction at the methyl groups.

(8) The rate constant used for these glycols are the 295 K rate constants tabulated by Atkinson (1986). The temperature dependences of these rate constants are not known and are ignored.

(9) The reaction of OH radicals with ethylene glycol is assumed to result in glycolaldehyde + HO_2, with the former being represented by acetaldehyde.

(10) The reaction of OH radicals with propylene glycol is estimated to occur at the 1-position 31.4% of the time, forming HO_2 + $CH_3CH(OH)CHO$, and at the 2-position the rest of the time, forming HO_2 + CH_3–CO–CH_2OH. The two organic products are represented by RCHO and MEK, respectively.

(11) This reaction is in the falloff region at atmospheric pressure. The expression for the temperature dependence at 760 torr of air given by Atkinson (1986) is used. The estimated mechanism is based on the data of Hatakeyama *et al.* (1986), who observed ~ 70% glyoxal and 40% formic acid in acetylene–NO_x photooxidations. The subsequent reactions of formic acid are ignored. The formation of glyoxal is assumed to involve the rearrangement of the vibrationally excited OH-acetylene adduct to CH_2CHO radicals, which adds O_2 and reacts with NO to form glyoxal, NO_2 and HO_2. The formation of formic acid is assumed to occur following stabilization of the initially formed adduct, which reacts with O_2 and rearranges to form formic acid + HCO radicals. The later reacts with O_2 form HO_2 and CO.

of the quantum yields for the photolyses of these species.

Reactions of phenols and cresols with OH *radicals.* The mechanisms of the reactions of OH radicals with phenolic compounds (i.e. PHEN and CRES in this mechanism) are unknown. While speculative mechanisms for these reactions have been incorporated in previous aromatic photooxidation mechanisms (e.g. Atkinson *et al.*, 1980, 1982; Leone and Seinfeld, 1984a,b), we do not consider that enough is known about them to justify attempting to represent them explicitly. The previously published speculative mechanisms are now known to be largely incorrect. (See discussion of the representation of the reactions of aromatic HCs below.) Thus, in this mechanism, a simple parameterized representation of these reactions is used, with the parameters being adjusted to fit the results of an *o*-cresol–NO_x–air chamber run (Atkinson *et al.*, 1980). These reactions are generally only of minor importance, since under most conditions reaction with NO_3 radicals is the major atmospheric fate of these compounds (Carter *et al.*, 1981; Atkinson, 1988 and references therein).

Inclusion of nitrophenol + NO_3 *radical reactions.* Nitrophenols are expected to be formed in the reactions of NO_3 radicals with phenol and cresols. Since

Table 9. Listing of kinetic and mechanistic parameters assigned to the non-ethene alkene species in the mechanism

Compound	Substituent codes*	p_N†	Rxn	Kinetic parameters‡ A	E_a	Refs.
Propene	1 2	0.000	OH	4.85E-12	−1.001	1,2
			O_3	1.32E-14	4.182	2,3
			NO_3	4.85E-12	3.699	4
			O	1.18E-11	0.644	5
1-Butene	1 3	0.000	OH	6.55E-12	−0.928	1,2
			O_3	3.46E-15	3.403	2,3
			NO_3	6.55E-12	3.732	4
			O	1.25E-11	0.648	5
trans-2-Butene	2 2	0.000	OH	1.01E-11	−1.091	1,2
			O_3	9.08E-15	2.258	2,3
			NO_3	1.01E-11	1.927	4
			O	2.26E-11	−0.020	5
cis-2-Butene	2 2	0.000	OH	1.10E-11	−0.968	1,2
			O_3	3.52E-15	1.953	2,3
			NO_3	1.10E-11	2.042	4
			O	1.21E-11	−0.235	6
Isobutene	1 4	0.000	OH	9.47E-12	−1.002	1,2
			O_3	3.55E-15	3.364	2,3
			NO_3	9.47E-12	2.025	4
			O	1.76E-11	0.085	6
2-Methyl-1-butene	1 5	0.000	OH	1.12E-11	−1.000	1,2,7
			O_3	3.55E-15	3.364	8
			NO_3	9.47E-12	2.025	8
			O	1.76E-11	0.085	8
2-Methyl-2-butene	2 4	0.000	OH	1.92E-11	−0.894	1,2
			O_3	6.17E-15	1.586	2,3
			NO_3	1.92E-11	0.429	4
			O	2.50E-11	−0.380	6
3-Methyl-1-butene	1 3	0.000	OH	5.32E-12	−1.059	1,2
			O_3	3.46E-15	3.403	9
			NO_3	6.55E-12	3.730	9
			O	1.25E-11	0.648	9
2,3-Dimethyl-2-butene	4 4	0.000	OH	2.03E-11	−1.000	1,2,7
			O_3	3.71E-15	0.690	2,3
			NO_3	2.03E-11	−0.611	4
			O	5.58E-12	−1.570	10
1-Pentene	1 3	0.100	OH	5.80E-12	−1.000	1,2,7,11
			O_3	3.46E-15	3.422	12
			NO_3	6.55E-12	3.732	9
			O	1.25E-11	0.648	9
1-Hexene	1 3	0.225	OH	6.84E-12	−1.000	1,2,7,13
			O_3	3.46E-15	3.369	12
			NO_3	6.55E-12	3.732	9
			O	1.25E-11	0.648	9
Cyclohexene	3 0	0.000	OH	1.25E-11	−1.000	1,2,7
			O_3	3.52E-15	2.109	14
			NO_3	1.10E-11	2.042	15
			O	1.21E-11	−0.354	16
Cyclopentene	3 0	0.000	OH	1.24E-11	−1.000	1,2,7
			O_3	3.52E-15	1.288	14
			NO_3	1.10E-11	2.042	15
			O	1.21E-11	−0.406	16
1,3-Butadiene	1 3	0.000	OH	1.48E-11	−0.890	2
			O_3	3.30E-14	4.968	2
			NO_3	1.48E-11	2.971	4
			O	2.10E-11		17
Isoprene	1 3	0.000	OH	2.54E-11	−0.815	1,2
			O_3	1.23E-14	4.000	2,3
			NO_3	2.54E-11	2.228	4
			O	6.00E-11		18
α-Pinene	3 0	0.000	OH	1.21E-11	−0.882	1,2,19
			O_3	9.90E-16	1.453	2
			NO_3	1.21E-11	0.435	4
			O	3.30E-11		17
β-Pinene	1 3	0.000	OH	2.38E-11	−0.709	1,2,20
			O_3	3.55E-15	3.199	21
			NO_3	2.38E-11	1.359	4
			O	2.10E-11		17

Table 9. (*Contd.*)

Compound	Substituent codes*	p_N†	Rxn	Kinetic parameters‡ A	E_a	Refs.
Unspeciated $C_{>5}$ terminal alkenes	1 3	See note 22	OH	6.84E–12	−1.000	22, 23
			O_3	3.46E–15	3.369	23
			NO_3	6.55E–12	3.732	23
			O	1.25E–11	0.648	23
Unspeciated $C_{\geq 5}$ internal alkenes	1 3	See note 22	OH	1.01E–11	−1.091	22, 24
			O_3	9.08E–15	2.258	24
			NO_3	1.01E–11	1.927	24
			O	2.26E–11	−0.020	24

*Substituent codes are as follows: (1) $=CH_2$, (2) $=CHCH_3$, (3) =CHR, (4) $=C(CH_3)_2$, (5) $=C(CH_3)$(R) or $=C(R)_2$, where R is not H or CH_3. See text.

†p_N = Nitrate yield in OH reaction.

‡"Rxn" = species reacting with alkene, "A" = Arrhenius A factor in cm^3 $molecule^{-2}$ s^{-1}, E_a = activation energy in kcal $mole^{-1}$.

Notes documenting references

(1) Atkinson (1986).
(2) Atkinson (1990).
(3) Atkinson and Carter (1984).
(4) k(298) of Atkinson (1990), A assumed to be the same as that for the OH radical reaction.
(5) Atkinson and Lloyd (1984).
(6) Atkinson and Pitts (1977).
(7) Activation energy estimated based on those for similar reactions.
(8) Rate constant assumed to be the same as that for isobutene.
(9) Rate constant assumed to be the same as that for 1-butene.
(10) Singleton *et al.* (1975).
(11) Nitrate yield estimated based on yields from alkanes with same number of carbons. This is based on nitrate yields estimated for the OH + 1-hexene reaction (see note 13).
(12) k(298) of Atkinson and Carter (1984) and Atkinson (1990); A of 1-butene.
(13) Nitrate yields in OH + *n*-hexene reaction derived based on model simulations of 1-hexene–NO_x–air chamber irradiations (Carter *et al.*, 1987).
(14) k (298) of Atkinson (1990), A of *cis*-2-butene.
(15) Rate constant assumed to be same as that for *cis*-2-butene.
(16) k(298) from Atkinson (1986), and references therein. A assumed to be same as for *cis*-2-butene.
(17) Atkinson (1986), and references therein. Temperature dependence not specified and assumed to be small.
(18) Estimated using correlation with rate constant for OH radical reaction (Atkinson, 1986).
(19) Nitrate yields of zero are assumed, since it gives better fits to results of model simulations of α-pinene–NO_x–air irradiations carried out in the UNC outdoor chamber (Jeffries *et al.*, 1982) than using yields estimated as indicated in footnote 22.
(20) Assumes same nitrate yield as used for α-pinene (i.e. zero).
(21) k(298) of Atkinson (1990). A assumed to be the same as that for isobutene.
(22) Nitrate yield parameters for the unspeciated alkanes are estimated based on the numbers of carbons in the alkenes as indicated in note 11. These estimates for 5–15 carbons are as follows: 0.100 (5 carbons), 0.225 (6), 0.270 (7), 0.330 (8), 0.360 (9), 0.380 (10), 0.395 (11), 0.400 (12), 0.410 (13), 0.412 (14), and 0.415 (15).
(23) All unspeciated $C_{>5}$ terminal monoalkenes are assumed to have the same rate constant as the corresponding reaction for 1-hexene.
(24) All unspeciated $C_{\geq 5}$ internal monoalkenes are assumed to have the same rate constant as the corresponding reaction for *trans*-2-butene.

this is the major atmospheric sink for these aromatic products, nitrophenols are predicted to be formed in non-negligible yields in the photooxidations of aromatic HCs. Most previous mechanisms have ignored their subsequent reactions. However, it is reasonable to expect that nitrophenols may also react with NO_3 radicals at significant rates, and thus represent an additional NO_x sink in these systems. Test calculations indicate that including the reactions of NO_3 radicals with nitrophenols results in somewhat lower O_3 yields in simulated aromatic–NO_x–air smog chamber experiments, more consistent with the results of these experiments than are calculations neglecting this reaction. Thus, the reactions of NO_3 with nitrophenols are included in this mechanism. However, the dinitrophenol products expected to be formed in the NO_3 + nitrophenol reactions are expected to be too nonvolatile to participate in gas-phase reactions, and their subsequent reactions are ignored.

Uncharacterized aromatic fragmentation products. Recent product studies of the photooxidations of toluene and other aromatics (Darnall *et al.*, 1979; Takagi *et al.*, 1982; Shepson *et al.*, 1984; Dumdei and O'Brien, 1984; Bandow *et al.*, 1985; Bandow and Washida, 1985a,b; Gery *et al.*, 1985; Tuazon *et al.*, 1986) indicate that the α-dicarbonyls represent only a relatively small fraction of the aromatic ring fragmentation process, and that the mechanism previously

assumed for this process (e.g. Atkinson *et al.*, 1980; Atkinson and Lloyd, 1984) is almost certainly incorrect. The products formed in this process are not well characterized, and the available data suggest that, in addition to the simple α-dicarbonyls, a large number of unsaturated oxygenated products are formed, with no single product being formed in large yield. Thus, we make no attempt to represent these products explicitly, but instead use two generalized 'aromatic unknown' species, called AFG1 and AFG2, in the present mechanism to represent the reactions of the reactive uncharacterized ring-opened products. The yields of these products are adjusted based on simulations of the chamber data, as discussed below. AFG1 is used to represent products not containing alkyl groups, which are formed in the reactions of benzene, the naphthalenes and tetralin. AFG2 is used to represent products which contain alkyl groups, and which appear to be generally much more reactive. These are formed in the toluene, xylenes, alkylnaphthalenes and other alkyl-substituted aromatics. The mechanisms used for these products are discussed in more detail below, in conjunction with the discussion of the aromatic photooxidation mechanisms.

General representation of organic peroxy and acyl peroxy radical reactions

The atmospheric photooxidations of most organic compounds involve the intermediacy of at least one, and in most cases several, unique peroxy or acyl peroxy radical species. The major removal processes for these peroxy radicals are either reaction with NO, NO_2, HO_2 or with other peroxy or acyl peroxy radicals. For example, alkyl peroxy radicals (RO_2) undergo the following types of reactions, with acyl peroxy radicals (RCO_3) reacting analogously:

$$RO_2 + NO \rightarrow NO_2 + RO.$$

$$RO_2 + NO \rightarrow RONO_2$$

$$RO_2 + NO_2 \rightarrow RO_2NO_2$$

$$RO_2 + HO_2 \rightarrow RO_2H$$

$$RO_2 + RO_2 \rightarrow \text{products.}$$

Because of the large number of organics emitted into polluted urban atmospheres, explicit representation of all of these individual reactions would require inclusion of a large number of species and reactions in the model, particularly if all the possible cross-combination reactions of the various organic peroxy and acyl peroxy radicals were included. To keep the total mechanism down to a practical and manageable size, atmospheric photooxidation mechanisms for realistic 'surrogate' mixtures have had to incorporate approximations concerning these reactions.

Most current atmospheric photooxidation mechanisms reduce the total number of peroxy radical reactions by neglecting the $RO_2 + NO_2$ reactions. This can be justified because organic peroxynitrates so formed undergo rapid thermal back-decomposition (Atkinson and Lloyd, 1984), resulting in no net loss process. Test calculations indicate that this approximation introduces no significant inaccuracies in the overall predictions in the mechanism, at least for temperatures greater than 270 K (Carter *et al.*, 1986b). Therefore, these $RO_2 + NO_2$ reactions are also neglected in this mechanism.

A much more severe approximation, incorporated in many previous chemical mechanisms (for example, the ALW mechanism (Atkinson *et al.*, 1982)) is to neglect all of the peroxy + peroxy and peroxy + HO_2 radical reactions on the basis that under daytime conditions when NO_x levels are high enough to promote O_3 formation, these reactions are much less important than reaction of peroxy radicals with NO. However, for mechanisms designed to be used for multi-day simulation purposes, including LRT and acid deposition modeling, the inclusion of these reactions is necessary, and indeed these are included in the acid deposition models of Lurmann *et al.* (1986) and NCAR (Stockwell, 1986; NCAR, 1987). Test calculations we have carried out show that these reactions can have significant effects on results of even single-day environmental chamber simulations. Thus, it is necessary to include these reactions in the mechanism.

However, to represent accurately all the reactions of peroxy radicals with HO_2 and other peroxy radicals, the numbers of reactions in the mechanism would increase substantially. This is due to the large numbers of different types of peroxy radicals involved in the photooxidations of the many types of organics emitted into the atmosphere. Thus, in this mechanism we do not represent the reactions of the peroxy radicals

Table 10. Peroxy radical pseudo-species used in the mechanism to represent overall processes common to peroxy radical reactions

Pseudospecies name	Products formed		
	Reaction with NO	Reaction with HO_2	Reaction RO_2/RCO_3
RO_2–R·	$NO_2 + HO_2$	–OOH	0.5 HO_2
RO_2–N·	RNO_3	–OOH + MEK	0.5 HO_2 + MEK
RO_2–XN·	(Loss of N)	–OOH	0.5 HO_2
RO_2–NP·	Nitrophenol	–OOH + (inert)	0.5 HO_2 + (inert)
R_2O_2	NO_2	None	None

explicitly, but instead use an approximate and condensed method to represent these reactions.

Representation of organic peroxy radical reactions. Instead of representing the formation of individual organic peroxy radicals explicitly, in any reaction where such a radical is formed the radical is replaced by the following: (a) the set of oxygenated product species (other than organic nitrates) which are expected to be ultimately formed when the peroxy radical reacts in the presence of NO; (b) a set of chemical 'operators' which are used to represent the various net effects of the peroxy radical reactions on NO consumption, NO_2 formation, HO_2 consumption and formation, organic nitrate formation and hydroperoxide formation and (c) the chemical operator $RO_2.$, which is used to calculate the total concentration of all organic peroxy radicals. These chemical operators are summarized in Table 10.

For example, *t*-butyl peroxy radicals are expected to react in the presence of NO_x as follows:

$$(CH_3)_3COO. + NO \rightarrow NO_2 + (CH_3)_3CO.$$
$$\downarrow$$
$$CH_3COCH_3 + CH_3. \xrightarrow{O_2} CH_3COCH_3 + CH_3OO.$$
$$CH_3OO. + NO \rightarrow CH_3O. + NO_2 \xrightarrow{O_2} HCHO + HO_2 + NO_2$$

or overall:

$$(CH_3)_3COO. \rightarrow CH_3COCH_3 + HCHO + (NO_2 - NO) + (HO_2 + NO_2 - NO).$$

In this mechanism, in any reaction forming $(CH_3)_3COO.$ that species would be replaced by the set of species: $CH_3COCH_3 + HCHO + R_2O_2. + RO_2\text{–}R. + RO_2.$, where the first two products represent the non-nitrate organic products formed in the presence of NO, the $R_2O_2.$ and RO_2–R. represent the two NO to NO_2 conversions, with RO_2–R. also representing the generation of HO_2 in the overall reaction, and the $RO_2.$ represents the contribution of formation of *t*-butyl peroxy radicals to the total formation of organic peroxy radicals.

The total organic peroxy radical operator, $RO_2.$, is used to calculate total rates of organic peroxy radicals with other peroxy radicals and with acyl peroxy radicals. The steady state approximation should not be used on this operator. Its rate of formation is calculated by including it as a product in any reaction forming organic peroxy radicals, and including the following pseudo-reactions in the mechanism:

$$RO_2. + NO \rightarrow NO \quad \text{(B1)}$$
$$RO_2. + HO_2 \rightarrow HO_2 \quad \text{(B5)}$$
$$RO_2. + RO_2. \rightarrow \quad \text{(B8)}$$
$$RO_2. + RCO_3. \rightarrow . \quad \text{(B9)}$$

($RCO_3.$ is the operator representing total acyl peroxy radical concentrations, calculated analogously as discussed below.) Reactions (B1)–(B9) are not true chemical reactions, but are included in the mechanism only for the purpose of calculating $RO_2.$ concentrations. They are written in the incomplete form above because the effects of reactions of peroxy radicals on NO, NO_2 and HO_2 are accounted for in the reactions of the other operators listed in Table 10. Note also that the operators $RO_2.$ and $RCO_3.$ represent no mass or radical centers, so all the above reactions are balanced in this regard.

With the total organic peroxy radical (and acyl peroxy radical) concentrations calculated as indicated above, the relative effects of the peroxy + peroxy radical reactions in competing with peroxy + NO and peroxy + HO_2 reactions can then be calculated. Since the operators RO_2–R., RO_2–N. (Table 10), $R_2O_2.$, etc. are used to calculate the effects of these reactions, this is represented by including the reactions of $RO_2.$ (and $RCO_3.$) with these chemical operators. For example, in the case of RO_2–R., the species used to represent NO to NO_2 conversion and HO_2 formation in the presence of NO, the effect of the competing peroxy radical reactions on NO, NO_2, HO_2 and organic hydroperoxide radical concentrations are represented as follows:

$$RO_2\text{–}R. + NO \rightarrow NO_2 + HO_2 \quad \text{(B11)}$$
$$RO_2\text{–}R. + HO_2 \rightarrow \text{–OOH} \quad \text{(B12)}$$
$$RO_2\text{–}R + RO_2. \rightarrow RO_2. + 0.5\,HO_2 \quad \text{(B13)}$$
$$RO_2\text{–}R + RCO_3. \rightarrow RCO_3. + 0.5\,HO_2. \quad \text{(B14)}$$

Note that $RO_2.$ is included as a product as well as a reactant in reaction (B13) because the consumption of $RO_2.$ due to reaction with other peroxy radicals is already represented in reaction (B8) above. Similarly, $RCO_3.$ is included as a product in reaction (B14).

The species –OOH is used to represent the formation of hydroperoxide groups in the reactions of HO_2 with organic peroxy radicals. The 0.5 HO_2 is included as a product in reactions (B13) and (B14) based on the assumption that the self-reactions of peroxy radicals occur approximately 50% of the time via radical producing routes. This in turn is based on data for

$$CH_3OO. + CH_3OO. \rightarrow 2\,CH_3O. + O_2;$$
$$\rightarrow HCHO + CH_3OH + O_2$$
$$CH_3O + O_2 \rightarrow HCHO + HO_2$$

occur at approximately equal rates (Atkinson and Lloyd, 1984; Atkinson, 1988). The products in the reactions used for the other peroxy radical operators are analogous, and are indicated in Table 10.

Representation of acyl peroxy radical reactions. The reactions of acyl peroxy radicals cannot be represented in as condensed a manner as used for the organic peroxy radicals, because the products formed from their reaction with NO_2 (e.g. PAN and its analogues) are relatively stable and cannot be neglected. Thus the nature of the products they form depends significantly on the NO to NO_2 ratio. This means that the use of the same set of species to represent the organic products regardless of the NO/NO_2 ratio, as for the other organic peroxy radicals, would not be an acceptable approximation for the acyl peroxy radical reactions. Therefore, the four acyl peroxy radicals formed from the species in this mechanism (i.e. $CCO\text{–}O_2.$, $C_2CO\text{–}O_2.$, $BZ\text{–}CO\text{–}O_2.$ and $HCOCO\text{–}O_2.$) and their corresponding PAN analogues (PAN, PPN, PBZN and GPAN) are represented explicitly. However, to permit calculation of the total acyl peroxy radical concentration, any reaction forming these acyl peroxy radicals also includes as a product the total acyl peroxy radical species $RCO_3.$ and destruction reactions for $RCO_3.$, analogous to those shown above for $RO_2.$, are also included in the mechanism. The use of $RCO_3.$ to represent the total acyl peroxy radical concentrations permits the use of the steady state approximation on the five individual acyl peroxy radical species. This means that a much smaller set of reactions are required to represent the reactions of the acyl peroxy radicals with themselves and with the organic peroxy radical operators.

Chemical approximations involved. This representation of peroxy radical reactions involves essentially no significant chemical approximation for conditions when the major fate of peroxy radicals is reaction with NO. This is generally the case when both NO_x and light are present, and when ozone formation is occurring. However, for low NO_x conditions when the peroxy + peroxy radical reactions become important, this representation becomes more approximate. It implicitly incorporates the approximations that (a) the set of oxygenated products formed when an organic peroxy radical or acyl peroxy radical reacts with itself or another peroxy radical can be represented by the oxygenated products formed when the radical reacts in the presence of NO, (b) that the organic hydroperoxides formed in organic peroxy + HO_2 reactions can be represented by the set of oxygenated products formed when the radical reacts with NO, plus the chemical operator –OOH which is used to represent formation and reactions of hydroperoxide groups; and (c) that a single rate constant can be used to represent all $RO_2 + RO_2$ radical reactions. The latter approximation is particularly extreme, since the rate constants for the organic peroxy + peroxy reactions differ by orders of magnitude, depending on whether the radical is primary, secondary or tertiary (e.g. see Atkinson and Lloyd, 1984; Atkinson, 1988, and references therein). However, use of these approximations permits a complete representation of all the peroxy + peroxy radical reactions without the need to include explicitly all of the possible combinations, which would require many hundreds of reactions. This is a significant improvement on other published mechanisms, which either ignore these reactions altogether or represent only a subset of all of the possible peroxy + peroxy combinations. Test calculations (Carter *et al.*, 1986b) indicate that this approximation does not have an adverse effect on predictions of O_3, PAN and most other species, even under conditions where neglecting peroxy + peroxy reactions introduces significant errors.

Representation of alkane and aromatic reactions

Although the details of their atmospheric reaction mechanisms are quite different, both alkanes and aromatic hydrocarbons react essentially only with hydroxyl radicals, and the net effect of these reactions can be represented in the mechanism by a single lumped reaction:

$$OH + \text{alkane/aromatic} \rightarrow \text{parm}_1\ \text{product}_1 + \text{parm}_2\ \text{product}_2 + \ldots$$

where $product_1$, $product_2$, etc., refer to the set of organic products ultimately formed and the various chemical operators ($RO_2.$, $RO_2\text{–}R.$, $R_2O_2.$, etc.) representing the other effects of these reactions, and where $parm_1$, $parm_2$, etc., represent the yields of these products or chemical operators. Both the rate constant and the product yields depend on the individual alkane or aromatic hydrocarbon represented. The types of product yield parameters used for the alkane and aromatic species are summarized in Table 4, and the values assigned for individual alkanes and aromatics are given in Tables 6 and 7, respectively. The derivation of these values is summarized below.

Derivation of mechanistic parameters for alkanes. The OH radical reaction rate constants and the product yield parameters for the alkanes are given in Table 6. These were derived based on the results of the evaluation of the atmospheric reactions of alkanes given by Carter and Atkinson (1985), as updated by the more recent evaluations of Atkinson (1987, 1988, 1990). Because of the large numbers of different types of alkyl peroxy and alkoxy radicals which can be involved in the atmospheric reactions of the higher molecular weight alkanes (due primarily to the variety of reactions which a number of the alkoxy radical intermediates can undergo), a computer program was employed to derive the major features of the overall

reaction mechanism. This program operated as follows.

(1) Using the estimation techniques developed by Atkinson (1986) and as recently updated (Atkinson, 1987), the rates of OH radical reactions with the various C–H bonds in the alkane were calculated. These were then used to derive both the total OH radical rate constant for the alkane and the relative yields of the various initially-formed radicals.

(2) For each initially formed radical, the distribution of products ultimately formed in the presence of NO_x, and the total amount of NO to NO_2 conversions, or NO and radical consumption due to organic nitrate formation, were calculated. These calculations used the alkoxy and alkyl peroxy radical branching ratio estimates given by Carter and Atkinson (1985), as updated by Atkinson (1988, 1990), except for decomposition rate constants assumed for the 2-butoxy radicals, where the experimentally derived value (see Carter and Atkinson, 1985; Atkinson, 1990, and references therein) was used. Since many of the initially-formed organic radicals are predicted to form other organic radicals, which in turn frequently form yet other radicals, this process is repeated for each of the radicals predicted to be formed until the reactions and products of all of the organic radical intermediates have been accounted for.

(3) Based on the total amounts of NO to NO_2 conversions, and the ultimate yields of HO_2 and organic nitrates, the total yields of the peroxy radical operators, RO_2–R., R_2O_2., RO_2–N. and RO_2–XN, are determined. (The reactions of $C_{\leq 3}$ nitrates are ignored, so the effects of nitrate formation from $C_{\leq 3}$ peroxy radicals is prepresented by RO_2–XN.)

(4) Based on the detailed distribution of organic products ultimately predicted to be formed from the various peroxy and alkoxy radical reactions, the program calculated the yields of the organic products in terms of the species used in this mechanism and for the oxygenated products as follows: formaldehyde (HCHO), acetaldehyde (CCHO), acetone (ACET) and CO are represented explicitly; propionaldehyde (RCHO) is used to represent the higher aldehydes; methyl ethyl ketone (MEK) is used to represent the higher ketones; the bi- and poly-functional products formed following alkoxy radical isomerization of the long chain alkanes were represented by RCHO and MEK, where RCHO represented all the –CHO groups in these species, and MEK represented the –OH or –CO– groups. If the use of MEK to represent all the –OH and –CO– groups in these species resulted in more carbons being represented than were present in the bifunctional products, then the yield of MEK was reduced so that the resulting mixture of RCHO and MEK had the same number of carbons as was present in the bi- and poly-functional products.

Note that a few cycloalkanes are predicted to form small yields of acyl peroxy radicals (Carter and Atkinson, 1985). This is not represented in this mechanism. Instead, in these cases the ultimate product yields are determined by assuming that these radicals all react with NO to form CO_2 and the corresponding alkoxy radical. The CO_2 yields listed in Table 6 indicate the extent to which acyl peroxy radicals are predicted to be formed, since this is the only source of CO_2 in our estimated alkane photooxidation mechanisms.

Although this automated procedure for deriving OH radical rate constants and product yield parameters for the alkane reactions is based on previously published evaluations and estimates, many of these estimates are highly uncertain, and the atmospheric reactions of the higher molecular weight alkanes cannot be considered to be well established. In particular, the estimates of the processes occurring following the 1,5-H shift isomerizations of long chain alkoxy radicals have never been verified by product studies. In addition, based primarily on fits to chamber data (Carter *et al.*, 1986b, 1987), we assume that alkyl nitrate formation from the reaction of NO with HO– or –CO– substituted peroxy radicals does not occur, despite the fact that it is clear that it can be important in the case of unsubstituted radicals (Carter and Atkinson, 1985). Moreover, fitting of model simulations to results of smog chamber experiments does not provide a good test of alkane–NO_x–air runs are highly sensitive to assumptions concerning the chamber radical source, which tends to vary from run to run (Carter *et al.*, 1982a).

The kinetic and mechanistic parameters given in Table 6 are those estimated for $T = 300$ K. Parameters for $T = 270$ and 330 K are given elsewhere (Carter, 1988a), and parameters for intermediate temperatures can be estimated by linear interpolation of these values.

Derivation of mechanistic parameters for aromatics. The kinetic and mechanistic parameters for the reactions of the aromatic HCs, and comments giving the derivation or sources of the rate constants and kinetic parameters employed, are given in Table 7. The OH radical rate constants for the individual aromatic HCs are based on the most recent recommendations of Atkinson (1990). Product yield parameters for benzene,toluene, *m*-xylene and 1,3,5-trimethylbenzene were derived, in part, from the recent evaluation of Atkinson (1990) and in part from the results of simulations of environmental chamber experiments, as discussed below. For the other alkylbenzenes, the product yields were assigned by using those of toluene for all monoalkylbenzenes, using those of *m*-xylene for all dialkyl benzenes, and those of 1,3,5-trimethylbenzene for all tri- and poly-alkyl benzenes. Mechanistic parameters for naphthalene, 2,3-dimethylnaphthalene and tetralin were derived from empirical fits of model calculations to chamber experiments, also discussed below. Parameters derived for 2,3-dimethylnaphthalene are used for all di- and poly-alkyl naphthalenes, and averages of mechanistic parameters for naphtha-

lene and 2,3-dimethylnaphthalene were assumed to apply to all monoalkyl naphthalenes.

The use of toluene, *m*-xylene, 1,3,5-trimethylbenzene, naphthalene and 2,3-dimethylnaphthalene as the standards for deriving parameters for related aromatic compounds is based primarily on the availability of environmental chamber data for those compounds. Many of the experiments for toluene and *m*-xylene have been published previously (Atkinson *et al.*, 1980; Jeffries *et al.*, 1982). Most or all of the chamber experiments for the other compounds, and some for toluene and *m*-xylene, were carried out more recently, and have not been published elsewhere except in a final project report (Carter *et al.*, 1987). In particular, the availability of chamber experiments employing 1,3,5-trimethylbenzene, the naphthalenes and tetralin permit mechanisms for these types of compounds to be derived.

Discussions of our current knowledge of the atmospheric reactions of aromatic hydrocarbons, and the many uncertainties involved, are given elsewhere (e.g. Atkinson, 1986, 1990). In the case of the alkylbenzenes, data are available concerning the yields of phenol and glyoxal from benzene, and of cresols, benzaldehyde or tolualdehydes and the α-dicarbonyls from toluene and the xylenes, add of aromatic aldehydes and α-dicarbonyls from the trimethylbenzenes (Atkinson, 1986, 1990, and references therein), and these data were incorporated into this mechanism. As with other aromatic mechanisms (e.g. Atkinson *et al.*, 1980, 1982; Leone and Seinfeld, 1984a,b; Lurmann *et al.*, 1986; Whitten *et al.*, 1985) formation of the phenolic products was assumed to involve generation of HO_2 radicals without any NO to NO_2 conversions, and the formation of the aromatic aldehydes and the aromatic ring fragmentation products were assumed to involve one NO to NO_2 conversion before yielding HO_2 radicals. In contrast with the earlier aromatic mechanisms of Atkinson *et al.* (1980, 1982) and the latest carbon bond mechanisms (Gery *et al.*, 1988), but consistent with more recent mechanisms (Lurmann *et al.*, 1986; Leone and Seinfeld, 1984b; Stockwell, 1988), organic nitrate formation from the reactions of NO with the peroxy radicals formed in alkylbenzene photooxidants was assumed to be unimportant.

However, the products listed above account for only a portion of the reacted carbon, and qualitative product studies on toluene (Shepson *et al.*, 1984; Dumdei and O'Brien, 1984) indicate that a large variety of other aromatic ring-opened compounds, other than the α-dicarbonyls, are also formed. Previous aromatic photooxidation mechanisms (e.g. Atkinson *et al.*, 1980, 1983; Leone and Seinfeld, 1984a,b; Lurmann *et al.*, 1986) have generally been based on the assumption, made originally by Atkinson *et al.* (1980), that most of the 'missing' products consist of compounds such as 2-butene-1,4-dial and its substituted analogues, and included speculative reactions based on estimates for such compounds. However, the most recent product studies indicate that, although products of this type are formed to some extent, their yields are relatively minor and many other types of unsaturated oxygenated compounds are formed, with no single type of compound dominating. We make no attempt to speculate on the nature and detailed reactions of the uncharacterized aromatic products, but instead use two idealized species designated AFG1 and AFG2 to represent the reactions of these reactive aromatic fragmentation products. These species are not intended to represent any specific molecules, but rather are included (at yields adjusted to optimize fits of model simulations to chamber data) to account for the contributions of the uncharacterized aromatic ring fragmentation products to the overall reactivities observed in NO_x–air irradiations of aromatic HCs. The notes to Table 7 indicate the data used to determine the yields of these products in the adjusted empirical mechanism.

The mechanisms for the idealized species used to represent the uncharacterized aromatic products are in many respects based on those for glyoxal and methylglyoxal. However, for model simulations to fit the results of aromatic–NO_x–air runs carried out in the SAPRC indoor Teflon chamber (ITC), as well as runs carried out in other chambers, it is necessary to assume that these species photolyze down to shorter wavelengths than do the α-dicarbonyls. As discussed by Carter *et al.* (1987), the SAPRC ITC employs a blacklight light source which has relatively low intensity in the wavelength region overlapping the longer wavelength absorption band of the α-dicarbonyls. Thus, the ratio of the photolysis rate of methylglyoxal to that of NO_2 is calculated to be approximately six times lower in the ITC than in the SAPRC evacuable chamber (EC) or in outdoor chambers using natural sunlight. Despite this, aromatic–NO_x–air chamber runs carried out in the ITC are comparable in reactively to those carried out in other chambers (Carter *et al.*, 1987) This indicates that a significant radical source in aromatic must be due to photolysis of some species at shorter wavelengths. In particular, if most of the radicals are assumed to be due to photolysis of α-dicarbonyls or compounds with similar spectral responses, then mechanisms which are adjusted to simulate results of aromatic runs carried out in the EC and in outdoor chambers would significantly underpredict reactivities observed in such runs carried out in the ITC. However, assuming that the uncharacterized ring fragmentation products AFG1 and AFG2 photolyze to form radicals rapidly at wavelengths below $\sim$ 350 nm allows the mechanism to account for the reactivities observed in aromatic–NO_x–air irradiations carried out in the ITC, as well as in other chambers.

This detailed mechanism also includes representations of the reactions of naphthalene, the alkyl naphthalenes and tetralin. Relatively little is known concerning the atmospheric reactions of these bicyclic aromatic compounds other than their initial rates of reaction with the OH radical (Atkinson, 1986, 1990),

and the fact that their reactions with O_3, NO_3 radicals and N_2O_5 are not important under atmospheric conditions (Atkinson, 1990). The results of NO_x–air irradiations of naphthalene, 2,3-dimethyl naphthalene and tetralin (carried out in the ITC) indicate that, despite their relatively high OH radical rate constants (which are comparable or higher to those for the xylenes), the naphthalenes and tetralin are considerably less reactive with respect to rates of ozone formation than are the alkylbenzenes (Carter *et al.*, 1984, 1987). Thus, models which assume that these bicyclic aromatics have similar mechanisms as alkylbenzenes will significantly overpredict their reactivities (Carter *et al.*, 1984). Table 7 indicates the specific empirical mechanistic parameters used to represent the reactivities of these species, and the specific sets of environmental chamber data used to derive the values used in the mechanisms. As far as we are aware, no other atmospheric photochemical reaction mechanism includes separate representations of the reactions of these species.

Representation of alcohols, ethers and acetylenes

Like alkanes and aromatics, the alcohols, ethers, acetylenes, and similar compounds react in the atmosphere primarily with hydroxyl radicals. Therefore, these compounds can also be represented using the generalized lumped reaction given above and the set of mechanistic parameters listed in Table 4. Table 8 gives the OH radical rate constant and mechanistic parameter assignments for these compounds. The rate constant assignments are based primarily on the most recent recommendations of Atkinson (1990), and the assignments for the product yield parameters are based primarily on estimates we have made for analogous radicals formed in alkane photooxidation systems, as discussed in detail elsewhere (Carter and Atkinson, 1985). The types of products these species form are in most cases analogous to those formed in alkane photooxidation systems, and in general their reactivities are comparable to alkanes. However, except for methanol, which was employed in a series of methanol substitution chamber experiments (Carter *et al.*, 1986a) and included in the set of chamber runs used to test this mechanism (Carter *et al.*, 1986b; Carter, 1988a), the assignments made for these species have not been tested against chamber data.

Representation of alkene reactions

Unlike the alkanes and the aromatic HCs, the alkenes can also react to a non-negligible extent with O_3 and NO_3 radicals. In addition, this mechanism also includes their reactions with $O(^3P)$ atoms, since these can be non-negligible under relatively high NO_x conditions which occur in some chamber experiments used to evaluate the mechanism, and also in plumes and other high-NO_x atmospheric modeling applications. Because of these additional reactions, the alkenes cannot be represented by the generalized scheme discussed above for species which react only with OH radicals. Instead, this mechanism represents the reactions of ethene explicitly, and represents the higher alkenes using a generalized scheme which is discussed below.

Generalized alkene + OH radical reactions. The rate constants used for the reactions of OH radicals with the individual alkene species in this mechanism are those recommended by Atkinson (1990) and are given in Table 9. These reactions are believed to occur via the following general mechanism:

$$\mathrm{OH} + \mathrm{R_1R_2C{=}CR_3R_4} \rightarrow \mathrm{R_1R_2\overset{HO}{\overset{|}{C}}\text{–}\dot{C}R_3R_4} \xrightarrow{O_2} \mathrm{R_1R_2\overset{HO\ OO.}{\overset{|\quad|}{C}}\text{–}CR_3R_4}$$

$$\mathrm{R_1R_2\overset{HO\ OO.}{\overset{|\quad|}{C}}\text{–}CR_3R_4} \xrightarrow{NO} \mathrm{R_1R_2\overset{HO\ O.}{\overset{|\quad|}{C}}\text{–}CR_3R_4} + NO_2 \qquad (a)$$

$$\xrightarrow{NO} \mathrm{R_1R_2\overset{HO\ ONO_2}{\overset{|\quad|}{C}}\text{–}CR_3R_4} \qquad (b)$$

$$\mathrm{R_1R_2\overset{HO\ O.}{\overset{|\quad|}{C}}\text{–}CR_3R_4} \rightarrow \mathrm{R_1R_2\dot{C}OH} + \mathrm{R_3R_4C{=}O} \xrightarrow{O_2} \mathrm{R_1R_2C{=}O} + \mathrm{R_3R_4C{=}O} + HO_2 \qquad (c)$$

$$\mathrm{H_2\overset{HO\ O.}{\overset{|\quad|}{C}}\text{–}CH_2} \xrightarrow{O_2} \mathrm{H_2\overset{HO}{\overset{|}{C}}\text{–}CHO} + HO_2. \qquad (d)$$

If we ignore process (d), which is believed to be important only in the case of ethene (Niki *et al.*, 1981; Atkinson, 1986, 1990), then the overall OH + alkene reactions in the presence of NO can be represented as

$$\mathrm{R_1R_2C{=}CR_3R_4} + \mathrm{OH} \rightarrow (1-p_N)(\mathrm{R_1R_2C{=}O} + \mathrm{R_3R_4C{=}O} + HO_2 - NO + NO_2) + p_N(\mathrm{R_1R_2\overset{HO\ ONO_2}{\overset{|\quad|}{C}}\text{–}CR_3R_4} - NO)$$

where p_N is $b/(a+b)$, the organic nitrate yield assumed in the reaction of the OH-substituted peroxy radical formed in the OH + alkene reaction.

In terms of the species used in this mechanism to represent reactive organic products and the effects of peroxy radical reactions, this overall process can be represented as follows:

$$\text{alkene} + \text{OH} \rightarrow (1-p_N)(\text{RO}_2\text{–R}. + p_1\,\text{HCHO} + p_2\,\text{CCHO} + p_3\,\text{RCHO} + p_4\,\text{ACET} + p_5\,\text{MEK}) + p_N\,\text{RO}_2\text{–N},$$

where p_1–p_5 are structural parameters indicating the substituents about the double bond where the reaction with OH radicals occurs. These are defined as follows:

p_1 = number of $=CH_2$ groups about the double bond
p_2 = number of $=CHCH_3$ groups
p_3 = number of $=CHR$ groups, where R not H or CH_3
p_4 = number of $=C(CH_3)_2$ groups
p_5 = number of $=C(CH_3)R$ or $=CR_2$ groups, where R not H or CH_3.

Note that for acyclic alkanes the values of these structural parameters must sum up to 2, and for dialkenes they refer to the substituents about the more reactive of the doube bonds. This generalized reaction scheme is also used for the cycloalkenes, where the structural parameters are assigned such that they sum up to 1. The values for the structural parameters used for the individual alkenes are given in Table 9.

The above scheme ignores reaction via routes such as abstraction from allylic hydrogens, e.g.

$$CH_3CH_2CH{=}CH_2 + OH \rightarrow CH_3\dot{C}H\text{–}CH\text{–}CH_2 + H_2O.$$

Atkinson *et al.* (1985) showed that in the case of 1-butene, this process occurs less than 10% of the time at room temperature, and clearly this reaction is relatively even less important for internal alkenes because of the more rapid reaction at the double bond. Reactions at other positions on long-chain alkenes are also estimated to be relatively unimportant (Atkinson, 1987, 1988, 1990), and are also ignored in this mechanism.

The organic nitrate yield parameter, p_N, must also be specified to completely characterize the alkene + OH radical reaction mechanism. As with alkanes, this is an important parameter affecting overall reactivity, since organic nitrate formation represents both a radical and a NO_x sink. Shepson *et al.* (1985) observed only 1.6% organic nitrate formation from propene at room temperature and atmospheric pressure, indicating it is essentially of negligible significance for that alkene. We also assume that it is not significant for the butenes. However, model simulations of 1-hexene–NO_x–air experiments carried out in the SAPRC ITC could only fit the data if it is assumed that organic nitrate formation occurs ~ 23% of the time (Carter *et al.*, 1987). This is comparable to the ~26% organic nitrate formation assumed for *n*-pentane (Table 6). Thus for the C_{5+} alkenes, we estimate that p_N is approximately the same as the fraction of nitrate formation in the peroxy radicals formed from the *n*-alkane with the same number of carbons. Note that this estimate is highly uncertain for the internal alkenes, since there are no data available for organic nitrate formation from these species, and also for the highest molecular weight alkenes, since this estimate involves a large extrapolation based on model simulations of only a single compound.

In particular, this estimation of p_N based on nitrate yields from *n*-alkanes does not appear to be valid for α-pinene, a C_{10} cyclic internal alkene. Model simulations of several α-pinene–NO_x–air irradiations carried out in the UNC outdoor chamber (Jeffries *et al.*, 1982), using the p_N value of 0.38 derived based on that estimated for *n*-decane, significantly underpredict the reactivity observed in those experiments. On the other hand, assuming $p_N = 0$ gives much better fits to these data. Therefore, we assume that organic nitrate formation in the OH radical reaction is negligible for α-pinene and other terpenes.

Generalized ozone reaction mechanisms. The rate constants used for the reactions of O_3 with the various alkene species represented in this mechanism are based on the recommendations of Atkinson and Carter (1984), as updated by Atkinson (1988, 1990), and are also given in Table 9. The mechanisms we assume for these reactions are discussed by Carter *et al.* (1986b) and by Atkinson (1988, 1990). They are believed to proceed initially as follows.

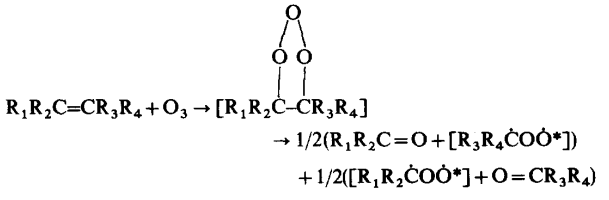

$$R_1R_2C{=}CR_3R_4 + O_3 \rightarrow [R_1R_2C(O_3)\text{–}CR_3R_4] \rightarrow 1/2(R_1R_2C{=}O + [R_3R_4\dot{C}O\dot{O}^*]) + 1/2([R_1R_2\dot{C}O\dot{O}^*] + O{=}CR_3R_4)$$

with the vibrationally excited Criegee intermediates (e.g. $[R_1R_2\dot{C}O\dot{O}^*]$) reacting further. This process can be expressed by the following general scheme, using the same set of structural parameters and oxygenated

product species employed for the OH radical reaction:

$$\begin{aligned}\text{alkene} + O_3 \rightarrow\ & p_1/2\ (HCHO + [HCHO_2^*]) \\ & + p_2/2\ (CCHO + [CCHO_2^*]) \\ & + p_3/2\ (RCHO + [RCHO_2^*]) \\ & + p_4/2\ (ACET + [C(C)CO_2^*]) \\ & + p_5/2\ (MEK + [C(R)CO_2^*])\end{aligned}$$

where $[HCHO_2^*]$, $[CCHO_2^*]$, etc., represent the various types of initially formed vibrationally excited fragmentation intermediates. The subsequent reactions of these species, which are assumed to be independent of the nature of the alkene from which they originated, are then derived as described by Carter *et al.* (1986b), and are briefly summarized below.

The species $[HCHO_2^*]$ represents the initially formed excited biradical formed in the reactions of O_3 with alkenes with terminal $=CH_2$ groups, and its mechanism is derived based on data for the ethene system. The reactions of $[HCHO_2^*]$ are the best characterized of the biradicals formed in the O_3 + alkene systems, and the mechanism we assume is based on that recommended by Atkinson (1988, 1990) [which is similar to that recommended by Atkinson and Lloyd (1984)]. A number of studies are reasonably consistent in indicating that $\sim 37\%$ of this initially formed radical is stabilized under atmospheric conditions [see Atkinson (1988, 1990) and references therein], with the remainder undergoing decomposition. The decomposition mechanism derived by Atkinson and Lloyd (1984) is assumed. Based on this, the overall reactions of this excited species (including stabilization) is then

$$[HCHO_2^*] \xrightarrow{M} 0.37\,HCHO_2 + 0.12\,HO_2 + 0.13\,H_2 + 0.19\,CO_2 + 0.44\,CO + 0.44\,H_2O$$

where $HCHO_2$ represents the stabilized biradical.

As discussed by Atkinson (1988, 1990), the stabilized biradical can react with CO, H_2O, NO_x, aldehydes or SO_2. Based on rate constants estimated by Atkinson (1990), the reaction with H_2O, forming formic acid, is estimated to dominate under atmospheric conditions. Thus, we assume that the primary fate of $HCHO_2$ is formation of formic acid, whose subsequent reactions are neglected in this mechanism. However, to account for possible effects of O_3 + alkene reactions on SO_2 oxidation to sulfate, which may be of concern in acid deposition modeling applications, this mechanism also has stabilized biradicals forming the chemical operator designated O_3OL-SB, a zero-carbon pseudo-species, which either reacts with H_2O to be destroyed or reacts with SO_2 to form H_2SO_4, with a H_2O/SO_2 rate constant ratio of 2.3×10^{-4} as derived from the data of Suto *et al.* (1985) and discussed by Atkinson (1988). (See discussion of SO_2 reactions in the notes to Table 2.) This representation is used for the other stabilized biradicals as well and permits the effects of the biradical reaction on SO_2 to be taken into account. However, it ignores the effect of SO_2 on the products of the O_3 + alkene reactions which, under most conditions, are expected to be small.

Therefore, the overall reactions used in this mechanism for the initially formed biradical formed in reactions of O_3 with alkenes containing terminal $=CH_2$ groups is as follows:

$$[HCHO_2^*] \rightarrow 0.37\,O_3OL\text{–}SB + 0.44\,CO + 0.12\,HO_2\cdot + 0.44\ -C.$$

Lost carbon (–C) is used to represent the formic acid and the CO_2 formed from the decomposition; the H_2 and H_2O which are also formed are ignored.

The species $[CCHO_2^*]$ represents the initially formed excited biradical formed when O_3 reacts with alkenes with $=CHCH_3$ groups. There are some data concerning its reactions from studies of O_3 + propene and O_3 + 2-butene reactions, but its reactions are much more uncertain than are those of $[HCHO_2^*]$, and it appears that not all the reaction routes can be accounted for. The data of Hatakeyama *et al.* (1984), based on oxidation of SO_2 by stabilized biradicals from the reactions of O_3 with a variety of alkenes, indicate that under atmospheric conditions $\sim 20\%$ of the $[CCHO_2^*]$ undergoes collisional stabilization. The observation of 14% yields of CH_4 in O_3 + *cis*-2-butene reactions (Niki *et al.*, 1977) indicates that $[CCHO_2^*]$ decomposes to form $CH_4 + CO_2 \sim 14\%$ of the time. Dodge and Arnts (1979) and Atkinson and Lloyd (1984) suggest that the remaining pathways, which would be 66% of the initially formed excited biradical, all involve fragmentations to form radicals. However, Carter *et al.* (1986b) found that assuming 66% radical formation from $[CCHO_2^*]$ results in significant and consistent overpredictions of rates of O_3 and PAN formation in model simulations of propene–NO_x–air environmental chamber experiments. The results of these experiments tend to be much better simulated if decomposition of $[CCHO_2^*]$ to radicals is assumed to occur only 30% of the time, which is somewhat smaller than the original estimate of 48% of Atkinson and Lloyd (1984) made before the stabilization data of Hatakeyama *et al.* (1984) were available.

Therefore, in this mechanism, we assume that $[CCHO_2^*]$ undergoes 20% stabilization [as indicated by the data of Hatakeyama *et al.* (1984)], 14% decomposition to methane + CO_2, 30% decomposition to radicals, and that the remaining 36% reacts via an unspecified, nonradical producing, decomposition route. The 0.72 carbons in the unknown product(s) resulting from the unspecified, nonradical forming route are arbitrarily represented by 0.18 MEK. By analogy with the reactions of stabilized $HCHO_2$ discussed above, the stabilized $CCHO_2$ is assumed to react in the atmosphere primarily with H_2O to form acetic acid, whose reactivity is also represented by MEK (in an amount with the same number of carbons). As with $HCHO_2$, chemical operator O_3OL-SB

is used to represent the possible contribution of this stabilized biradical to oxidation of SO_2. Therefore, assuming the relative rates of the various possible radical fragmentation processes derived by Atkinson and Lloyd (1984) and Dodge and Arnts (1979), the overall reactions assumed for excited biradicals formed in O_3 reactions with alkenes with $=CHCH_3$ groups are represented in this mechanism by

$$[CCHO_2^*] \rightarrow 0.2\,O_3OL\text{–}SB + 0.28\,MEK + 0.15\,CO + 0.3\,HCHO + 0.27\,RO_2\text{–}R. + 0.27\,RO_2. + 0.21\,HO_2 + 0.12\,HO. + 0.43\,\text{–}C.$$

The species $[RCHO_2^*]$ represents the initially formed excited biradical formed when O_3 reacts with alkenes containing =CHR groups, where R is an alkyl group other than methyl. The subsequent reactions of this species is even more uncertain than is the case for $[CCHO_2^*]$, discussed above. We assume, in analogy with our assumptions for $[CCHO_2^*]$, that this species is stabilized 20% of the time, decomposes to CO_2 + ethane 14% of the time, decomposes to radicals 30% of the time, with the remainder decomposing to form unspecified reactive products, and are represented by MEK with the same number of carbons. Assuming the radical fragmentation pathways analogous to those assumed for the methyl-containing species, and using an analogous representation of the stabilization processes, the mechanism we assume for the overall reactions of this species is then

$$[RCHO_2^*] \rightarrow 0.2\,O_3OL\text{–}SB + 0.42\,MEK + 0.15\,CO + 0.3\,CCHO + 0.27\,RO_2\text{–}R. + 0.27\,RO_2. + 0.21\,HO_2. + 0.12\,HO. + 0.57\,\text{–}C.$$

It should be emphasized that this mechanism is in many ways arbitrary and is extremely uncertain.

The species $[C(C)CO_2^*]$ represents the excited biradical initially formed when ozone reacts with alkenes with $=C(CH_3)_2$ groups. Its reactions under atmospheric conditions are also extremely uncertain. The total amount of formation of biradical stabilization observed by Hatakeyama *et al.* (1984) when O_3 reacts with isobutene is only 17–19%, which can all be accounted for if it is assumed that $[HCHO_2^*]$ is formed 50% of the time in this reaction. Thus, in this mechanism, we assume that stabilization of $[C(C)CO_2^*]$ is not important. This excited biradical could either undergo immediate fragmentation to form radicals

$$[(CH_3)_2\dot{C}O\dot{O}^*] \rightarrow 2\,CH_3. + CO_2 \qquad (a)$$

or could isomerize via an H-atom abstraction (via a five-member ring transition state) to form an excited hydroperoxide, which could either decompose or be stabilized

$$[(CH_3)_2\dot{C}O\dot{O}^*] \rightarrow [CH_2{=}C(CH_3)OOH^*] \xrightarrow{M} CH_2{=}C(CH_3)OOH \qquad (b)$$

$$\rightarrow .CH_2COCH_3 + OH \qquad (c)$$

$$CH_3COCH_2. \xrightarrow{O_2} \xrightarrow{NO} NO_2 + CH_3COCHO.$$

The only basis to choose among these alternative routes are model simulations of a single isobutene–NO_x–air chamber experiment carried out in the SAPRC ITC (Carter *et al.*, 1984, 1986b). As discussed by Carter *et al.* (1986b), the rates of ozone formation are, in that run, best fit if it is assumed that there is no radical formation from $[C(C)CO_2^*]$ [i.e. that pathway (b) dominates], while the high PAN yields observed in that experiment can only be fit if pathway (c) is assumed to be important. Thus, the data from that run are consistent with none of these mechanisms. In this mechanism, we arbitrarily assume that pathways (b) and (c) are equally important [with pathway (a) being assumed to be insignificant], and arbitrarily use MEK to represent the stabilization product. Thus, the overall fate of the biradical formed when ozone reacts with alkenes with $=C(CH_3)_2$ groups is represented by

$$[C(C)CO_2^*] \rightarrow 0.2\,(HO. + MGLY + RO_2\text{–}R. + RO_2.) + 0.8\,MEK + -0.8\,\text{–}C.$$

(The -0.8 –C is added for carbon balance.) This is obviously highly uncertain.

Finally, the species $[C(R)CO_2^*]$ is used to represent the excited biradicals initially formed when ozone reacts with alkenes with $=C(R)(CH_3)$ or $=CR_2$ groups, where R represents an alkyl group other than methyl. There are no data concerning the reactions of these species, and we assume that their reactions are analogous to the arbitrary mechanism discussed above for $[C(C)CO_2^*]$, except that instead of $CH_3COCH_2.$ being the radical formed in the decomposition process, 0.5 $CH_3COCH(\cdot)CH_3$ + 0.5 $CH_3COCH_2CH_2.$ are assumed to be formed, with their subsequent reactions being as discussed by Carter *et al.* (1986b). Thus, the overall process used to

represent the reactions of this species in this mechanism is

$$[C(R)CO_2^*] \rightarrow 0.2\ HO. + 0.1\ (HCHO + CCHO + CCO\text{–}O_2. + C_2CO\text{–}O_2.) + 0.2\ RCO_3. + 0.3\ (R_2O_2. + RO_2.) + 0.8\ MEK.$$

This is even more uncertain than the mechanisms assumed for the other excited biradical species, since it is not based on any experimental data.

The species $[HCHO_2^*]$, $[CCHO_2^*]$, etc., are not represented explicitly in this mechanism. Instead they are combined with the initial reaction forming them to yield an overall lumped O_3 + alkene reaction, given in Table 2, which represents the set of products, radicals and chemical operators which are ultimately formed. For any given alkene, the yield coefficients for the products in this overall reaction are calculated from the values of the structural parameters (p_1, p_2, p_3, etc.) based on assuming the sets of reactions given above. The resulting equations relating the product yields to the structural parameters are given in Table 5.

Representation of alkene + NO_3 radical reactions. The rate constants used for the reactions of NO_3 radicals with alkenes are those recommended by Atkinson (1988), and are given in Table 9. The temperature dependencies of these rate constants are not known, but are estimated by assuming the Arrhenius *A* factor to be the same as those for the corresponding OH radical reaction. The reactions of NO_3 radicals with alkenes are assumed to proceed as follows,

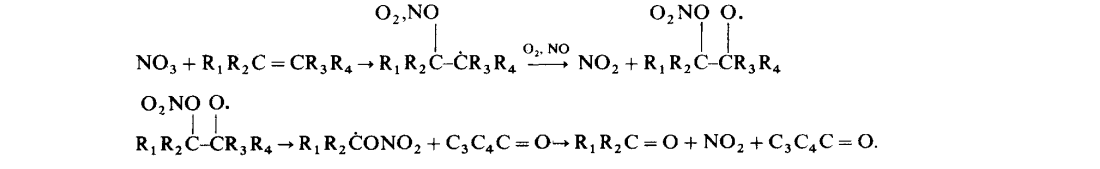

Note that this is analogous to the general scheme used for the reactions of OH radicals with the alkenes (other than ethene), except that no alkyl nitrate formation is assumed (though it may well occur), and that NO_2 is generated instead of HO_2. Thus, an analogous generalized reaction for this overall process, with the organic products being determined based in the structural parameters (p_1, p_2, etc.), can be employed. This is shown in Table 2.

Representation of $O(^3P)$ reactions. Although the reactions of $O(^3P)$ with alkenes are relatively unimportant in the concentration regime which usually occurs in the atmosphere, they are non-negligible in some of the chamber experiments used to evaluate the mechanism, and possibly also under some high NO_x conditions as may occur in plumes. Therefore, they are included in this mechanism to improve its range of validity. The rate constants used for these reactions are listed in Table 9.

The mechanisms for the reactions of $O(^3P)$ with representative alkenes are discussed by Atkinson and Lloyd (1984) and Carter *et al.* (1986b). Based primarily on the discussion in Atkinson and Lloyd (1984), Carter *et al.* (1986b) assumed the following overall processes for the reactions with propene, 1-butene, the 2-butenes and isobutene (given in terms of the species and chemical operators used in this mechanism):

$$O(^3P) + \text{propene} \rightarrow 0.6\ RCHO + 0.2\ CCHO + 0.4\ HCHO + 0.2\ CO + 0.6\ (RO_2\text{–}R. + RO_2.) + 0.2\ HO_2.$$

$$O(^3P) + \text{1-butene} \rightarrow 0.44\ MEK + 0.39\ (RCHO + -C) + 0.17\ CCHO + 0.17\ HCHO + 0.17\ CO + 0.34\ HO_2.$$

$$O(^3P) + \text{2-butene} \rightarrow MEK + 0.4\ HO_2.$$

$$O(^3P) + \text{isobutene} \rightarrow 0.5\ MEK + 0.5\ (RCHO + -C) + 0.4\ HO_2.$$

These mechanisms do not lend themselves to the generalized reaction schemes based on structural parameters as do the other reactions of the alkenes. Since this reaction is usually relatively unimportant, we did not attempt to generally develop a scheme which duplicates the above mechanism for the various types of compounds, but instead approximated them by the following overall process, which is used for all alkenes other than ethene,

$$O(^3P) + C_{3+}\ \text{alkene} \rightarrow 0.5\ MEK + 0.5\ RCHO + 0.4\ HO_2.$$

Reactions of ethene. The rate constants and mechansim used for the reactions of ethene are given in Table 2, and notes in the table give the sources of the rate constants employed. Ethene is treated separately in

this mechanism because of its importance in urban emissions, and because it reacts significantly slower in the atmosphere than the other alkenes. Also, the mechanism for its reaction with OH radicals and $O(^3P)$ atoms is sufficiently different that it does not fit into the generalized scheme used in this mechanism for the higher alkenes. In the case of the OH radical reaction, the OH-substituted alkoxy radical formed (discussed above) decomposes sufficiently slowly that a non-negligible fraction [$\sim$22% at 298 K and atmospheric pressure, based on the data of Niki *et al.* (1981)] reacts with O_2 to form glycolaldehyde. This makes the generalized scheme shown above for the higher alkenes not applicable to ethene. (Glycolaldehyde is represented by acetaldehyde in this mechanism since test calculations show that this approximation has only minor results on simulations, even of ethene–NO_x–air irradiations.) In the case of the $O(^3P)$ reaction, the mechanism we assume [based on that recommended by Atkinson and Lloyd (1984)] amounts to complete fragmentation to form radicals, making the generalized $O(^3P)$ reaction used for the higher alkenes inapplicable to ethene. However, the general discussions given above for the mechanisms of the O_3 and the NO_3 radical reactions are also applicable to ethene, and the reactions shown in Table 2 for ethene are consistent with the general scheme used for these reactions.

Representation of reactions of complex mixtures of organics

In principle, the detailed reaction mechanisms discussed in the previous sections can permit separate representation of the atmospheric reactions of over 100 individual alkenes, aromatics, alkenes, alcohols and other compounds. This is useful when evaluating the mechanism against results of environmental chamber experiments containing only a limited number of organics, but is not practical in most air quality simulation applications when most, if not all, of these $\geqslant 100$ compounds may be emitted and contribute, at least to some extent, to the overall reactivity. In such cases, it is more practical to use a limited number of lumped species to represent these compounds, with their rate constants and mechanistic product yield parameters derived based on weighted averages of those for the sets of species they represent. In such cases, the detailed assignments of the kinetic and mechanistic parameters for the $\geqslant 100$ different species can be used to derive the parameters for the lumped groups. Thus, maximum advantage of detailed chemical composition data (when available) can be taken in deriving lumped mechanisms which best represent the sets of species emitted into the airsheds being modeled. Computer software has been developed which can utilize detailed emissions data to derive the most appropriate set of parameters for lumped species based on this detailed mechanism (Carter, 1988b), but a discussion of this is beyond the scope of this paper. Methods for condensing this mechanism will be the subject of a subsequent manuscript.

CONCLUSIONS

The gas-phase photochemical reaction mechanism described in this paper should represent our current knowledge of atmospheric chemistry. However, it should be recognized that despite continuing laboratory studies of the kinetics and mechanisms of the atmospheric reactions of emitted organics, there continue to be significant uncertainties. For example, we still know very little of the chemical processes accounting for much of the ring fragmentation routes for the aromatic HCs, and recent laboratory studies tend to indicate that we know even less about these processes than we once thought we did (Atkinson, 1990; Atkinson *et al.*, 1989a). Likewise, significant uncertainties remain in the photooxidation mechanisms of the higher alkanes (and their reaction products), in many important details of the O_3–alkene reaction mechanisms (particularly with regard to radical formation) and in the photolysis reactions of many of the oxygenated products. The representations of many of these processes in the photochemical mechanism continue to be largely speculative or are based on empirical models derived from fits to environmental chamber data.

A major characteristic of the mechanism developed in this program is its capability to explicitly represent the kinetics and reaction mechanisms of over 100 detailed model species representing a wide variety of emitted organic compounds. However, although the initial rates of reaction for most of these species are reasonably well established, either by direct measurement or by experimentally validated estimation techniques, this cannot be said for the product yields and mechanisms assumed for most of these compounds. For most compounds, these had to be estimated based on our knowledge of analogous, but generally lower molecular weight, compounds whose mechanisms themselves (as indicated above) may be uncertain. Only for a minority of the species in this mechanism are environmental chamber data available to evaluate the assumptions or estimations made for their mechanistic or product yield parameters. The parameters assumed for the higher molecular weight compounds, which constitute a non-negligible fraction of the emissions, are particularly uncertain.

However, despite these uncertainties we believe that using these estimates for the detailed model is preferable to the alternative of ignoring our best estimates for the mechanisms of the many emitted species entirely, and just representing their reactions by the much smaller number of surrogate species (or lumped structure groups) used in most current lumped mechanisms. As discussed elsewhere (Carter, 1988b), techniques exist for utilizing these detailed estimates for deriving condensed mechanisms for use in practical air quality simulation applications such that advantage is

taken of the detailed information contained in the mechanism and the emissions data. As more data become available concerning the kinetics and reaction mechanisms of the many classes of emitted organic compounds, as well as chamber data to test their reaction mechanisms, our representation of the detailed model species, and condensed mechanism derived based on them, will become increasingly accurate. The procedures developed for incorporating parameters assigned for the detailed species into lumped models (Carter, 1988b) provides a framework for this new knowledge to become readily incorporated into the airshed models, without the need to develop and then totally re-evaluate new lumped mechanisms.

Acknowledgements—The development of the mechanism described in this paper is primarily a result of funding from the U.S. Environmental Protection Agency (Contract No. 60–02–4104), the U.S. Air Force (Contract No. F08635-83-0278) and the California Air Resources Board (Contract No. A5-12-32). The author is grateful to Dr Roger Atkinson for reviewing this manuscript and for many helpful discussions. Helpful discussions with Dr Marcia C. Dodge and Frederick W. Lurmann are also gratefully acknowledged.

REFERENCES

Addison M. C., Burrows J. P., Cox R. A. and Patrick R. (1980) Absorption spectrum and kinetics of the acetylperoxy radical. *Chem. Phys. Lett.* **73,** 283–287.

Atkinson R. (1987) A structure–activity relationship for the estimation of rate constants for the gas-phase reactions of OH radicals with organic compounds. *Int. J. Chem. Kinet.* **19,** 799–828.

Atkinson R. (1988) Gas-phase atmospheric chemistry of organic compounds. Report, California ARB Contract No. A5-122-32, October.

Atkinson R. (1990) Gas-phase tropospheric chemistry of organic compounds: a review. *Atmospheric Environment* **24A,** 1–41.

Atkinson R. and Aschmann S. M. (1986) Kinetics of the reactions of naphthalene, 2-methylnaphthalene, and 2,3-dimethylnaphthalene with OH radicals and with O_3 at 295 $\pm$ 1 K. *Int. J. Chem. Kinet.* **18,** 569–573.

Atkinson R. and Aschmann S. M. (1987) Kinetics of the gas-phase reactions of alkylnaphthalenes with O_3, N_2O_5 and OH radicals at 298 $\pm$ 2 K. *Atmospheric Environment* **21,** 2323–2326.

Atkinson R. and Aschmann S. M. (1988) Kinetics of the gas-phase reactions of acenaphthene and acenaphthylene and structurally-related aromatic compounds with OH and NO_3 radicals, N_2O_5 and O_3 at 296 $\pm$ 2 K. *Int. J. Chem. Kinet.* **20,** 513–539.

Atkinson R. and Aschmann S. M. (1989) Rate constants for the gas-phase reactions of the OH radical with a series of aromatic hydrocarbons at 296 $\pm$ 2 K. *Int. J. Chem. Kinet.* **21,** 355–365.

Atkinson R., Aschmann S. M., Arey J. and Carter W. P. L. (1989a) Formation of ring-retaining products from the OH radical-initiated reactions of benzene and toluene. *Int. J. Chem. Kinet.* **21,** 801–827.

Atkinson R., Baulch D. L., Cox R. A., Hampson R. F., Jr., Kerr J. A. and Troe J. (1989b) Evaluated kinetic and photochemical data for atmospheric chemistry. Supplement III. *J. Phys. Chem. Ref. Data* **18,** 881–1097.

Atkinson R. and Carter W. P. L. (1984) Kinetics and mechanisms of the gas-phase reactions of ozone with organic compounds under atmospheric conditions. *Chem. Rev.* **84,** 437–470.

Atkinson R., Carter W. P. L., Darnall K. R., Winer A. M. and Pitts Jr. J. N. (1980) A smog chamber and modeling study of the gas phase NO_x–air photooxidation of toluene and the cresols. *Int. J. Chem. Kinet.* **12,** 779–836.

Atkinson R., Carter W. P. L. and Winer A. M. (1983) Effects of pressure on product yields in the NO_x photooxidations of selected aromatic hydrocarbons. *J. phys. Chem.* **87,** 1605–1610.

Atkinson R. and Lloyd A. C. (1984) Evaluation of kinetic and mechanistic data for modeling of photochemical smog. *J. Phys. Chem. Ref. Data* **13,** 315–444.

Atkinson R., Lloyd A. C. and Winges L. (1982) An updated chemical mechanism for hydrocarbon/NO_x/SO_2 photooxidations suitable for inclusion in atmospheric simulation models. *Atmospheric Environment* **16,** 1341.

Atkinson R. and Pitts Jr. J. N. (1977) Absolute rate constants for the reaction of O(3*p*) atoms with a series of olefins over the temperature range 298–439 K. *J. Chem. Phys.* **67,** 38.

Atkinson R., Tuazon E. C. and Carter W. P. L. (1985) Extent of H-atom abstraction from the reaction of the OH radical with 1-butene under atmospheric conditions. *Int. J. Chem. Kinet.* **17,** 725–734.

Atkinson R., Winer A. M. and Pitts Jr. J. N. (1986) Estimation of night-time N_2O_5 concentrations from ambient NO_2 and NO_3 radical concentrations and the role of N_2O_5 in night-time chemistry. *Atmospheric Environment* **20,** 331–339.

Bandow H. and Washida N. (1985a) Ring-cleavage reactions of aromatic hydrocarbons studied by FT-IR spectroscopy. II. Photooxidation of *o*-, *m*-, and *p*-xylenes in the NO_x–air system. *Bull. Chem. Soc. Jpn.* **58,** 2541–2548.

Bandow H. and Washida N. (1985b) Ring-cleavage reactions of aromatic hydrocarbons studied by FT-IR spectroscopy. III. Photooxidation of 1,2,3-, 1,2,4- and 1,3,5-trimethylbenzenes in the NO_x–air system. *Bull. Chem. Soc. Jpn.* **58,** 2549–2555.

Bandow H., Washida N. and Akimoto H. (1985) Ring-cleavage reactions of aromatic hydrocarbons studied by FT-IR spectroscopy. I. Photooxidation of toluene and benzene in the NO_x–air system. *Bull. Chem. Soc. Jpn.* **58,** 2531–2540.

Basco N. and Parmar S. S. (1985) Spectra and reactions of acetyl and acetylperoxy radicals. *Int. J. Chem. Kinet.* **17,** 891–900.

Bass A. M., Glasgow L. C., Miller C., Jesson J. P. and Filken D. L. (1980) Temperature dependent absorption cross sections for formaldehyde (CH_2O): the effect of formaldehyde on stratospheric chlorine chemistry. *Planet. Space Sci.* **28,** 675–679.

Bass A. M. and Paur R. J. (1985) In *Atmospheric Ozone, Proceedings of Quadrennial Ozone Symposium in Halkidiki*, pp. 606–616. Reidel, Dordrecht.

Baulch D. L., Cox R. A., Hampson Jr. R. F., Kerr J. A., Troe J. and Watson R. T. (1984) Evaluated kinetic and photochemical data for atmospheric chemistry: Supplement II. *J. Phys. Chem. Ref. Data* **13,** 1259–1380.

Carter W. P. L. (1988a) Documentation of a gas-phase photochemical mechanism for use in airshed modeling, Report, California ARB Contract No. A5-122-32, October.

Carter W. P. L. (1988b) Documentation for the SAPRC atmospheric photochemical mechanism preparation and emissions processing programs for implementation in airshed models, Report, California Air Resources Board Contract No. A5-122-32, October.

Carter W. P. L. and Atkinson R. (1985) Atmospheric chemistry of alkanes. *J. atmos. Chem.* **3,** 377–405.

Carter W. P. L., Atkinson R., Winer A. M. and Pitts Jr J. N. (1982a) Experimental investigation of chamber-dependent radical sources. *Int. J. Chem. Kinet.* **14,** 1071–1103.

Carter W. P. L., Long W. D., Parker L. N. and Dodd M. C. (1986a) Effects of methanol fuel substitution on multi-day air pollution episodes, Final Report, California Air Resources Board Contract No. A3-125-32, April.

Carter W. P. L., Lurmann F. W., Atkinson R. and Lloyd A. C. (1986b) Development and testing of a surrogate species chemical reaction mechanism, EPA-600/3-86-031, August.

Carter W. P. L., Winer A. M., Atkinson R., Dodd M. C. and Aschmann S. A. (1984) Atmospheric photochemical modeling of turbine engine fuels. Phase I. Experimental studies. Volume I of II. Results and discussion. Final Report, U.S. Air Force, ESL-TR-84-32, September.

Carter W. P. L., Winer A. M., Atkinson R., Heffron S. E., Poe M. P. and Goodman M. A. (1987) Atmospheric photochemical modeling of turbine engine fuels. Phase II. Computer model development, Report, U.S. Air Force Contract No. F08635-83-0278, Engineering and Services Laboratory, Air Force Engineering and Services Center, Tyndall AFB, FL, August.

Carter W. P. L., Winer A. M. and Pitts Jr J. N. (1981) Major atmospheric sink for phenol and the cresols. Reaction with the nitrate radical. *Envir. Sci. Technol.* **15,** 829–831.

Carter W. P. L., Winer A. M. and Pitts Jr J. N. (1982b) Effects of kinetic mechanisms and hydrocarbon composition on oxidant–precursor relationships predicted by the EKMA isopleth technique. *Atmospheric Environment* **16,** 113–120.

Calvert J. G. and Pitts Jr. J. N. (1966) *Photochemistry*. John Wiley, New York.

Darnall K. R., Atkinson R. and Pitts Jr. J. N. (1979) Observation of biacetyl from the reaction of OH radicals with *o*-xylene. Evidence for ring cleavage. *J. phys. Chem.* **83,** 1943–1946.

Dodge M. C. (1977) Combined use of modeling techniques and smog chamber data to derive ozone–precursor relationships. *Proceedings International Conference on Photochemical Oxidant and Its Control, Research Triangle Park*, NC, EPA-600/3-80-028a.

Dodge M. C. and Arnts R. R. (1979) A new mechanism for the reaction of ozone with olefins. *Int. J. Chem. Kinet.* **11,** 399–410.

Dumdei B. E. and O'Brien R. J. (1984) Toluene degradation products in simulated atmospheric conditions. *Nature* **311,** 248–250.

EPA (1987) Workshop on Evaluation/Documentation of Chemical Mechanisms, EPA-600/9-87-024, October.

Falls A. H. and Seinfeld J. H. (1978) Continued development of a kinetic mechanism for photochemical smog. *Envir. Sci. Technol.* **12,** 1398–1406.

Gery M. W., Fox D. L., Jeffries H. E., Stockburger L. and Weathers W. S. (1985) A continuous stirred tank reactor investigation of the gas-phase reaction of hydroxyl radicals and toluene. *Int. J. Chem. Kinet.* **17,** 931–955.

Gery M. W., Fox D. L., Kamens R. M. and Stockburger L. (1987) Investigation of hydroxyl radical reactions with *o*-xylene and *m*-xylene in a continuous stirred tank reactor. *Envir. Sci. Technol.* **21,** 339–348.

Gery M. W., Whitten G. Z. and Killus J. P. (1988) Development and testing of the CBM-IV for urban and regional modeling, Final Report, EPA Contract No. 68–02–4136, Atmospheric Sciences Research Laboratory, Research Triangle Park, NC, January.

Graham R. A. and Johnston H. S. (1978) The photochemistry of NO_3 and the kinetics of the N_2O_5–O_3 system. *J. phys. Chem.* **82,** 254–268.

Hatakeyama S., Kobayashi H. and Akimoto H. (1984) Gas-phase oxidation of SO_2 in the ozone–olefin reactions. *J. phys. Chem.* **88,** 4736–4739.

Hatakeyama S., Washida N. and Akimoto H. (1986) Rate constants and mechanisms for the reaction of OH (OD) radicals with acetylene, propyne, and 2-butyne in air at 297 ± 2 K. *J. phys. Chem.* **90,** 173–178.

Heicklen J., Desai J., Bahta A., Harper C. and Simonaitis R. (1986) The temperature and wavelength dependence of the photooxidation of propionaldehyde. *J. Photochem.* **34,** 117–135.

Hough A. M. (1988) An intercomparison of mechanisms for the production of photochemical oxidants. *J. geophys. Res.* **93,** 3789–3812.

Jeffries H. E., Sexton K. G. and Salmi C. N. (1981) The effects of chemistry and meteorology on ozone control calculations using simple trajectory models and the EKMA procedure. EPA-450/4-81-034, November.

Jeffries H. E., Kamens R. M., Sexton F. G. and Gerhardt A. A. (1982) Outdoor smog chamber experiments to test photochemical models. EPA-600/3-82-016A, April.

Kenley R. A. and Hendry D. G. (1982) Generation of peroxy radicals from peroxynitrates ($ROONO_2$). Decomposition of peroxybenzoyl nitrate (PBzN). *J. Am. Chem. Soc.* **104,** 220–224.

Killus J. P. and Whitten G. Z. (1982) A new carbon-bond mechanism for air quality simulation modeling. EPA-600/3-82-841, April.

Kircher C. C. and Sander S. P. (1984) Kinetics and mechanism of HO_2 and DO_2 disproportionations. *J. phys. Chem.* **88,** 2082–2091.

Langford A. O. and Moore C. B. (1984) Collision complex formation in the reactions of formyl radicals with nitric oxide and oxygen. *J. Chem. Phys.* **80,** 4211–4221.

Leone J. A., Flagan R. C., Grosjean D. and Seinfeld J. H. (1985) An outdoor smog chamber and modeling study of toluene–NO_x photooxidation. *Int. J. Chem. Kinet.* **17,** 177–216.

Leone J. A. and Seinfeld J. H. (1984a) Evaluation of chemical reaction mechanisms for photochemical smog. Part II. Quantitative evaluation of the mechanisms. EPA-600/3-84-063 revised, November.

Leone J. A. and Seinfeld J. H. (1984b) Updated chemical-mechanism for atmospheric photooxidation of toluene. *Int. J. Chem. Kinet.* **16,** 159–193.

Lurmann F. W. and Carter W. P. L. (1989) A performance evaluation of the SAPRC and RADM chemical reaction mechanisms. Presented at the 82nd Annual APCA Meeting, 25–30 June, Anaheim, California.

Lurmann F. W., Carter W. P. L. and Coyner L. A. (1987) A surrogate species chemical reaction mechanism for urban-scale air quality simulation models. Volume I—Adaptation of the mechanism. Final Report, EPA Contract No. 68–02-4104, Atmospheric Sciences Research Laboratory, Research Triangle Pàrk, NC.

Lurmann F. W., Lloyd A. C. and Atkinson R. (1986) A chemical mechanism for use in long-range transport/acid deposition computer modeling. *J. geophys. Res.* **91,** 10,905–10,936.

Magnotta F. and Johnston H. S. (1980) Photodissociation quantum yields for the NO_3 free radical. *Geophys. Res. Lett.* **7,** 769–772.

Majer J. R., Naman S-A. M. A. and Robb J. C. (1969) Photolysis of aromatic aldehydes. *Trans. Faraday Soc.* **65,** 1846–1853.

McRae G. J., Goodin W. R. and Seinfeld J. H. (1982) Development of a second-generation mathematical model for air pollution—I. Model formulation. *Atmospheric Environment* **16,** 679–696.

McRae G. J. and Seinfeld J. H. (1983) Development of a second-generation mathematical model for urban pollution—II. Model performance. *Atmospheric Environment* **17,** 501–523.

Meyrahn H., Pauly J., Schneider W. and Warneck P. (1986) Quantum yields for the photodissociation of acetone in air and an estimate for the lifetime of acetone in the lower troposphere. *J. atmos. Chem.* **4,** 277–291.

Molina M. J. and Arguello G. (1979) Ultraviolet absorption spectrum of methylhydroperoxide vapor. *Geophys. Res. Lett.* **6,** 953–955.

Moortgat G. K., Seiler W. and Warneck P. (1983) Photodissociation of HCHO in air: CO and H_2 quantum yields at 220 and 300 K. *J. Chem. Phys.* **78,** 1185–1190.

NASA (1987) Chemical kinetics and photochemical data for use in stratospheric modeling. Evaluation number 8. JPL Publication 87–41, Jet Propulsion Laboratory, Pasadena, CA, September.

NCAR (1987) Development and implementation of chemical

mechanisms for the Regional Acid Deposition Model (RADM). Final Report, on EPA Interagency Agreement DW49930144-01-4, Atmospheric Sciences Research Laboratory, Research Triangle Park, NC 1 April.

Niki H., Maker P. D., Savage C. M. and Breitenbach L. P. (1977) Fourier transform i.r. spectroscopic observation of propylene ozonide in the gas phase reaction of ozone–*cis*-2-butene–formaldehyde. *Chem. Phys. Lett.* **46,** 327–330.

Niki H., Maker P. D., Savage C. M. and Breitenbach L. P. (1981) An FT–IR study of mechanisms for the HO radical initiated oxidation of C_2H_4 in the presence of NO: detection of glycolaldehyde. *Chem. Phys. Lett.* **80,** 499–503.

Niki H., Maker P. D., Savage C. M. and Breitenbach L. P. (1983) A Fourier transform infrared study of the kinetics and mechanism for the reaction $HO + CH_3OOH$. *J. phys. Chem.* **87,** 2190–2193.

Penner J. E. and Walton J. J. (1982) Air quality model update. Lawrence Livermore Laboratory Report UCID-193000.

Pitts Jr. J. N., Atkinson R., Carter W. P. L., Winer A. M. and Tuazon E. C. (1983) Chemical consequences of air quality standard and of control implementation programs. Final Report, California Air Resources Board Contract No. A1-030-32, April.

Pitts Jr. J. N., Darnall K., Carter W. P. L., Winer A. M. and Atkinson R. (1979). Mechanisms of photochemical reactions in urban air. EPA-600/3-79-110, November.

Plum C. N., Sanhueza E., Atkinson R., Carter W. P. L. and Pitts Jr. J. N. (1983) OH radical rate constants and photolysis rates of α-dicarbonyls. *Envir. Sci. Technol.* **17,** 479–484.

Schafer T. B. and Seinfeld J. H. (1985) Evaluation of chemical reaction mechanisms for photochemical smog. Part III. Sensitivity of EKMA to chemical mechanism and input parameter. EPA-600/3-85-042.

Shepson P. B., Edney E. O. and Corse E. W. (1984) Ring fragmentation reactions in the photooxidations of toluene and *o*-xylene. *J. phys. Chem.* **88,** 4122–4126.

Shepson P. B., Edney E. O., Kleindienst T. E., Pittman J. H., Namie G. R. and Cupitt L. T. (1985) The production of organic nitrates from hydroxyl and nitrate radical reaction with propylene. *Envir. Sci. Technol.* **19,** 849–854.

Singleton D. L., Furuyama S., Cvetanovic R. J. and Irwin R. S. (1975) Temperature dependence of the rate constants for the reactions 0(3P) +2,3-dimethyl-2-butene and 0(3P) + NO + M determined by a phase shift technique. *J. Chem. Phys.* **63,** 1003–1007.

Stockwell W. R. and Calvert J. G. (1978) The mechanism of $HO–SO_2$ reaction. *Atmospheric Environment* **17,** 2231–2235.

Stockwell W. R. and Calvert J. G. (1983) The mechanism of NO_3 and HONO formation in the night-time chemistry of the urban atmosphere. *J. geophys. Res.* **88,** 6673–6682.

Stockwell W. R. (1986) A homogeneous gas-phase mechanism for use in a regional acid deposition model. *Atmospheric Environment* **20,** 1615–1632.

Suto M., Manzanares E. R. and Lee L. C. (1985) Detection of sulfuric acid aerosols by ultraviolet scattering. *Envir. Sci. Technol.* **19,** 815–820.

Sverdrup G. M., Spicer C. W. and Ward G. F. (1987) Investigation of the gas-phase reaction of dinitrogen pentoxide with water vapor. *Int. J. Chem. Kinet.* **19,** 191–205.

Takagi H., Washida N., Akimoto H. and Okuda M. (1982) observation of 3-hexene-2,5-dione in the photooxidation of 1,2,4-trimethylbenzene in the $NO–H_2O$–air system. *Spectros. Lett.* **15,** 145–152.

Tuazon E. C., Atkinson R., Plum C. N., Winer A. M. and Pitts, Jr. J. N. (1983) The reaction of gas-phase N_2O_5 with water vapor. *Geophys. Res. Lett.* **10,** 953–956.

Tuazon E. C., Mac Leod H., Atkinson R. and Carter W. P. L. (1986) α-Dicarbonyl yields from the NO_x–air photooxidations of a series of aromatic hydrocarbons in air. *Envir. Sci. Technol.* **20,** 383–387.

Vaghjani G. L. and A. R. Ravishankara (1989) Kinetics and mechanisms of OH reactions with CH_3OOH. *J. phys. Chem.* **93,** 1948–1959.

Wallington T. J., Neuman D. E. and Kurylo M. J. (1987) Kinetics of the gas-phase reaction of hydroxyl radicals with ethene, benzene, and a series of halogenated benzenes over the temperature range 234–438 K. *Int. J. Chem. Kinet.* **19,** 725–739.

Witte F., Urbanik E. and Zetzsch C. (1986) Temperature dependence of the rate constants for the addition of OH to benzene and to some monosubstituted aromtics (aniline, bromobenzene, and nitrobenzene) and the unimolecular decay of the adducts. Kinetics into a quasi-equilibrium. 2. *J. phys. Chem.* **90,** 3251–3259.

Whitten G. Z., Killus J. P. and Johnson R. G. (1985) Modeling of auto exhaust smog chamber data for EKMA development. EPA-600/3-85-025, April.